UNIVERSIDAD DE CÓRDOBA

Facultad de Ciencias

Departamento de Genética

Identification of compounds secreted by tomato roots that elicit chemotropic growth in *Fusarium oxysporum*

Mennat El Ghalid

Córdoba, 2015

TITULO: *Identification of compounds secreted by tomato roots that elicit chemotropic growth in Fusarium oxysporum*

AUTOR: *Mennat el Ghalid*

Campus de Rabanales
Ctra. Nacional IV, Km. 396 A
14071 Córdoba

www.uco.es/publicaciones
publicaciones@uco.es

TÍTULO DE LA TESIS: Identification of compounds secreted by tomato roots that elicit chemotropic growth in *Fusarium oxysporum*

DOCTORANDO/A: Mennat El Ghalid

INFORME RAZONADO DEL/DE LOS DIRECTOR/ES DE LA TESIS

La Tesis doctoral de Dña. Mennat El Ghalid se ha llevado a cabo en el Departamento de Genética de la Universidad de Córdoba en el seno del grupo "Genética Molecular de la Patogénesis fúngica (BIO-3138). Su desarrollo ha permitido a la doctoranda adquirir una sólida formación en Genética, Bioquímica y Biología Molecular. Durante la realización de la tesis, la candidata ha purificado, a partir de exudados de raíz de tomate, las moléculas que actuan como señales químicos para el crecimiento dirigido del hongo patógeno *F. oxysporum*, identificadas como peroxidasas de clase III. Además ha caracterizado la respuesta quimiotrópica del hongo a dichas señales, y ha confirmado, mediante expresión heteróloga en *Escherichia coli*, que la actividad enzimática de las peroxidasas es esencial para su función en dicho proceso.
Los resultados obtenidos se han comunicado en varios congresos nacionales e internacionales, y se han recogido en unartículo aceptado en la revista Nature.

Por todo ello, se autoriza la presentación de la tesis doctoral

Córdoba, Septiembre 2015

Firma de los directores

Fdo.: Antonio Di Pietro **Fdo.: David Turrà**

This work has been conducted in the Department of Genetics of the University of Córdoba and financially supported by the ARIADNE Marie Curie Research Training Network (FP7-PEOPLE-ITN-237936).

“*La gloire n’est pas de ne jamais tomber*
mais de se relever à chaque chute”

Confucius

A ma mere,

Acknowledgement

Que difícil!!! Además lo intento en español! ☺

La primera persona que quiero agradecer es mi director de tesis Antonio Di Pietro. Gracias por embarcarme en este tema de tesis tan estimulante! Como todas tesis, hay altos y bajos pero al final del camino, uno se da cuenta, que los esfuerzos quedan recompensados y ahorra entiendo el porque de algunas cosas que no había comprendido antes. Me acuerdo que un día que yo no tenia las ideas claras, me dijiste "confía en mi", y lo cierto es que teñiste razón. Aprendí mucho de ti que sea a nivel profesional o personal. Supiste sacar de facetas de mi carácter que ni siquiera conocía! Gracias por todas las enseñanzas…son muchas!

En segundo lugar, quiero agradecer a mi co-director de tesis David Turra. Eres sin duda un excelente científico y me alegro de haber tenido la oportunidad de trabajar contigo y aprender de ti.

Lugo, quiero agradecer a todos los profesores que me apoyaron, empezando por Reyes quien nunca se canso de mis problemas administrativos y quien me apoyo por lo todo lo que necesitaba! A Concha quien estuvo siempre disponible para escucharme y levantarme el animo! Y por supuesto a Carmen y Encarna quienes me apoyaron en varias ocasiones durante estos cuatros anos y sin olvidar a los profesores del grupo de Veterinaria quienes me hicieron sentir una mas de su grupo.

Ahorra quiero agradecer a mis compis y amigos del laboratorio. Miles gracias a Loida, quien me adopto desde mi primer día en Córdoba, me enseno a hablar español con tanta paciencia y con quien compartí alegrías y penas! Una verdadera amiga. Gracias a Katja con quien tuve charlas interminables y por cierto súper constructivas ;)! Y por todos los momentazos de risas! Gracias a David Segorve por seguir estas charlas con migo cuando ella se fue y compartir los duros momentos de final de tesis. Gracias a Elena por escucharme y darme los mejores consejos cuando mas lo necesitaba. Gracias a Esther, el pilar de este laboratorio, por tu apoyo durante los experimentos y para hacer empezar los días de buen humor cuando venia temprano ☺. Gracias a Gus por su ayuda en el laboratorio en varios momentos de la tesis y por su tranquilidad, que siempre se agradece en un lugar de trabajo. Da paz! ☺. Gracias a Daniela y Tania, dos chicas maravillosas quien llevaron aire nuevo y fresco al entrar últimamente en el laboratorio. Gracias a Rafita quien era al final de la tesis como mi hermana pequeña y con quien compartí mucho de la cultura francesa. Y gracias a muchas otras personas del laboratorio Cris[3], Estefania, Manu, Isa, Picolo para compartir estos anos de tesis. Quiero también agradecer a los chicos de plantas Lola, Tere, Marivi quienes me guiaron y aconsejaron con mis experimentos con plantas, a Angel por su apoyo informático, a Casi y a Jara con quien teñí muchos momentos de risas especialmente con su baile de la proteína soluble!! Por cierto, tenemos que sacar un clip, seguro que ganaremos mas que en cienca! ☺

Graciass a los chicos de Ariadne! Tuve suerte de estar en este consortium y poder conocerles.

Ahorra quiero dar la gracias Marce, Suzi, Tere y Fransisco por todos las buenos momentos especialmente los que hemos tenido en rabanales a la hora de comida! Me lo pase realmente súper bien! Me acuerdos de los días que regresaba al laboratorio con los ojos hinchados de haber llorado de risa! ☺

Millones y millones de gracias a Gaby, Latifa, Carmen, Ire y Sara, mis amigas quien han estado a mi lado en estos cuatro anos de tesis y con quien compartí todas las penas y alegrías. Tuve muchas suerte en teneros. Chicas, sabéis que nada de lo que puedo escribir será suficiente para agradeceros! Pero desafortunadamente, aquí se trata de hacerlo corto! ;). Quiero agradecer a mis amigos de toda la vida, Mona, Didou, May, Faty, Imene, Rim, Anne Marie, Margot, Nas, Romi, Jessica, Imene, Monia, Darine, Julie, Nermine….quienes nunca jamas agradacere lo suficiente por tanto amor, pacienca y presencia!!! Os quiero!

Y finalmente quiero dar las gracias a mis padres…por los pasados 28 anos! La situación se podría resumir simplemente en una frase: si podía elegir, no podría elegir mejores padres. Lo cierto es que gane a la lotería de los padres! ☺ Je vous aime plus que tout.

Index

Table of contents

List of figures

List of tables

Resumen

La ruta de la proteína quinasa activada por mitógenos (MAPK) Fmk1 es la cascada de señalización mejor caracterizada en el hongo patógeno *F. oxysporum*, y regula varios mecanismos esenciales para la infección. Los métodos actualmente disponibles para medir el estado de activación de esta ruta son lentos y laboriosos. El primer objetivo de este trabajo ha sido el desarrollo de un método rápido y reproducible que consiste en la determinación de los niveles de transcripción de genes effectores regulados por la ruta. Estudios anteriores mostraron que el gen *fpr1*, que codifica una proteína secretada, muestra una expresión marcadamente reducida en mutantes de la ruta Fmk1. Hemos probado si la expression de *fpr1* estaba, además, regulada por otras rutas MAPK tales como la de la integridad de la pared celular. Utilizando mutantes específicos de ambas MAPKs encontramos que tanto Fmk1 como Mpk1 contribuyen a la expresión de *fpr1*. Para buscar nuevos genes regulados por la ruta Fmk1 se seleccionaron diez genes descritos anteriormente como por la cascada MAPK ortóloga en *S. cerevisiae.* expresión reveló ninguno de esos genes candidatos se reguló diferencialmente en los mutantes de la ruta Fmk1. En conclusión, los resultados de este estudio demuestran que la regulación de los genes que funcionan aguas abajo de la ruta MAPK Fmk1 no está conservada entre *F. oxysporum* y *S. cerevisiae*. Se necesitan más estudios para identificar genes indicadores adecuados para la activación de la cascada Fmk1.

Los hongos patógenos y simbiontes del suelo son capaces de dirigir el crecimiento hacia las raíces de las plantas. Actualmente se desconocen las señales que inducen la respuesta quimiotrópica. Estudios previos demostraron que las hifas de *F. oxysporum* muestran una respuesta quimiotrópica significativa hacia el exudado de raíces de tomate. El objetivo del presente trabajo fue caracterizar los compuestos secretados por las raíces del tomate que elicitan la respuesta quimiotrópica en *F. oxysporum*. El fraccionamiento por exclusión de tamaño y cromatografía de intercambio aniónico seguido por espectrometría de masas (LC-ESI-MS), identificaron los compuestos quimioatrayentes como peroxidasas de tipo III. Las peroxidasas de tipo III existen como familias multigénicas en todas las plantas terrestres y estan asociados a una variedad de procesos fisiológicos y de desarrollo tales como la elongación celular, la organización de la pared celular y la defensa a patógenos. La peroxidase de tipo III de rábano (horseradish peroxidase, HRP) comercial también provocó una respuesta quimiotrópica en *F. oxysporum*, mientras que inhibidores específicos de las peroxidasas

abolieron la actividad quimioatrayente de los exudados de raíces de tomate y de la HRP. Las peroxidasas de tomate TMP2 y CEVI-1, expresada de manera heteróloga en *E. coli* también quimiotrópica del hongo. Dicha respuesta no se observó con $TMP2_{R38SH42E}$, una versión mutada de TMP2 que carece de actividad enzimática. Además, especies reactivas de oxígeno (ERO) como el H_2O_2 provocaron una fuerte respuesta quimiotrópica en *F. oxysporum*. El quimiotropismo inducido por la peroxidasa y por los ERO requiere del receptor de feromona Ste2 y de la MAPK Mpk1. Los exudados de raíces de trigo también provocaron una respuesta quimiotrópica en el hongo que dependía de la actividad peroxidasa. Nuestros resultados indican que las peroxidasas secretadas de tipo III podrían representar un mecanismo general para la detección quimiotrópica de raíces de plantas por los hongos fitopatogenos.

Summary

The Fmk1 mitogen-activated protein kinase (MAPK) pathway is the best-characterized signaling cascade in the vascular wilt pathogen *F. oxysporum* and governs multiple infection-related processes. The current methods for measuring the activation status of this pathway are slow and laborious. The first objective of this work was to develop a fast and reproducible method consisting in monitoring the transcript levels of an effector gene regulated by the Fmk1 pathway. Previous studies showed that *fpr1*, encoding a secreted protein is drastically downregulated in mutants impaired in the Fmk1 MAPK pathway. We tested whether *fpr1* expression was also regulated by additional MAPK pathways such as the cell wall integrity cascade. Using specific pathway mutants we found that both Fmk1 and Mpk1 MAPK pathways contribute to *fpr1* gene expression. To search for additional genes specifically regulated by the Fmk1 pathway, we selected ten genes previously shown to be regulated by the orthologous MAPK pathway in *S. cerevisiae* and monitored their expression in *F. oxysporum*. Surprisingly, none of these candidate genes was differentially regulated in the Fmk1 pathway mutants. In conclusion, this study revealed that the regulation of genes functioning downstream of the Fmk1 MAPK pathway is not conserved between *F. oxysporum* and *S. cerevisiae*. Further studies are required to identify suitable reporter genes for monitoring Fmk1 cascade activation.

Soil-inhabiting fungal pathogens and symbionts exhibit directed hyphal growth towards plant roots, but the chemoattractant signals are currently unknown. Previous studies demonstrated that germ tubes of *F. oxysporum* display a significant chemotropic response towards root exudates of the host plant tomato. The objective of the present work was to characterize the compounds that elicit this chemotropic response. Fractionation of tomato root exudates by size exclusion and anion-exchange chromatography followed by liquid chromatography-electrospray ionization-mass spectrometry (LC-ESI-MS) analysis, identified class III peroxidases as the chemoattractant compounds. Class III peroxidases exist as large multigene families in all land plants and have been associated with a variety of physiological and

developmental processes such as cell elongation, cell wall organization, and pathogen defense. Importantly, commercial class III peroxidase from horseradish also triggered a robust chemotropic response in *F. oxysporum*, while specific peroxidase inhibitors abolished the chemoattractant activity of tomato root exudates and horseradish peroxidase. The tomato peroxidases TMP2 and CEVI-1 heterologously expressed in *E. coli* elicited a strong chemotropic response in the fungus which was abolished in $TMP2_{R38S,H42E}$, a mutant version TMP2 lacking enzymatic activity. Additionally, radicalized and non-radicalized Reactive Oxygen Species (ROS) such as H_2O_2 elicited a strong chemotropic response in *F. oxysporum*. Similar to plant-induced chemotropism, directed growth towards a gradient of ROS required both the seven transmembrane pheromone receptor Ste2 and the cell wall integrity MAPK Mpk1. Root exudates from the monocotiledoneous plant wheat also elicited a robust chemotropic response in *F. oxysporum* that required peroxidase enzymatic activity. Our results indicate that secreted class III peroxidases could represent a general mechanism for chemotropic sensing of plant roots by soil-inhabiting fungi.

Introduction

Fusarium species

Fusarium species are distributed worldwide and are adapted to a wide range of geographical sites, climate conditions, ecological habitats and host plants (Backhouse, Burgess et al. 2001). The diversity of plant species colonized by the genus *Fusarium* is amazing. *Fusarium* has been isolated from gymnosperms and from the monocotyledonous and dicotyledonous angiosperms (Kuldau and Yates. 2000). *Fusaria* can be saprophytes, endophytes or pathogens. The genus collectively represents the most important group of fungal plant pathogens, causing disease on almost every economically important plant species. *Fusaria* can also cause a broad spectrum of diseases in humans, ranging from superficial or localized infections in healthy hosts to lethal disseminated fusarioses in immunocompromised patients (Dignani and Anaissie 2004).

The soil-borne ascomycete *Fusarium oxysporum* is the causal agent of vascular wilt, a devastating disease affecting a large variety of economically important crops worldwide (Beckman 1987b). Vascular wilt disease is a major limiting factor in the production of many agricultural crops, including tomato, banana, cabbage, onion, cotton, flax, muskmelon, pea, watermelon, carnation, chrysanthemum, gladiolus and tulip (Armstrong and Armstrong 1981). The widespread distribution of the species complex stems from its ability to grow on a wide range of substrates and on its efficient high persistence in the soil (Burgess 1981). Our study will focus essentially on *F. oxysporum* f. sp. *lycopersici* which infects tomato plants.

Management of *Fusarium* vascular wilt

Disease management of *Fusarium* vascular wilt has evolved over the years. Chemical treatment with methyl bromide was applied as early as in the 1930s (Rosskopf, Chellemi et al. 2005). Because of its adverse effects on human health and the environment, its use was gradually reduced from the late 90s until its final ban (Fravel , Olivain et al. 2003), leading to the development of new methods for disease control.

Resistant tomato and melon cultivars are highly successful in conferring resistance to certain races of *F. oxysporum* f. sp. *lycopersici* and *F. oxysporum* f. sp. *melonis*, respectively (Ori, Eshed et al. 1997; Joobeur, King et al. 2004). In cases where no resistance against *Fusarium* wilt is available, such as in banana (f. sp. *cubense*), the disease can only be controlled by preventing the introduction of the pathogen through destruction of diseased plants. Under greenhouse and field conditions, studies on biological control of Fusariosis have focused on the application of antagonistic bacteria or non-pathogenic strains of *F. oxysporum.* The mechanisms contributing to the biocontrol capacity of these agents include antibiosis, competition for nutrients, reduction of chlamydospore germination, competition on the host root and induction of plant defense and systemic resistance (Larena, Melgarejo et al. 2002; Larkin and Fravel 2002; Khan, Fischer et al. 2006)

History and taxonomy

The genus *Fusarium* was first described in by Johann H. F. Link in 1824 (Link 1809). The necessity of a precise and reliable system of classification became apparent when it was realised that fusaria caused serious diseases on many plants. Wollenweber published the first taxonomy of the genus in 1931 (Wollenweber 1931) and a revised version (Wollenweber and Reinking 1935). The taxonomy of the genus has been revised, restructured and modified many times during the last century. Synder and Hansen greatly contributed to its simplification by organizing all the taxa into nine species with no varieties or forms and by grouping all the taxa of section *elegans* into a single species named *F. oxysporum*. They designated 25 formae speciales (f. spp.) species based on their pathogenicity on different plant species (Snyder and Hansen 1940). To date, more than 150 f. spp. have been reported (Michielse, van Wijk et al. 2009).

Table 1. Taxonomic classification of *F. oxysporum*.

Taxonomy (From NCBI, http://www.ncbi.nlm.nih.gov)	
Phylum	Ascomycota
Class	Sordariomycete
Order	Hypocreales
Family	Nectriaceae
Genus	*Fusarium*
Species	*F. oxysporum*
Formae speciales	e.g. *F. oxysporum* f. sp. *lycpoersici* (tomato)

Due to the lack of reliable morphological characters for defining species and subgenus groupings of *Fusarium*, molecular tools are currently used for identification and determination of evolutionary relationships. These include ribosomal spacer sequencing, Restriction Fragment Length Polymorphism (RFLP) and Random Amplified Polymorphic DNA (RAPD) markers. Interestingly, molecular phylogenetic studies in *F. oxysporum* revealed substantial genetic diversity among isolates, supporting the current view that it represents a species complex. In 1998, a pioneering study established that different field isolates of a f. sp. have polyphyletic origins, suggesting that the capacity to infect a given plant host has arisen multiple times during evolution (O'Donnell, Kistler et al. 1998).

The genome sequence of the tomato pathogenic *F. oxysporum* f. sp. *lycopersici* isolate 42-87 was published in 2010 (Ma, van der Does et al. 2010). Since then, the sequences of eleven additional *F. oxysporum* strains have become public. The availability of the complete genome sequences, as well as of molecular tools and well-established pathogenicity assays has been instrumental for addressing the genetic bases and evolutionary origins of pathogenicity and host range in *F. oxysporum*.

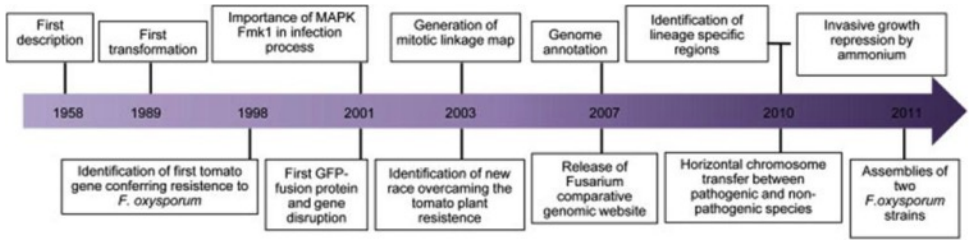

Figure 1. Key milestones in the history of *F. oxysporum* research (Perez-Nadales, Almeida Nogueira et al. 2014).

Biology of *F. oxysporum*

F. oxysporum changes its morphology and color depending on the environmental conditions. The culture conditions affect growth rate, shape, size and abundance of conidia as well as number of septa and pigmentation (Booth 1971). In general, the aerial mycelium appears first in white and then turns to a variety of colors that range from pink to dark purple. The species produces three types of asexual spores: microconidia, macroconidia and chlamydospores (Figure 2) (Agrios 1997).

Figure 2. Type of *F. oxysporum* conidia. A. Macroconidia. **B.** Microconidia. **C.** Chlamydospores.

Microconidia are single-celled dispersal structures that are abundantly produced under most conditions. Macroconidia contain three to five cells, are gradually pointed and curved toward the ends and are commonly found on the surface of dead plants killed by the pathogen. Chlamydospores are thick-walled cells generally developed through the modification of hyphal and conidial cells. Their formation is induced by aging or unfavorable environmental conditions such as low temperatures or carbon starvation. Chlamydospores represent the principal structure for long-time survival during unfavorable periods in the soil, and play an important role as primary inoculum for

plant root infection. Chlamydospore germination is stimulated when carbohydrates are released from decaying plant tissue or from roots (Stevenson and Becker 1972; Nelson 1981; Couteaudier and Alabouvette 1990; Kono, H. Yamamoto et al. 1995). The fungus can travel long distances within infected plants, soil or by wind in the form of microconidia. In short distances, *F. oxysporum* propagates mainly through water irrigation or contaminated equipment. Although it can infect fruit tissue and contaminate seeds, propagation rarely happens via the seed (Agrios 1997).

Overview of the *F. oxysporum* genome

Genome sequencing, assembly and annotation of *F. oxysporum* f. sp. *lycopersici* was performed by the Broad Institute as part of the Fusarium Comparative Sequencing Project. A striking feature of the genome is that 28% corresponds to repetitive sequences, including many retroelements and short interspersed elements (SINEs) as well as class II transposable elements (TEs) (Table 2).

Table 2. Overview on *F. oxysporum* genome data.

Genome Size (Mb)	61.36
Chromosomes	15
GC content (%)	48.4
Number of genes	17708
Non-coding RNAs (tRNAs)	308
Introns	Unknown
Average gene size	1.3 Kb
Transposons	28% is constituted by repetitive sequence: Retroelements (copia-like and gypsy-like, LINEs (long interspersed nuclear elements) and SINEs (short interspersed nuclear elements) and DNA transposons (Tc1-mariner, hAT-like, Mutator-like, and MITEs)
Mithocondrial DNA (Kb)	34.48
References	www.broadinstitute.org and (Takken and Rep 2010)

Lineage specific chromosomes

Comparison of the *F. oxysporum* genome with those of *F. graminearum* and *F. verticillioides* led to the discovery of four supernumerary chromosomes that are enriched for TEs and genes putatively related to host–pathogen interactions (Ma, van der Does et al. 2010). These so-called lineage-specific (LS) regions contain more than 95% of all DNA transposons. Only 20% of the predicted genes in the LS regions could be functionally classified on the basis of homology to known proteins. Many encode predicted secreted effectors, virulence factors, transcription factors and proteins involved in signal transduction but less house keeping proteins. Recent data suggest that LS regions of *F. oxysporum* strains with different host specificities may differ considerably in sequence.

Sequence characteristics of the genes present on the LS genome regions indicate a distinct evolutionary origin from the core genome, suggesting that they could have been acquired through horizontal transfer from another Fusarium species. This idea was experimentally supported by the finding that co-incubation of two strains of *F. oxysporum* can result in transfer of small LS chromosomes from a tomato pathogenic to a non-pathogenic strain, converting the latter in a tomato pathogen. This led to the hypothesis that horizontal chromosome transfer in *F. oxysporum* can generate new pathogenic lineages (Ma, van der Does et al. 2010). The genetic and cellular mechanisms underlying these processes are currently subject to intensive study.

Plant infection cycle

Spores present in the soil germinate in response to signals from the plant host and differentiate infection hyphae, which adhere to the plant roots and penetrate them directly without the need for specialized infection structures. Root penetration appears to occur predominantly through natural openings at the intercellular junctions of cortical cells or through wounds (Perez-Nadales and Di Pietro 2011). Once inside the root, hyphae grow inter- and intracellularly to invade the cortex and cross the

endodermis, until they reach the xylem vessels. The fungus then uses the xylem as a conduct to colonize the host (Figure 3).

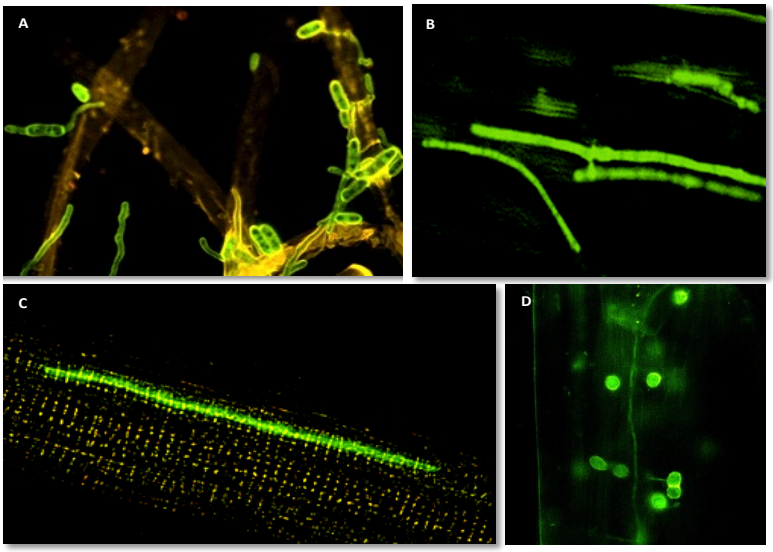

Figure 3. Penetration and colonization of tomato plants. A. Germinated microconidia and penetration hyphae of *F. oxysporum* f. sp. *lycopersici* strain 4287 attaching to the root surface, 24h after inoculation. **B.** Infection hyphae growing in the root cortex, 5 days after inoculation. **C.** Hypha growing in the root xylem vessels, 7 days after inoculation. **D.** Chlamydospores produced on dying plant tissue. Pictures taken from (Di Pietro, Garcia-MacEira et al. 2001).

A defence response based on a gene-for-gene interaction is induced in the xylem contact cells (Rep, van der Does et al. 2004). Unlike the classical hypersensitive response (HR), this response mainly involves callose deposition, accumulation of phenolics and formation of tyloses and gels in the infected vessels. Disease symptoms include wilting, chlorosis, necrosis, premature leaf loss, browning of the vascular system and stunting, which eventually will lead to plant death (Michielse and Rep 2009). *F. oxysporum* can survive in soil for extended time periods, either as chlamydospores or by growing saprophytically on organic compounds until a new cycle of infection starts (Agrios 2005b) (Figure 4).

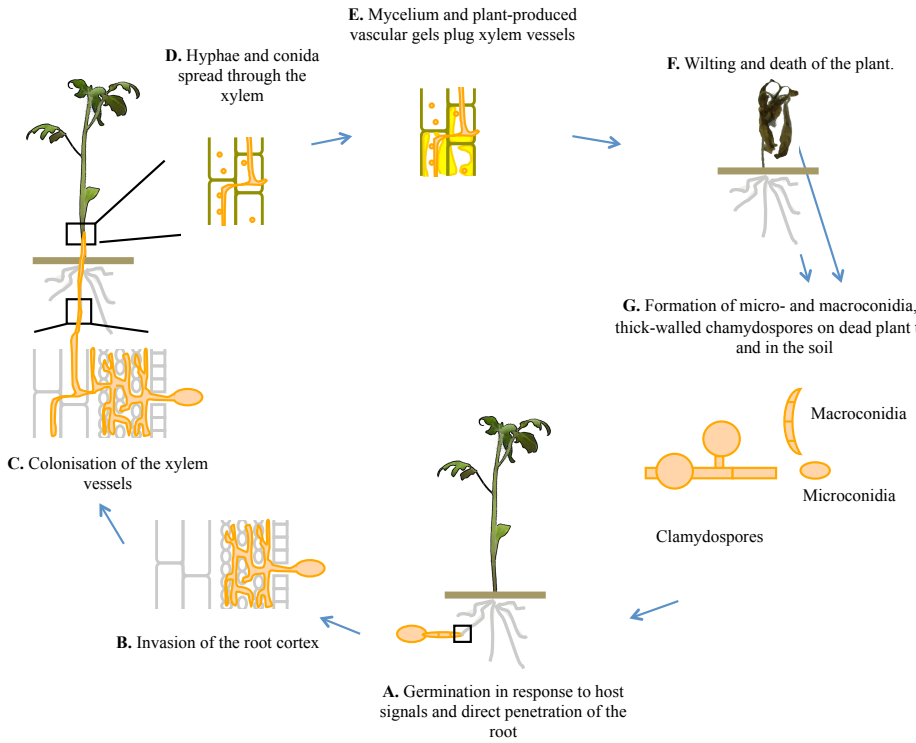

Figure 4. Life cycle of *F. oxysporum*. A. Germination in response to host signals and direct penetration of the root. **B.** Invasion of the root cortex. **C.** Colonization of the xylem vessels. **D.** Hyphae and conidia spread through the xylem. **E.** Fungal mycelium and plant-produced vascular gels plug the xylem vessels. **F.** Wilting and death of the plant. **G.** Formation of micro- and macroconidia, and thick-walled chlamydospores on the dead plant tissue and in the soil (Perez-Nadales, Almeida Nogueira et al. 2014).

Although a sexual stage has not yet been described for *F. oxysporum*, the genome contains apparently functional mating type idiomorphs (*MAT1-1* and *MAT-1-2*) similar to those found in sexual *Fusarium* species. The *MAT1-1* idimorph is composed of three genes including a gene encoding a protein with an alpha-box motif *FoMAT1-1-1* (motif found in all ascomycete *MAT1-1* idiomorph), whereas the *MAT1-2* idimorph contains a single gene *FoMAT1-2-1* encoding for a transcription factor with a high-mobility-group (HMG) DNA binding domain (motif found in all ascomycete *MAT1-2* idiomorph). *F. oxysporum MAT* genes are expressed and all the predicted introns are correctly processed (Arie, Kaneko et al. 2000). These observations indicate that, similar to other

fungal pathogens previously thought to lack sex, a cryptic sexual cycle may remain to be discovered in *F. oxysporum*.

Plant-pathogen interaction

Plant-pathogen interaction is a complex process with several stages and levels of recognition that determine success or failure of the infection process (Callow 1987). Pathogen detection is the first step for activation of plant defence mechanisms. Plants respond to attacks by pathogens at two levels (Dangl and McDowell 2006). First, the plant is able to recognize molecules commonly produced by all microbes, called pathogen-associated molecular patterns (PAMPS), including polysaccharides and glycoproteins present at the fungal surface, and mounts an innate immunity response. Successful pathogens have evolved mechanisms to overcome this first layer of defense, either by evading detection or by suppressing the immune response by the means of secreted effectors. In these cases, the plant becomes a host for a given pathogen species, establishing a compatible interaction. However, plants have acquired a second level of defense based on the capacity to recognize specific secreted virulence effectors and to mount a hypersensitive response involving localized cell death (Dangl and McDowell 2006). The gene-for-gene hypothesis established by Flor (Flor 1947; Flor 1971) proposes that for every avirulence gene (*avr*) in the pathogen there is a corresponding host resistance gene (*R*), and that the loss or mutation of an *avr* gene leads to the breakdown of resistance mediated by the corresponding *R* gene (Farman, Eto et al. 2002). The gene-for-gene model was recently demonstrated for the *F. oxysporum* f. sp. *lycopersici*-tomato interaction. In this f. sp. there are three known races, named in order of discovery race 1, 2 and 3 (Table 3). These are defined by their capacity to produce vascular wilt on tomato cultivars carrying different resistance genes. Tomato genes *I-1, I-2* and *I-3* confer resistance against race 1, 2 and 3, respectively (Beckman 1987a). The *I-2* resistance gene as well as several avirulence genes from *F. oxysporum* f. sp. *lycopersici* have been cloned, providing molecular support for the gene-for-gene hypothesis (Takken and Rep 2010). One of these avirulence proteins is Six1, which is secreted during colonisation of the xylem and mediates recognition by resistance gene

I-3. Strains defective in *six1* are thus virulent on *I-3* plants, while those expressing the gene are not. However, loss of Six1 comes at a cost for the pathogen, causing a global reduction of virulence (Rep, van der Does et al. 2004).

Table 3. Races and resistance genes described in the *F. oxysporum* f. sp. *lycopersici*-tomato interaction. From (Takken and Rep 2010)

Race		**Resistance genes in tomato cultivars**	
	I-1	***I-2***	***I-3***
Race 1	Avirulent	Virulent/Avirulent	Virulent/Avirulent
Race 2	Virulent	Avirulent	Virulent/Avirulent
Race 3	Virulent	Virulent	Avirulent

Fungal genes required for pathogenicity on plants

The number of pathogenic isolates resistant to fungicides is increasing and causes a need for the development of new active principles for agriculture and human health. However, a deeper understanding of the molecular mode of infection is required to develop novel strategies for disease control. The information provided by fungal genome sequencing is aiding the identification of new genes and proteins that could be useful for the design of targeted drugs (Isaacson 2002). In F. oxysporum and in other fungal pathogens, two main strategies have been used to identify pathogenicity genes. The first is reverse genetics, involving targeted deletion of candidate genes whose products may be involved in known biological functions relevant for infection (Pietro, Madrid et al. 2003). This strategy has been facilitated recently through the sequencing of the genome of F. oxysporum (Ma, van der Does et al. 2010). A second strategy known as forward genetics involves generation of pathogenicity mutants by random insertional mutagenesis followed by identification of the affected genes in these mutants (Madrid, Di Pietro et al. 2003). Genes that have a significant impact on

pathogenicity are often regulatory genes such as those encoding signalling components and transcription factors.

MAPK signaling cascades

Adaptation to changes in the environment is crucial for viability of all organisms. In fungi, conserved signal transduction pathways control fundamental aspects of growth, development and reproduction. Two important classes of fungal signalling pathways are mitogen-activated protein kinase (MAPK) cascades and the calcium-calcineurin pathway. MAPK cascades comprise a conserved module of three kinases: the MAPK, the MAPK kinase (MAPKK), and the MAPKK kinase (MAPKKK) that sequentially activate each other by phosporylation (Chang and Karin 2001). The upstream signals are sensed by specific receptors that stimulate the MAPK module directly or through intermediate signalling components. MAPKs phosphorylate a diverse set of components, including transcription factors, translational regulators, protein kinases, phosphatases and other classes of proteins that regulate metabolism, cellular morphology, cell cycle progression and gene expression in response to a variety of extracellular stresses and signals (Cyert 2003; Kraus and Heitman 2003; Qi and Elion 2005).

Role of MAPK pathways in Saccharomyces cerevisiae

Due to its relative simplicity, the yeast *S. cerevisiae* has been used as a model to decipher the functioning of the MAPK signaling network. In this organism, three MAPK cascades were found to signal through a common MAPKKK named Ste11 (Saito 2010). These are the Fus3 pheromone response pathway, the Kss1 filamentation/invasive growth pathway and the Hog1 hyperosmotic stress pathway.

Fus3 and Kss1 MAPK pathways

The sequential MAPK module of these two pathways is composed of the MAPKKK Ste11 and the MAPKK Ste7 (Wang and Dohlman 2004). Two MAPKs regulate distinct signalling outputs downstream of Ste7. Fus3, is essential for mating, whereas Kss1

controls invasive growth and pseudohyphal development (Madhani, Styles et al. 1997) (Figure 5).

The Fus3 MAPK cascade or pheromone response pathway in *S. cerevisiae* has been characterized in detail (Kurjan 1993; Gustin, Albertyn et al. 1998; Elion 2000; Wang and Dohlman 2004). Signaling is initiated when pheromone binds to the cell surface receptors Ste2 and Ste3. This leads to activation of a cascade that culminates in phosphorylation of Fus3, which in turn activates the transcription factor Ste12 leading to cell cycle arrest in G1, polarized growth after the remodeling of the cytoskeleton and the cell wall, formation of specialized fusion tubes called shmoos and finally fusion with the mating partner (Elion, Satterberg et al. 1993) (Figure 5).

Under nutrient-limiting conditions, yeast cells undergo a developmental switch called filamentous growth (FG), during which the cells become elongated, and mother and daughter cells remain attached to each other forming filaments of cells named pseudohyphae. The FG pathway is activated by a mucin-like protein, Msb2 (Cullen, Sabbagh et al. 2004) and controls cell adhesion, cell elongation, and the reorganization of cell polarity through the transcription factors Ste12 and Tec1 (Madhani, Styles et al. 1997). It is thought that the FG response allows yeast cells to forage for nutrient resources under unfavorable conditions (Figure 5).

The Mpk1 cell wall integrity pathway

The Mpk1 cell wall integrity cascade is responsible for orchestrating changes in the cell wall throughout the cell cycle and in response to various forms of stress (Levin 2005). This pathway is activated by the integrin-like membrane proteins Wsc1,2,3 (Verna, Lodder et al. 1997) which subsequently trigger the kinase module composed of the MAPKKK Bck1, the MAPKKs Mkk1 and Mkk2 and the MAPK Mpk1 (Levin 2005). Mpk1 regulates several nuclear targets such as Rlm1, Mbp1, Swi4, Swi6 and genes implicated in cell wall biogenesis and function (Nasmyth and Dirick 1991; Jung and Levin 1999; Jung, Sobering et al. 2002) (Figure 5).

The High Osmolarity Glycerol (HOG) pathway

The HOG pathway mediates responses to hyperosmotic shock and other stresses. This MAPK cascade was not the focus of the present work. Detailed information can be found in (Hohmann, Krantz et al. 2007) (Figure 5).

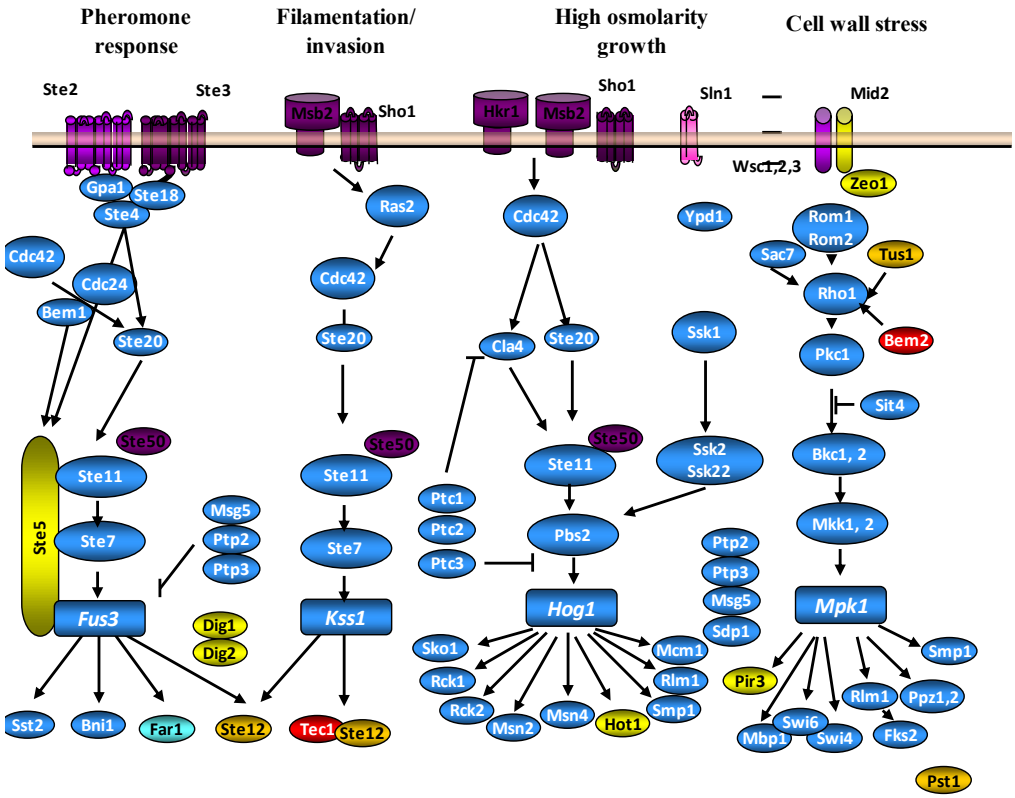

Figure 5. Schematic view of MAPK pathways in *S. cerevisiae*. Colors indicate different degrees of conservation among the fungal species *S. cerevisiae*, *A. gossypii* and *C. albicans* (hemiascomycetes), *S. pombe* (archiascomycetes), *A. fumigatus*, *F. graminearum*, *M. grisea* and *N. crassa* (euascomycetes), *R. oryzae* (zygomycetes) and *U. maydis* (basidiomycetes): blue, components detected in all species studied; green, all except zygomycetes; orange, all except basidiomycetes; cyan, all except zygomycetes and archiascomycetes; pink, all except zygomycetes, basidiomycetes and archiascomycetes; red, all except euascomycetes; purple, only ascomycetes; yellow: only hemiascomycetes (modified from (Rispail, Soanes et al. 2009)).

The role of MAPK pathways in plant pathogenic fungi

The Pathogenicity MAPK pathway

In plant pathogenic fungi, the Pathogenicity MAPK cascade, orthologous to the Kss1 pathway in *S. cerevisiae*, is involved in the control of infection-related morphogenesis and invasive growth (Turra, Segorbe et al. 2014). The first mutational analysis of a MAPK was performed in the rice blast fungus *Magnaporthe oryzae* (Xu and Hamer 1996). The mutants in the Kss1 ortholog Pmk1 were unable to form appressoria and to penetrate the rice leaf cuticle. Moreover, they failed to infect rice leaves through wounds, suggesting that the role of this pathway in pathogencity reaches beyond the differentiation of penetration structures. Kss1 orthologs were subsequently shown to be essential for plant infection in phylogenetically and biologically diverse phytopathogens (Zheng, Campbell et al. 2000; Di Pietro, Garcia-MacEira et al. 2001; Mey, Oeser et al. 2002; Jenczmionka, Maier et al. 2003) including obligate biotrophs (Panwar, McCallum et al. 2013). Currently, this MAPK is considered as a key player in infectious growth on living plant tissue and is the most studied pathogenicity factor in fungi. Additional components of the Kss1 MAPK module, such as Ste7 and Ste11 were also found to be essential for differentiation of penetration structures and plant infection in different pathogens (Banuett and Herskowitz 1994; Andrews, Egan et al. 2000; Muller, Weinzierl et al. 2003; Shim and Dunkle 2003; Izumitsu, Yoshimi et al. 2009; Schamber, Leroch et al. 2010). Interestingly, all studies so far confirmed the evolutionarily conserved role of the Kss1 pathway in plant infection, although its precise function is not completely understood. This cascade was described to play a major role in different steps of infection, such as host sensing (Xu and Hamer 1996; Lanver, Mendoza-Mendoza et al. 2010; Liu, Zhou et al. 2011; Perez-Nadales and Di Pietro 2011), develpment of infection structures (Xu and Hamer 1996), re-organisation of the actin cytoskeleton during host penetration (Park, Xue et al. 2002), invasion of the host tissue (Xu and Hamer 1996; Di Pietro, Garcia-MacEira et al. 2001), and expression of secreted plant cell wall-degrading enzymes (CWDEs) (Di Pietro, Garcia-MacEira et al. 2001; Lev and Horwitz 2003; Jenczmionka and Schafer 2005; Rispail and Di Pietro 2009; Zhang, Xue et al. 2011).

On the other hand, the Kss1 MAPK pathway also controls developmental processes such as conidiation (Lev, Sharon et al. 1999; Ruiz-Roldan, Maier et al. 2001; Jenczmionka, Maier et al. 2003; Shim and Dunkle 2003; Izumitsu, Yoshimi et al. 2009) sexual development (Lev, Sharon et al. 1999; Jenczmionka, Maier et al. 2003; Muller, Weinzierl et al. 2003; Izumitsu, Yoshimi et al. 2009), and vegetative hyphal fusion (Prados-Rosales and Di Pietro 2008), but is dispensable for vegetative hyphal growth, especially during liquid culture. This MAPK cascade shows how a conserved signaling pathway for developmental transitions in fungi has evolved to regulate new functions such as plant infection-related processes.

The Cell Wall Integrity MAPK pathway

As its name reflects, the cell wall integrity pathway is involved in the maintenance of the cell wall. Mutants of *M. oryzae* and *F. graminearum* lacking the Mpk1 ortholog presented normal hyphal growth in submerged culture but severely restricted colonies on solid media, which were partially restored by an osmotic stabilizer (Xu, Staiger et al. 1998; Hou, Xue et al. 2002; Kojima, Kikuchi et al. 2002). Besides its function in vegetative growth, Mpk1 is also important for developmental processes such as conidiation (Xu, Staiger et al. 1998; Kojima, Kikuchi et al. 2002; Mey, Held et al. 2002; Rui and Hahn 2007), female fertility (Xu, Staiger et al. 1998; Hou, Xue et al. 2002), and vegetative hyphal fusion (Hou, Xue et al. 2002). Although the mutants in this MAPK still produce melanised appressoria, they are defective in penetration and invasion of the host living tissue as well as virulence (Xu, Staiger et al. 1998; Kojima, Kikuchi et al. 2002; Mey, Held et al. 2002; Rui and Hahn 2007). These studies suggest that the cell wall integrity MAPK cascade is recruited for penetration and for subsequent steps of infection, which ensure the successful establishment of fungus-plant interaction, such as escape from the host immune response. Up- and downstream components of this pathway such as Bck1, Rlm1 and Swi6 are aslo involved in these biological processes (Jeon, Goh et al. 2008; Mehrabi, Ding et al. 2008; Qi, Wang et al. 2012).

Nitrogen sources control morphogenetic transition and virulence in fungi

In the model fungus *S. cerevisiae*, the orthologous MAPK Kss1 regulates a dimorphic switch to pseudo-filamentous growth and agar invasion in response to nutrient limitation (Truckses, Garrenton et al. 2004; Qi and Elion 2005). The transition between the unicellular form and filamentous growth form is also required in a wide range of fungal pathogens for infectious growth and virulence. It is for example the case for *Candida albicans*, *C. dubliniensis*, *Malassezia* spp., *Aspergillus fumigatus*, *Trichophyton rubrum* and *T. mentagrophytes,* among others (Brand 2012). In budding yeast, exogenous signals such as poor availability of ammonium and solid surfaces trigger the dimorphic switch to filamentous form growth (Prinz, Avila-Campillo et al. 2004). In plant pathogenic fungi, nitrogen limitation has been also proposed as a key signal for activating the expression of virulence genes (Snoeijers, Perez-Garcia et al. 2000; Tavernier, Cadiou et al. 2007). Previous studies demonstrated that in planta–induced genes such as *Magnaporthe oryzae mpg1* encoding a hydrophobin required for pathogenicity, or *Cladosporium fulvum* avirulence gene *Avr9* are strongly upregulated under conditions of nitrogen limitation (Talbot, Ebbole et al. 1993; van den Ackerveken, van Kan et al. 1994). In agreement with these findings, many genes identified in screens for nitrogen starvation-induced transcripts were also upregulated during plant infection (Coleman, Henricot et al. 1997; Stephenson, Green et al. 1997; Divon, Rothan-Denoyes et al. 2005; Donofrio, Oh et al. 2006).

Nitrogen is a critical element for the synthesis of proteins and nucleic acids, and its utilisation is a highly regulated process. Although fungi are able to use a wide variety of nitrogen sources, readily assimilated compounds such as amonium and glutamine, are used preferentially over more complex sources (Marzluf 1997). This is accomplished by a process known as nitrogen catabolite repression, whereby genes required for exogenous nitrogen source utilization are downregulated in the presence of the preferred source.

The Fmk1 MAPK cascade is essential for virulence-related functions in *F. oxysporum*

In our study, we focused on the *F. oxysporum* MAPK Fmk1, the ortholog of the yeast Fus3/Kss1 MAPKs. Fmk1 is dispensable for vegetative growth and conidiation of *F. oxysporum*in solid and liquid culture, but essential for the regulation of multiple virulence-related functions such as plant root adhesion and penetration, secretion of pectinolytic enzymes, and invasive growth (Di Pietro, Garcia-MacEira et al. 2001; Delgado-Jarana, Martinez-Rocha et al. 2005; Prados Rosales and Di Pietro 2008).

To date, five additional components of the Fmk1 pathway have been characterized in *F. oxysporum*: the homeodomain transcription factor Ste12, the MAPKKK Ste11, the MAPKK Ste7, and two upstream transmembrane components, the mucin-like protein Msb2 and the tetraspan protein Sho1 (Rispail and Di Pietro 2009; Perez-Nadales and Di Pietro 2011; Perez-Nadales and Di Pietro 2014). Ste11, Ste7 and Ste12 are all required for invasive growth, the most critical of the Fmk1-regulated functions for plant infection (Rispail and Di Pietro 2009). Msb2 is an upstream component of both the Fmk1cascade, promoting invasive growth and plant infection, and of the Mpk1 MAPK cascade contributing to maintenance of cell wall integrity (Perez-Nadales and Di Pietro 2011). Both *msb2*Δ and *fmk1*Δ mutants share characteristic phenotypes, such as defects in hyphal growth under poor nitrogen conditions, penetration of cellophane membranes, and colonization of living fruit tissue, root penetration, and virulence on tomato plants. Sho1 is an additional regulator of the Fmk1 pathway and cooperates with Msb2 to regulate virulence functions such as extracellular pectinolytic activity, cellophane penetration, plant tissue colonization and virulence on tomato plants. *Sho1*Δ mutants are also hypersensitive to cell wall perturbing compounds and show defects in activation of the Mpk1 MAPK signaling pathway (Perez-Nadales and Di Pietro 2014).

Chemotropic sensing in fungi

Discovery and history of chemotropism in fungi

Filamentous hyphal growth is critical for the lifestyle of fungi. Most are sessile and grow by extending the tip of the germ tube to form expanding hyphal networks (Brand and Gow 2009). Fungi have evolved elaborated mechanisms to respond to external stimuli and activate the appropriate developmental response such as vegetative growth, mating or formation of fruiting structures. Therefore, the ability to orient hyphae within a mycelium is vital for saprofitic, symbiotic and parasitic fungi.

Tropism is a biological phenomenon consisting of the growth or turning movement of an organism in response to environmental signals. The response depends on the type and the direction of the stimulus. There are different types of tropsims such as geotropism (in response to gravity), heliotropism (in response to the direction of the sun), hydrotropism (in response to the water), phototropism (in response to a light source), electrotropism (in response to an electric field) or thigmotropism (in response to a contact stimulus), among others. The topic of the present work was chemotropism, defined as directed growth in response to a chemical gradient. Chemotropism enables fungi to search for nutrients, mating partners or host organisms, to invade and colonize substrates and form multicellular structures such as fruiting bodies (Brand and Gow 2009; Leeder, Palma-Guerrero et al. 2011).

The probably first observation of chemotropism in fungi was made by Anton de Bary, the father of modern plant pathology who reported that oogonia from certain Phycomycetes can attract the male reproductive organs. In further studies on plant-fungus interactions, he asked whether "the bending of a germ-tube towards the epidermis of its proper host, but not towards any membrane or moist surface, may be brought about by a specific reaction in the parasite, induced by physical or chemical stimuli which may operate through unknown secretions from the host plant" (de Bary 1884).

Parallel studies also reported observations on fungal chemotropism. Pfeffer observed that hyphae of Saprolegnia turned towards nutrient substances and proposed that chemical compounds might determine the direction of fungal growth fungus (Pfeffer 1883). Brefeld postulated that a directional chemical influence could explain the fact that adjacent sporidia of *Ustilaginaceae* conjugate in pairs (Brefeld 1883). Woronin suggested that it is through chemical influence that germ-tubes of *Peziza baccarum* reach the wound of the host plant (Woronin 1888).Thus, these early studies already reported chemotropic growth of fungi towards nutrients, mating partners and host organisms. However, these studies were mostly opinions or byproducts during the course of observations of other phenomena. Moreover, the existence of positive chemotropism in fungi remained controversial. Strange in 1890 questioned positive chemotropism in fungi and speculated that the phenomena described by his colleagues could be rather explained by faster growth of the fungus in the presence of an attractive substance (Strange 1890).

Miyoshi was the first to make chemotropism of fungi the subject of systematic and extensive experimental studies, improving the existing chemotropic assays and scoring methods (Miyoshi 1894). He defined positive and negative chemotropism, respectively, as the deviation of germ tubes from their original direction of growth towards or away from the diffusing substance. Chemical substances were classified into three types: attractive (positive chemotropism), repellent (negative chemotropism) or neutral (no chemotropism). Additionally, he observed that the direction and the extent of turning was concentration-dependent and that the optimal chemotropic response depended on the substance and the fungus. Generally, the concentration that elicited chemotropism was very low for most attractive substances. Among a large list of substances tested, compounds such as ammonium nitrate, sugar, peptone and meat extract were found to act as attractants while acids, bases or alcohols were classified as repellents. Interestingly, certain chemoattractants could turn into repellents at supra-optimal concentrations. In light of these observations, Swingle proposed that copper hydroxide could prevent the germ tubes of pathogenic fungi to enter the host plant through its negative chemotropic action (Swingle 1896).

Massee was the first to focus the research more in depth on the nature of the chemoattractants. He proposed that fungi are attracted to their hosts by specific substances in the cell sap. He distinguished between saprophytes and facultative parasites which were both attracted by saccharose, and obligate pathogens such as *Monilia fructigena* and *Cercospora cucumis,* which were attracted by malic acid and pectate, respectively (Massee 1904). However, except for a few studies, little attention was given to the nature of the chemical factors involved in directed hyphal growth, and most of the work focused on the causes of tropism.

All this body of work served as a basis for postulating the existence of chemotropism in fungi, and for suggesting that fungal pathogens and symbionts can orient hyphal growth towards host stimuli. However, during the subsequent century only very few studies were performed on this topic, and none of them elucidated the nature of the chemoattractants nor the mechanisms underlying the chemotropic response. Indeed, a number of authors still questioned the concept of positive fungal chemotropism. They studies proposed an alternative concept termed "the staling reaction", which states that oriented hyphal growth is determined by negative autotropism away from staling products rather than by positive chemotropism (Fulton 1906; Stadler 1952). Further studies suggested that fungi switch between positive and negative autotropism depending on the concentration of CO_2 or during aging of the germ tubes to mature hyphae (Jaffe 1966; Robinson, Park et al. 1968). These contributions helped to understand the mechanisms of positive and negative autotropism and their importance during colony development (Leeder, Palma-Guerrero et al. 2011).

The modern era in fungal chemotropism

Towards the end of the last century, and thanks to the technological progress, several studies have started to elucidate the nature of the compounds and the mechanisms eliciting directed hyphal growth in fungi (Arkowitz 2009; Leeder, Palma-Guerrero et al. 2011). Sexual development and vegetative hyphal fusion are two phenomena involving positive chemotropic sensing, which were intensively studied in the model organisms *S.*

cerevisiae and *Neurospora crassa*. During sexual development, genetically distinct individuals of opposite sex are chemotropically attracted towards each other by the means of secreted mating type-specific peptides pheromone (Arkowitz 2009). By contrast, during vegetative fusion genetically identical hyphae, often from the same individual, approach each other guided by an unknown chemoattactant signal (Fleissner, Leeder et al. 2009; Leeder, Palma-Guerrero et al. 2011).

Cellular components and pathways involved in chemotropic sensing prior to mating

The Fus3 and Kss1 MAPK pathways

During mating, a- and α-pheromones bind respectively to the Ste3 and Ste2 receptors to activate downstream signaling through a conserved MAPK cascade that leads to cell polarization towards the partner cells. In *S. cerevisiae* and *Schizosaccharomyces pombe*, the molecular link between the pheromone receptor and the induction of hyphal polarization differs between these two yeasts (Merlini, Dudin et al. 2013). In *S. cerevisiae*, the chemotropic response towards the α-pheromone is governed by the Fus3 MAPK and the cell wall integrity cascade (Buehrer and Errede 1997). As explained in section previously, the Fus3 and Kss1 MAPK pathways target the transcription factor Ste12 which regulates genes involved in mating, as well as Far1 which mediates cell-cycle arrest and chemotropism (Valtz, Peter et al. 1995). Far1 associates with Cdc24, the guanine nucleotide exchange factor for Cdc42, and with the G*β* subunit Ste4 to form a chemotropic complex that induces the cytoskeleton orientation in response to the pheromone gradient (Nern and Arkowitz 1998; Nern and Arkowitz 1999). This complex leads to spatial activation of the Rho-type GTPase Cdc42 at pheromone-occupied receptor-enriched sites, promoting actin polymerization and exocytosis (Nern and Arkowitz 1999; Kelley, Dixit et al. 2015). During shmoo formation, Ste4 also recruits the GTPase Rho1, which functions in the cell wall integrity MAPK pathway, to the site of polarized growth (Bar, Ellicott et al. 2003). Phosphorylation of Ste4 before its polarization seems to be involved in the formation of the intracellular signaling gradient (Deflorio, Brett et al. 2013). Active Gα also binds the MAPK Fus3 (Metodiev,

Matheos et al. 2002) which stimulates recruitment of Scp160, an RNA-binding protein that delivers mRNAs involved in polarization and maintaining the mating signal to the shmoo tip (Gelin-Licht, Paliwal et al. 2012). In fission yeast, conjugation exclusively depends on the Mating Pheromone-responsive MAPK Spk1, the orthologue of *S. cerevisiae* Fus3/Kss1 (Neiman, Stevenson et al. 1993).

Orientation of the tip depends on the chemattractant concentration. Segall showed that the direction of orientation of the initial protusion becomes more random at higher pheromone concentrations. Subsequent studies also demonstrated that yeast cells sense spatial gradients with high accuracy at low concentration and when the gradient slope is steep, although cells can sense gradients over a 1000-fold range of concentration (Segall 1993; Paliwal, Iglesias et al. 2007; Moore, Chou et al. 2008). In *S. pombe*, low levels of pheromone stimulate dynamic exploration of the cell periphery by active Cdc42 zones, which recruit the polarization effectors. Subsequently, when the partner cells engage in mating, a single stable zone of activated Cdc42 is established at the site of the protusion formation (Bendezu and Martin 2013). Therefore, spatially and temporally regulated recruitment of polarity proteins appears to be important for reliable and precise gradient tracking during chemotropic hyphal growth.

Cellular components and pathways involved in chemotropic sensing prior to vegetative hyphal fusion

Another type of chemotropic sensing occurs prior to vegetative hyphal fusion (anastomosis), a process that has been studied in detail in *N. crassa*. Anastomosis takes place between genetically identical cells both during colony initiation by means of conidial anastomosis tubes (CATs) and in the mature colony via fusion bridges between hyphae (Read, Goryachev et al. 2011). Prior to fusion, cells alternate between two physiological states of signal sending and receiving to allow recognition and behavioral changes. Such coordinated switching allows the cells to generate transient signal molecule gradients and thus avoid an inadequate responding response to their own external signals. The conserved MAPK MAK-2 (orthologous to the Fus3/Kss1) and soft (SO), a conserved protein whose molecular function is yet unknown, are two key

players in the chemotropic sensing and are recruited alternatively to the plasma membrane region of the two communicating hyphal tips (Read, Goryachev et al. 2011) (Fleissner, Leeder et al. 2009). Interestingly, SO was recently shown to function as a scaffold for the cell wall integrity MAPK pathway in *Sordaria macrospora,* a close relative of *N. crassa* (Teichert, Steffens et al. 2014).

Chemotropic sensing of nutrients and plant signals

Although directed hyphal growth is now a generally accepted phenomenon in fungi, besides the above mentioned studies on mating and vegetative fusion little is known about other types of chemotropism such as growth towards nutrients and host organisms. It has been reported that zoospores of the marine chytrid fungus *Rhizophydium littoreum* show a positive chemotaxis towards distinct sources of nutrients such as sugars, polysaccharides and proteins which was concentration-dependent (Muehlstein, Amon et al. 1988). The oomycte *Achlya bisexualis* has the ability to reorient germ tubes towards a gradient of amino acids or amino acid analogues such as methionine, phenylalanine, glutamate, tyrosine or α-aminoisobutyric acid (Schreurs, Harold et al. 1989). Interestingly, the chemotropic response towards a certain amino acid was not abolished in presence of isotropic concentrations of a different amino acid, suggesting the existence of different hierarchies for recepetor-mediated perception during the chemotropic response. However, the cellular components and the mechanisms ruling the chemotropic sensing towards nutrient are still undeciphered.

Only few studies have addressed the chemotropic response of filamentous pathogens towards plant signals. Both chemotactic and chemotropic responses of the soil-inhabiting plant pathogenic oomycete *Phytophthora cinnamomi* were observed towards roots of avocado seedlings (Zentmyer 1961). Another study reported that *P. sojae* hyphal germlings were chemotropically attracted by daidzein and genistein, two specific host isoflavones (Morris, Bone et al. 1998). In 1981, Cameron *et al.* proposed that chemotactic sensing of roots may mediated by specific fungal receptors, demonstrating that the chemoattractant isovaleraldehyde binds in a specific and saturable manner to zoospores of *P. palmivora* (Cameron and Carlile 1981).

Chemotropic growth was also reported in the fungal pathogen *Cochliobolus sativus* towards barley roots and roots exudates (Jansson, Johansson et al. 1988). This phenomenon was also seen in symbiotic and saprophytic fungi. Germ tubes of *Gigaspora gigantea*, an arbuscular mycorrhizal (AM) fungus, grew through the air and successfully located and contacted roots of bean and corn plants, suggesting that the fungus responds to a volatile chemoattractant released by the roots (Koske 1982). Another AM fungus, *Glomus mosseae*, was able to reorient hyphal growth across a filter membrane towards the roots of the host plant, but not towards non-hosts (Sbrana and Giovannetti 2005). Selective chemotropism was reported for the ectomycorrhizal fungi *Pisolithus tinctorius* and *Paxillus involutus* which grew preferentially towards the root apices of the eucalypt host but not towards culture media. Since both fungi were separeted from the eucalypt host and the culture media with a membrane, it was proposed that chemoattractants are diffusing from root apices (Horan and Chilvers 1990).

In light of these earlier studies, the identification of the host compounds inducing chemotropic growth in fungal pathogens and symbionts, and of the underlying mechanisms such as the fungal receptors and signaling pathways is important to advance our understanding of the early stages of plant-fungus interaction.

Objetivos/Aims

Objetivos

A pesar de la importancia de las cascadas MAPK de hongos en la infección de las plantas, se desconocen las señales de activación y la mayoría de los procesos regulados por estas vías de señalización.

- El primer objetivo de esta tesis era el desarrollo de un método simple y reproducible para determinar el estado de activación de las rutas MAPK Fmk1 y Mpk1.

- El segundo objetivo de esta tesis era la identificación de los compuestos secretados por raíces de tomate que inducen el crecimiento quimiotrópico en *F. oxysporum* y la caracterización del mecanismo de dicha respuesta.

Aims

In spite of the importance of fungal MAPK cascades in plant infection, the activating signals and most of the downstream processes regulated by these signaling pathways remain unknown.

- The first objective of this thesis was to develop a simple and reproducible method for monitoring the activation status of the Fmk1 and Mpk1 MAPK pathways.

- The second objective of this thesis was to identify the compounds secreted by tomato roots that elicit chemotropic growth in *F. oxysporum* and to characterize the mechanisms underlying this response.

Materials and Methods

Fungal and bacterial strains, plant species and plasmids

F. oxysporum and bacterial strains, plant species and plasmids used in this work are listed in the tables below.

Table 4. *F. oxysporum* f. sp. *lycopersici* strains used in this study

Strain	Background	Genotype	Origin and reference
Wild-type (wt)	Wild-type, race 2 isolate 4287 (FGSC 9935)		J. Tello, University of Almeria, Spain
wt-GFP	4287	*Pgpda-GFP*; *HYG*	(Di Pietro, Garcia-MacEira et al. 2001)
*fmk1*Δ	4287	*fmk1::PHLEO*	(Di Pietro, Garcia-MacEira et al. 2001)
*ste12*Δ	4287	*ste12::HYG*	(Rispail and Di Pietro 2009)
msb2Δ	4287	*msb2::HYG*	(Perez-Nadales and Di Pietro 2011)
*msb2*Δ*fmk1*Δ	*fmk1*Δ	*fmk1::PHLEO; msb2::HYG*	(Perez-Nadales and Di Pietro 2011)
*msb2*Δ+*msb2*	*msb2*Δ	*msb2::HYG; msb2,PHLEO*	(Perez-Nadales and Di Pietro 2011)
*sho1*Δ	4287	*sho1::HYG*	(Perez-Nadales and Di Pietro 2015)
*msb2*Δ*sho1*Δ	*msb2*Δ	*msb2::HYG; sho1::PHLEO*	(Perez-Nadales and Di Pietro 2015)
*ste2*Δ	4287	*ste2::HYG*	(Turra, El Ghalid et al. 2015)
*ste2*Δ+ *ste2*	*ste2*Δ	*ste2::HYG; ste2,PHLEO*	(Turra, El Ghalid et al. 2015)
*mpk1*Δ	4287	*mpk1::HYG*	(Turra, El Ghalid et al. 2015)
*mpk1*Δ + *mpk1*	*mpk1*Δ	*mpk1::HYG; mpk1,PHLEO*	(Turra, El Ghalid et al. 2015)

Table 5. Bacterial strains used in this study

Species	Strain	Genotype	Origin
Escherichia coli	DH5α	F– Φ80*lac*ZΔM15 Δ(*lac*ZYA-*arg*F) U169 *rec*A1 *end*A1 *hsd*R17 (rK–, mK+) *pho*A *sup*E44 λ– *thi*-1 *gyr*A96 *rel*A1	Invitrogen
	BL21 (DE3) CodonPlus	F^{-} *dcm*$^{-}$ *omp*T hsdS (r_B^- m_B) gal λ(DE3) Hte[*argU, ileY, leuW,* Cam^r]*ung*$^{-}$*151*	Gift from Prof. Rafael Ariza
	E. coli strains generated in this study and used for heterologous production of class III peroxidases		
	DH5α::pGEM-*TMP2*	DH5α::pGEM-*TMP2,* Ampicillin	This study
	DH5α::pGEM-$TMP2_{R38S,H42E}$	DH5α::pGEM-$TMP2_{R38S,H42E}$, Ampicillin	This study
	DH5α::pGEM-*CEVI-1*	DH5α::pGEM-*CEVI-1,* Ampicillin	This study
	DH5α::pET28a-*TMP2*	DH5α::pET28a-*TMP2,* Kanamycin	This study
	DH5α::pET28a-$TMP2_{R38S,H42E}$	DH5α::pET28a-$TMP2_{R38S,H42E}$, Kanamycin	This study
	DH5α::pET28a-*CEVI-1*	DH5α::pET28a-*CEVI-1,* Kanamycin	This study
	BL21::pET28a-*TMP2*	BL21::pET28a-*TMP2,* Chloramphenicol, Kanamycin	This study
	BL21::pET28a-$TMP2_{R38S,H42E}$	BL21::pET28a-$TMP2_{R38S,H42E}$, Chloramphenicol, Kanamycin	This study
	BL21::pET28a-*CEVI-1*	BL21::pET28a-*CEVI-1,* Chloramphenicol, Kanamycin	This study
	E. coli strains generated in this study and used for VIGS assay		
	DH5α::pGEM-*TMP*	DH5α::pGEM-*TMP,* Ampicillin	This study
	DH5α::pGEM-*CEVI*	DH5α::pGEM-*CEVI,* Ampicillin	This study
	DH5α::pGEM-*CEVI*	DH5α::pGEM-*CEVI,* Ampicillin	This study
	DH5α::pTRV-*RNA2*::*TMP*	DH5α::pTRV-*RNA2*::*TMP,* Kanamycin	This study
	DH5α::pTRV-*RNA2*::*CEVI*	DH5α::pTRV-*RNA2*::*CEVI,*	This study

		Kanamycin	
	DH5α::pTRV-*RNA2*::*AP*	DH5α::pTRV-*RNA2*::*AP,* Kanamycin	This study
Agrobacterium tumefaciens	GV3101::pMP90	Chromosomal background: C58. Marker gene: Rif.Ti. Plasmid: pMP90 (pTiC58DT-DNA). Ti plasmid marker gene: Gentamycin Opine: Nopaline	Gift from Prof. Bart Thomma
	GV3101::pMP90, TRV1	GV3101::pMP90, RNA1, Gentamycin, Kanamycin	Gift from Prof. Bart Thomma
	GV3101::pMP90, TRV2::*GFP*	GV3101::pMP90, RNA2::*GFP*, Gentamycin, Kanamycin	Gift from Prof. Bart Thomma
	A. tumefaciens strains generated in this study and used for VIGS assay		
	GV3101::pMP90, TRV2::*TMP*	GV3101::pMP90,RNA2::*TMP*, Gentamycin, Kanamycin	This study
	GV3101::pMP90, TRV2::*CEVI*	GV3101::pMP90, RNA2::*CEVI*, Gentamycin, Kanamycin	This study
	GV3101::pMP90, TRV2::*AP*	GV3101::pMP90,RNA2::*AP*, Gentamycin, Kanamycin	This study

Table 6. Plant species used in this study

Species	**Cultivars**	**Origin**
Tomato (*Lycopersicon esculentum*)	Monika	/
Wheat (*Triticum aestivum*)	Mexican Creole wheat landraces HGO94 (CWI60550)	Gift from Prof Juan Bautista Alvarez Cabello
Arabidospsis thaliana	Columbia	Gift from Prof. Rafael Ariza

Table 7. Plasmids used in this study

Plasmid	Characteristics	Origin
pGEM®-T	Derived from plasmid pGEM®-5Zf(+), linearized with EcoRV and with a T added in both 3' ends	Promega
pET-28a(+)	Encodes a N-terminal His-tag/thrombin cleavage site/T7-tag sequence and an optional C-terminal His-Tag sequence. pET plasmids are the archetypal expression vectors for *E. coli*.	Novagen
pTRV-*RNA1*	Encodes a 134 and 194 kDa replicase proteins from the tobacco rattle virus (TRV) genomic RNA, 29 kDa movement protein and 16 kDa cysteine-rich protein from subgenomic RNAs. It is placed between duplicated CaMV 35S promoter and nopaline synthase terminator (NOSt) in an Agrobacterium T-DNA vector.	Gift from Prof. Bart Thomma
pTRV-*RNA2*	Encodes the coat protein gene from the TRV genomic RNA and a MCS for cloning the target gene sequences. It is placed between duplicated CaMV 35S promoter and nopaline synthase terminator (NOSt) in an Agrobacterium T-DNA vector.	Gift from Prof. Bart Thomma
pTRV-*RNA2*::*GFP*	Derived from pTRV-*RNA2* and used to silence *GFP* (green fluorescent protein) transcripts in a plant expressing the *GFP* gene. A *GFP* cDNA fragment was cloned into pTRV-*RNA2*	Gift from Prof. Bart Thomma
Plasmids generated in this study and used for the heterologous production of class III peroxidases		
pGEM-*TMP2*	Generated by cloning tomato*TMP2*cDNA (excluding the signal peptide, Uniprot accession number P15004) into pGEM®-T.	This study
pGEM-$TMP2_{R38S,H42E}$	Derived from pGEM-*TMP2*, where *R38S* and *H42E* mutations where introduced by site-directed mutation in *TMP2*. For *R38S* mutation, the first cytosine in nucleotide triplet encoding R38 was substituted by an adenine. For *H42E* mutation, the first cytosine and the third thymine in the nucleotide triplet encoding H42 were both substituted by guanine.	This study
pGEM-*CEVI-1*	Generated by cloning tomato *CEVI-1* cDNA (excluding the signal peptide, Uniprot accession number Q9LWA) into pGEM®-T.	This study
pET28a-*TMP2*	*TMP2* cDNA previously cloned into pGEM®-T (pGEM-*TMP2*) was excised from the latter plasmid using the restriction enzymes *Xho*1 and *Nde*1 and cloned into pET-28a(+) previously digested with the same enzymes.	This study
pET28a-$TMP2_{R38S,H42E}$	$TMP2_{R38S,H42E}$ cDNA previously cloned into pGEM®-	This study

	T (pGEM-*TMP2*$_{R38S,H42E}$) was excised from the latter plasmid using the restriction enzymes *Xho*1 and *Nde*1 and cloned into pET-28a(+) previously digested with the same enzymes.	
pET28a-*CEVI-1*	*CEVI-1* cDNA previously cloned into pGEM®-T (pGEM-*CEVI-1*) was excised from the latter plasmid using the restriction enzymes *Xho*1 and *Nde*1 and cloned into pET-28a(+) previously digested with the same enzymes.	This study
Plasmids generated in this study and used for VIGS assay		
pGEM-*TMP*	Generated by cloning a 307-bp *TMP2* cDNA fragment corresponding to bases 406-692, obtained by PCR amplification from pGEM-*TMP2,* into pGEM®-T.	This study
pGEM-*CEVI*	Generated by cloning a 328-bp *CEVI-1* cDNA fragment corresponding to bases 533-798, obtained by PCR amplification from pGEM-*CEVI-1,* into pGEM®-T.	This study
pGEM-*AP*	Generated by cloning a 388-bp *CEVI-1* cDNA fragment corresponding to bases 130-476, obtained by PCR amplification from pGEM-*CEVI-1*, into pGEM®-T.	This study
pTRV-*RNA2*::*TMP*	pTRV-*RNA2*::*TMP* plasmid was used to silence simulataneously *TMP1* and *TMP2* genes. It was generated by cloning a 307-bp *TMP2* cDNA fragment excised from pGEM-*TMP* using *Eco*RI and *Xho*I restriction enzymes, into the EcoRI-XhoI-cut pTRV2 plasmid.	This study
pTRV-*RNA2*::*CEVI*	pTRV-*RNA2*::*CEVI* plasmid was used to silence the *CEVI-1* gene. It was generated by cloning a 328-bp *CEVI-1* cDNA fragment excised from pGEM-*CEVI* using *Eco*RI and *Xho*I restriction enzymes, into the EcoRI-XhoI-cut pTRV2 plasmid.	This study
pTRV-*RNA2*::*AP*	pTRV-*RNA2*::*AP* plasmid was used to silence simultaneously utmost class III peroxidase genes. It was generated by cloning a 388-bp *CEVI-1* cDNA fragment excised from pGEM-*CEVI* using *Eco*RI and *Xho*I restriction enzymes, into the EcoRI-XhoI-cut pTRV2 plasmid.	This study

Media and culture conditions

Media

All media were prepared with Milli-Rho deionized water (dH_2O) and sterilized either by autoclaving at 120 °C for 20 min or by filtration (0.22 µm pore size, Millipore).

Table 8. Media and buffer solutions used in this work

Media and solutions	Ingredients and preparation (1 L)
Potato Dextrose Broth (PDB) [1]	Boil 200 g of peeled potatoes in 0.6 L of water for 1h. Stir and add 20 g of glucose. Add H_2O to a final volume of 1 L.
Potato Dextrose Agar (PDA) [1]	Dissolve 3.9 % potato dextrose agar (w/v) in 1L H_2O.
Luria Broth (LB) [1]	10 g of tryptone, 5 g of yeast extract and 10 g of sodium chloride. Add H_2O to a final volume of 1 L. Adjust the pH to 7.0.
Luria Agar (LA) [1]	10 g of tryptone, 5 g of yeast extract, 10 g of sodium chloride and 20 g of agar. Add H_2O to a final volume of 1 L. Adjust the pH to 7.0.
Puhalla's minimal medium (MM) [1]	0.5 g $MgSO_4$ x $7H_2O$, 1 g KH_2PO_4, 0.5 g KCl, 2 g $NaNO_3$ and 30 g sucrose. Add 20 g bacto agar for solid medium. After autoclaving add trace elements (200 µl).
Trace elements [2]	0.05 g citric acid, 0.05 g $ZnSO_4$, 0.048 g $FeSO_4$ x $7H_2O$, 0.01 g $Fe(NH_4)SO_4$ x 6 H_2O, 0.0025 g $CuSO_4$ x $5H_2O$, 0.0005 g $MnSO_4$ x H_2O, 0.0005 g HBO_3, 0.0005 g Na_2MoO_4 x $2H_2O$ (Puhalla 1968).
Synthetic medium (SM)[1]	10 g glucose, 10 g tryptone, 1 g yeast extract, 1 g $MgSO_4$ x $7H_2O$, 1.9 g KH_2PO_4, 0.6 g K_2HPO_4 and 20 g bacto agar. Add H_2O to a final volume of 1 L. Adjust pH to 6.0 - 6.4 with KOH.
Buffer TE	2 ml 0.5 M EDTA pH 8.0 and 10 ml 1 M Tris-HCl pH 8.0. Add H_2O to a final volume of 1 L.
Lysis buffer [2]	10 mM Tris-HCl pH 8.0, 2 M NaCl, 10 mM DTT and 1 µl/ml PMSF protease inhibitor.
Buffer A [2]	20 mM Tris-HCl pH 8.0 and 1 mM EDTA pH 8.0.

Folding buffer [2]	50 mM Tris-HCl pH 8.0, 1 mM EDTA pH 8.0, 2 M urea, 5 mM $CaCl_2$, 5 µM bovine hemin, 0.7 mM oxidized glutathione and 100 µM reduced DTT
NaI 6M buffer [2]	900 g NaI and 15.2 g Na_2SO_3. Add H_2O to a final volume of 1 L.
Glass milk solution	100 mg/ml silice powder in 1X PBS.
PBS 1X [1]	8 g NaCl, 0.02 g KCl and 1,44 g Na_2HPO_4. Add H_2O to a final volume of 1 L. Adjust pH to 7.4.
Washing buffer [2]	20 mM Tris pH 7.4, 1 mM EDTA and 100 mM NaCl.
CTAB extraction buffer	12.1 g Trizma base, 7.44 g EDTA, 81.8 g NaCl and 20 g cetyltrimethylammonium bromide. Add H_2O to a final volume of 1 L. Heat to 60 °C to dissolve and adjust pH to 8.0.
STET solution	8 % saccharose (w/v), 0.1% Triton X-100 (v/v), 50 mM EDTA pH 8.0, 50 mM Tris-HCl pH 8.0.
Protein loading buffer (5X)	50 mM Tris-HCl pH 6.8, 8% glycerol (v/v), 1.6 % SDS (w/v), 4% β-mercaptoethanol (v/v) and 0.1 % bromophenol blue.
Separating gel (10%)	1.67 ml 30% acrylamide/Bis, 1.25 ml 1.5 M Tris-HCl pH 8.8, 25 µl 20% SDS, 25 µl 10% ammonium persulfate, 2.5 µl TEMED and 2 ml H_2O.
Staking gel (5%)	0.51 ml 30% acrylamide/Bis, 0.375 ml 1 M Tris-HCl pH 6.8, 15 µl 20% (w/v) SDS, 15 µl 10% ammonium persulfate, 1.5 µl TEMED and 2 ml H_2O.
Electrophoresis running buffer (10X)	30.3 g Tris-base, 144 g glycine and 10 g SDS. Add H_2O to a final volume of 1 L.
Coomassie Blue Staining	2,5 g Coomassie Brilliant Blue R250, 100 ml Glacial acetic acid and 900 ml MetOH:H_2O (1:1; v/v).
Low Destain solution	7% Glacial acetic acid and 5% MetOH:H_2O.
High Destain solution	10% Glacial acetic acid and 50% MetOH:H_2O.

[1] Autoclave sterilized.[2] Filter-sterilized.

Culture conditions

F. oxysporum *growth conditions*

F. oxysporum strains were grown in liquid PDB (Table 8) at 28°C with orbital shaking at 170 rpm. For transformants carrying an antibiotic resistance cassette, appropriate antibiotics (hygromycin B at 55 µg/ml or phleomycin at 5.5 µg/ml) were added to the medium. To collect microconidia, 3 to 5 day-old cultures were filtered through a nylon filter (mesh size 10 µm). Conidia were pelleted by centrifugation at 10000 g for 10 min and resuspended in sterile H_2O. Conidia were counted with a hemocytometer and concentration adjusted with water to the desired density. For long-term storage of the different strains, microconidia from 3 to 4 day-old cultures were collected by filtration as previously described, resuspend in 30% glycerol and stored at -80ºC. These suspensions were used for later inoculation to obtain fresh microconidia (Di Pietro, Garcia-MacEira et al. 2001).

Bacterial growth conditions and transformation

E. coli DH5α and BL21 (DE3) CodonPlus strains were cultured in LB medium (Table 8) (Sambrook 1989) at 37°C using the appropriate antibiotics when necessary (Table 5). *A.tumefaciens* GV3101 strains were cultured in LB medium at 28°C using the appropriate antibiotics when necessary (Table 5).

For preparation of *E. coli* BL21 (DE3) CodonPlus competent cells, cells were streaked on LB plates containing chloramphenicol (34 mg/ml) and grown O.N. at 37°C. A single colony was then inoculated into 10 ml of LB supplemented with chloramphenicol (34 mg/ml) and grown O.N. at 37°C. A 500 µl aliquot of the culture was transferred into 50 ml of LB supplemented with chloramphenicol (34 mg/ml) and grown at 37°C and 200 rpm until OD_{600} reached 0.4. The culture was transferred to a centrifuge bottle, placed on ice for 20 min and centrifuged at 3000 g for 10 min. All the following steps were performed in ice. The supernatant was poured off and the pellet resuspended in 3 ml of cold 0.1 M $CaCl_2$, incubated on ice for 30 min and centrifuged at 3000 g for 10 min. The supernatant was removed and the pellet was further resuspended in 800 µl of cold

0.1M $CaCl_2$ containing 15% glycerol. 100 µl of cells were aliquoted in Ependorff tubes and stored at -80°C.

For transformation of *E. coli*, 1 to 100 ng of plasmidic DNA were added to 100 µl of *E. coli* competent cells. The mixture was incubated on ice for 30 min, placed in a water bath at 42°C for 30 sec and incubated again on ice for 2 min. 250 µl of pre-warmed (37°C) LB was added to the mix and incubated at 37°C for 1h at 200 rpm. For selection of recombinant *E. coli* cells, 20 µl and 200 µl of the transformation reaction were spread onto LA plates containing the appropriate antibiotics and incubated at 37°C O.N.

For preparation of *A. tumefaciens* GV3101 competent cells we used the freeze/thaw method as described in Wang 2006 (Wang 2006). Briefly, 2 ml of LB containing the appropriate antibiotics were inoculated and cells grown O.N. at 28°C with orbital shaking at 200 rpm. The 2 ml culture was then tranferred to a 250 ml flask containing 50 ml of the same medium and incubated again until it reached an OD_{600} between 0.5 and 1. The culture was then chilled on ice. Cells were pelleted by centrifugation at 4°C for 10 min at 10000 g. The supernatant was discarded and the pellet was resuspended in 5 ml of cold 20 mM $CaCl_2$. The centrifugation was repeated, the supernatant was discarded and the cells resuspended in 1 ml of cold 20 mM $CaCl_2$. 100 µl of cells were aliquoted in pre-chilled Ependorff tubes and stored at -80°C.

For transformation of *A. tumefaciens* GV3101, frozen competent cells were retrieved from the freezer and thawed on ice. One µg of plasmid DNA was added to the cells. The cells/DNA mixture was freezed by lowering the tube into liquid nitrogen for 5 min. Then the mixture was thawed for 10 min at RT. Cells were transferred to a culture tube containing 2 ml of LB and incubated for 3h with shaking at 28°C. Cells were then pelleted centrifugation at 4°C for 2 min at 10000 g in a microcentrifuge, then resuspend in 1 ml of LB containing the appropriate antibiotics. Finally 200 µl of cells were spread onto LA plates containing the appropriate antibiotics and incubated at 28°C O.N..

Solanum lycopersicum *growth conditions and treatments*

Tomato seeds were surface sterilized (Lopez-Berges, Rispail et al. 2010), placed in a Petri dish on top of a humidified sterile moist filter paper or planted in moist vermiculite and maintained at 28°C in the dark until the length of the roots reached 1 cm approximately or in a growth chamber (15/9 h light/dark photoperiod, 28°C) for the desired time, respectively.

For *CEVI-1* cDNA amplification, leaves of 2 weeks-old tomato plants were wounded with a sterile scalpel and plants were left in a growth chamber (15/9 h light/dark photoperiod, 28°C) for an incubation period of 55h. Wounded leaves were then collected, flesh-frozen in liquid nitrogen and stored at -80°C until RNA extraction.

For VIGS experiments tomato seeds were surface sterilized as described above, planted in moist vermiculite and maintained in a growth chamber (15/9 h light/dark photoperiod, 28°C) for 2 weeks. Seedlings were then transplanted into soil and agro-inoculated with *A. tumefaciens* strains carrying pTRV1 and pTRV-*RNA2*::*GFP*, pTRV-*RNA2*::*TMP*, pTRV-*RNA2*::*CEVI* or pTRV-*RNA2*::*AP* plasmids as follows. A 5 ml culture of each strain was grown at 28°C for 2 days in the appropriate antibiotic selection medium. Further, the culture was transferred to 50 ml of LB medium containing the appropriate antibiotics, 10 mM MES and 20 µM acetosyringone (induction medium) and grown at 28°C for 2 days (200 rpm). Cell culture concentration was then adjusted to an OD_{600} of 1. *A. tumefaciens* strains containing pTRV1 and pTRV2 derivatives were mixed in a 1:1 ratio. Cultures were then harvested by centrifugation at 10000 g for 10 min, resuspended in infiltration media (10 mM $MgCl_2$, 10mM MES, 200 µM acetosyringone, pH 5.5) and adjusted to an OD_{600} of 0.4- 0.6. Mixed cultures were left at RT for 3h with shaking at 80 rpm. Finally, each infiltration mixture was injected into the abaxial side of tomato leaves with a needless syringe and plants incubated in a growth chamber (15/9 h light/dark photoperiod, 28°C) for 5 weeks (Liu, Schiff et al. 2002).

Molecular methodology

Restriction mapping and subcloning

Restriction mapping and subcloning were carried out according to standard methods (Sambrook 1989) and using the reagents according to the manufacturer's instructions. Cutting sites for restriction enzymes were predicted with NEBcutter V2.0 (Table 10). *E. coli* competent cells were transformed with purified plasmids by the heat shock method described by Hanahan (Hanahan 1985). Restriction enzymes were provided by Roche (Barcelona, Spain). Ligations were carried out using T4 DNA ligase from Roche. DNA fragments were isolated by migration on a 1% agarose gel, excision and elution from the gel. For elution and purification, excised DNA fragments were transferred to a 2 ml Eppendorf tube and incubated with NaI 6M buffer (3V) (Table 8) for 5 min at 55°C. The solution was vortexed until the complete dissolution of agarose. 15 µl of glass milk solution (Table 8) were added and samples were incubated 10 min on ice and vortexed every minute. DNA fragments attached to glass milk were pooled down by 1 min centrifugation at 13000 g. To break the interaction and to recover the purified DNA fragments, the pellet was resuspended in a washing buffer (Table 8) and centrifuged 1 min at 13000 g. The washing step was repeated 3 times. The pellet was then dried by an additional centrifugation step and resuspend in 20 µl H_2O. Samples were incubated for 5 min at 55°C to ensure complete dissolution of the DNA fragments. Supernatant was obtained after a 1 min centrigation step at 13000 g and transferred into a clean Eppendord tube to remove any glass milk residues.

Plasmid DNA isolation from E. coli *and* A. tumefaciens *cell cultures*

Plasmid DNA was extracted from bacterial cells using the CTAB method (Murray and Thompson 1980). A single colony grown O.N. at 37ºC on a LA plate (Table 8) containing the appropriate antibiotics was peaked and grown O.N. in 5 ml LB solution containing the same antibiotics. Two ml culture were transferred into an Eppendorf tube and centrifuged 2 min at 13000 g. The supernatant was removed and other 2 ml of culture were added. Another step of centrifugation was performed and the supernatant removed again. 200 µl of STET solution (Table 8) supplemented with 4 µl of lysozyme

(50 mg/ml) and 4 µl of RNAse (10 mg/ml) were added to the pellet and the mixture was incubated 10 min at RT, transferred in a water-bath at 100ºC for 45 sec. The mixture was further centrifuged 10 min at 13000 g and the pellet removed using a sterile wood stick. 10 µl of CTAB extraction buffer (Table 8) was added to the supernatant to precipitate the DNA and the mixture was left 5 min at RT. After 10 min of centrifugation at 13000 g, the supernatant was removed and 300 µl of 1.2 M NaCl and 750 µl 100% ice-cold ethanol were added. The pellet was vortexed and then centrifuged for 10 min at 13000 g. Finally the precipitate was washed with 70% ethanol, dried and resuspended in 20 µl H_2O. For *A. tumefaciens* plasmid DNA isolation, the following modifications were made to the protocol: *A. tumefaciens* cells were cultured for 2 days at 28ºC and the initial volume of liquid culture used to extract plasmid DNA was of 100 ml. The volumes of all the reagent above mentioned for the extraction of plasmid DNA from *E. coli* cells were therefore multiplied by a factor of 20 folds.

RNA extraction

Approximately 100 mg of frozen mycelium or plant tissues were ground to a fine powder with a mortar and a pestle under liquid nitrogen and transferred to a pre-chilled 2 ml Eppendorf tube. TRIzol Isolation Reagent (Invitrogen) (4V) was added to the tube and the sample vortexed and incubated on ice for 5 min. The supernatant obtained after 10 min centrifugation (12000 g) at 4°C was transferred to a new vial and chloroform (1/5 of TRIzol volume) was added. The mix was gently vortexed for 15 sec. Mix was then incubated 3 min on ice. Three phases were obtained after 20 min centrifugation (12000 g) at 4°C; the upper clean phase with high-quality RNA was taken and transferred to a clean Ependorf tube pre-chilled with 750 µl Isopropanol. The tube was mixed by inversion, incubated on ice for 10 min, then centrifuged 20 min (12000 g) at 4°C to precipate RNA. The pellet was washed with 1 ml of 75 % ethanol (v/v) and centrifuged 5 min at 7500 g at 4°C. The pellet was then air dried for 5-10 min and resuspended in 20-50 µl RNAse free water.

Nucleic acid quantification

DNA and RNA were quantified in a Nanodrop® ND-1000 spectrophotometer at 260nm and 280 nm wavelengths, respectively. In addition, the quality of the DNA and RNA obtained was monitored by electrophoresis in a 0.7% and 1% agarose gel, respectively.

Amplification reactions

Standard PCR

PCR amplifications were performed in a termocycler using the thermostable DNA polymerase of the Roche Expand High Fidelity PCR System. Each reaction contained 300 nM primers, 2.5 mM $MgCl_2$, 0.8 mM of a dNTPs mix and 0.05 U/µl of polymerase. Genomic DNA was added at 20 ng/µl and plasmid DNA at 2 ng/µl final concentration. PCR cycling conditions were: an initial step of denaturation (5 min, 94ºC) followed by 35 cycles of 35 sec at 94ºC, 30 sec at the calculated primer annealing temperature and 35 sec at 72ºC (or 68ºC for templates larger than 3 kb), and a final extension step at 72ºC (or 68ºC) for 10 min. Fusion PCR or overlap extension strategy was used to generate site-directed mutations (Ho, Hunt et al. 1989; Yang, Ukil et al. 2004). Complementary primers in a standard PCR reaction were used to generate two DNA fragments with overlapping ends. These fragments were combined in a subsequent 'fusion' reaction in which the overlapping ends annealed, allowing the 3' overlap of each strand to serve as a primer for the 3' extension of the complementary strand. The resulting fusion product was further amplified by PCR.

Reverse transcriptase PCR

Prior to cDNA synthesis, the RNA was treated with DNaseI (Fermentas). First strand cDNA was synthesized with Moloney murine leukemia virus reverse transcriptase following the instructions of the manufacturer (Invitrogen). Briefly, 1 µg of total RNA was used in a final reaction volume of 20 µl containing 100 pmol of oligodT primers. The mixture was incubated at 70ºC for 10 min to allow RNA denaturation. Next, the tube was transferred to ice and 0.4 mM dNTPs, 1x First Strand Buffer (Invitrogen), 4

U/µl of RNasin® Plus RNase Inhibitor (Promega) and 5 mM dithiothreitol (DTT) were added and the mix was incubated at RT for 10 min. Then, the retrotranscriptase (10 U/µl) was added followed by a 50 min incubation step at 37ºC and a final 15 min incubation step at 70ºC to inactivate the enzyme. Efficacy of reverse transcription was verified by amplifying the cDNAs from the fungal and plant housekeeping genes actin and Efα-1, respectively, in a standard PCR reaction using the primer pairs act-2/act-q6 and Efα-1-1/Efα-1-2, respectively (Table 9).

Real-time quantitative PCR

Quantitative real-time PCR reactions (qRT-PCR) were performed in an iCycler apparatus (BioRad, USA) using iQ SYBR Green Supermix (BioRad, USA), 400 ng cDNA template and 300 nM of each gene-specific primer in a final reaction volume of 15 µl. All primer pairs amplified products of 70-200 bp. The following PCR program was used for all reactions: an initial step of denaturation (5 min, 94°C) followed by 40 cycles of 30 sec at 94°C, 30 sec at 60°C, 30 sec at 72°C, and 20 sec at 80°C for measurement of fluorescence emission. A melting curve program was run for which measurements were made at 0.5°C temperature increments every 5 sec within a range of 55-95°C. Once Ct values were obtained (Ct=number of cycles required for the fluorescent signal to cross the threshold), comparison of multiple samples was performed using relative quantification by the 2-ΔΔCt method (Livak and Schmittgen 2001; Pfaffl 2001). For this, the control fungal strain or plant was chosen as the calibrator and the expression of the target gene in all other fungal strains or plants was expressed as an increase or decrease relative to the calibrator. To determine the relative expression of a target gene in the test sample and calibrator sample, a reference gene (actin for *F. oxysporum* and Efα-1 for plants) was used as the normalizer.

Synthetic oligonucleotides

Oligonucleotides used in amplification and sequencing reactions were designed with the software Oligo 6 (version 6.65; Molecular Biology Insights, Inc. USA, Table 10), analyzing internal stability, duplex and hairpin formation and different physico-chemical parameters (Tm, %G+C, %A+T) in each case. Oligonucleotides were

synthesized by StabVida. Oligonucleotides used in this work are listed in the table below.

Table 9. Oligonucleotides used in this study

Name	**Sequence (5'-3')**
Oligonucleotides used for qRT-PCR analysis of Fmk1-regulated gene candidates	
act-2	GAGGGACCGCTCTCGTCGT
act-q6	GGAGATCCAGACTGCCGCTCAG
FOXG_07921-for (*rnr1*)	TGGACGCTGATGTGCCCCA
FOXG_07921-rev	ATTTCAGTGCACAGGTTGGAG
FOXG_00980-for (*sfp1*)	ACCGTGGTGACAATGCGAAC
FOXG_00980-rev	TATTTCGGGCTGTGTTCGGG
FOXG_05349-for (*tkl2*)	ATGTCTGGCGATCTTCCCGA
FOXG_05349-rev	TAGTCACCGAGACCAGTGGA
FOXG_09346-for (*car2*)	CAAGCCCGATCTTGTTACCC
FOXG_09346-rev	GGCATTGAGCAGACCCTTTC
FOXG_09428-for (*yps1*)	CGGAAAGGAGCCCAACAAGT
FOXG_09428-rev	ACAGACTCTCCCTCCTCGTA
FOXG_00795-for (*ssa4*)	CGGAAAGGAGCCCAACAAGT
FOXG_00795-rev	TCGGACTTCTTGGTGGGGAT
FOXG_08172-for (*htb2*)	CGTCGCTTCTGAGGCTTCC
FOXG_08172-rev	AGAGACGGCGTGCTTGGCA
FOXG_12722-for (*dhh1*)	CCGTCGCATTAACTGGTCGA
FOXG_12722-rev	AGAGACGGCGTGCTTGGCA
FOXG_03730-for (*rpn12*)	CCGTCGCATTAACTGGTCGA
FOXG_03730-rev	TCTCAACGTCAACGCCACCA
FOXG_04438-for (*grr1*)	CAGGTGGAAGATGCTTGCCA
FOXG_04438-rev	AGCCTCTTGATAAAGTCGCGA
Oligonucleotides used for VIGS assay	

TMP1-2_for	CGGGAATTCTATTGCTGCTCGTGATTCCCT
TMP1-2_rev	CGGCTCGAGCAAATCGGAATCAGTTAGCGT
CEVI-1_for	CGGGAATTCAGTTGCCTTGGTTGGAGGTC
CEVI-1_rev	CGGCTCGAGAGTATTCCCATTGTTTCCACCT
Sil-all-perox_for	CGGGAATTCCCGAAATTGTACGTGGTGTCA
Sil-all-perox_rev	CGGCTCGAGAGGCTTTCAAATGGAGTTGGG
Oligonucleotides used for the production of recombinant peroxidases in *E. coli*	
Tap1/2_for	CTCGAGTCACATAGAAGGCACAGAAG
Tap2_for1	CTCTGTTTCTTCCAAATAGAC
Tap1/2_rev	CTCGAGTCACATAGAAGCCACAGAAG
Cevi1_for	CATATGCAATTAAGTGCAACATTTTACG
Cevi1_rev	CTCGAGCTAATCAACTAATTAACCCTCT
Oligonucleotides used for qRT-PCR analyses of peroxidase genes expression in wt and/or VIGS tomato plants (underlined and italic primers are used for VIGS plants and for both wt and VIGS plants, respectively). Bold primers were also used for the production of recombinant peroxidases in *E. coli* and are as well listed in the previous category.	
Tap1_for1	CTTTAATTTGTTTCCTCGATAG
Tap1_rev	TCTATAAATAGCAACACCTGC
Tap2_for1	CTCTGTTTCTTCCAAATAGAC
Tap2_rev	TCATGGCCTCATAAGTATTTC
Cevi1_for (used to monitor *CEVI-1* transcript levels in CEVI-1 silenced plants)	CATATGCAATTAAGTGCAACATTTTACG
Cevi1_rev (used to monitor *CEVI-1* transcript levels in CEVI-1 silenced plants)	CTCGAGCTAATCAACTAATTAACCCTCT
CEVI-1 qRT-PCR-for (used to monitor *CEVI-1* transcript levels in AP silenced plants)	TGCTGGTGCTAAAATTATTCG
CEVI-1 qRT-PCR-rev (used to	CGCAGTTTTAATATCATCCAC

monitor *CEVI-1* transcript levels in AP silenced plants)	
Efα-1-1	TACTGGTGGTTTTGAAGCTGG
Efα-1-2	AACTTCCTTCACGATTTCATCA
Oligonucleotides used for site-directed mutation of *TMP2*	
Tmp2FPCR-for	ATTAGTCTACATTTCGAGGACTGC
Tmp2FPCR-rev	GTCCTCGAAATGTAGACTAATGAG

Protein methods

Ethyl acetate partitioning

An equal volume of ethyl acetate was added to the aqueous root exudate. The mixture was vortexed for 30 sec and centrifuged at 13000 g for 30 min. The upper phase (organic phase) was removed and the lower (inorganic phase) was extracted again. The extraction was repeated 3 times. Pooled ethyl acetate fractions were then concentrated in a centrifugal vacuum concentrator (Speedvac) without heating.

Sodium dodecyl sulfate polyacrylamide gel electrophoresis

The gel cassette was assembled as described by Laemmli (Laemmli 1970). The separating gel was prepared to a final volume of 5 ml as explained in Table 8. The gel solution was transferred to the casting chamber using a 1 ml pipette. A small layer of H_2O was added to the top of the gel prior to polymerization to straighten the upper front of the gel. Once the gel polymerized, the water was removed by soaking it with a filter paper. The staking gel solution was then prepared in a total volume of 3 ml and added above the separating gel. Finally the comb was inserted. Once the separating gel was solidified, the comb was removed carefully. 6 µl of 5x protein sample buffer was added to each protein sample in a final volume of 30 µl (Table 8) and the mix was boiled in a water bath for 10 min before centrifuging it at 13000 g for 1 min.

For electrophorisis, the gel cassette was removed from the casting stand and placed in the electrode assembly with the short plate on the inside. 1x electrophoresis running

buffer (Table 8) was poured into the opening of the casting stand, a protein MW marker and protein samples were slowly added into each well. The electrophoresis tank was connected to the power supply.

For the protein detection, the gel was incubated in Coomassie blue staining (Table 8) O.N. with shaking. The dye solution was removed, the gel was incubated in a high destain solution (Table 8) for 2h then kept in a low destain solution (Table 8) at RT.

Elution of protein bands from SDS-PAGE gels

To elute protein bands from the SDS-PAGE gel, bands were excised from the gel with a scalpel, inserted in an Eppendorf tube containing 150 µl H_2O and grinded using a mixer (IKA I-10 basic ULTRA-TURRAX). Samples were incubated at 4°C O.N., then centrifuged at 13000 g for 5 min. Supernatants were recovered and the centrifugation step was repeated twice. Finally, supernatants were pooled, desalted using a 3 kDa ultrafiltration device (see section 4.4), and resuspended in 50 µl H_2O.

Centrifugal ultrafiltration

For small volumes (up to 5 ml), solvent exchange or desalting steps were performed using a 3kDa MWCO Amicon Ultra-0.5 ml device as recommended by the manufacturers (Millipore). Briefly, the device was placed into a microcentrifugal tube, 500 µl of H_2O were added to the assembled device and centrifuged at 14000 g for 10 min. The water was removed from the centrifuged tube and 500 µl of sample were added to the assemble device. Centrifugation was repeated as previously described. To recover the concentrated solute, the Amicon device was placed upside down in a clean centrifuge tube and spinned at 1000 g for 2 min. The same procedure was used for the 10, 30 and 50 kDa MWCO Amicon Ultra-0.5 devices. In this study, devices were used to fractionate and concentrate protein samples.

Dialysis

Dialysis tubing (Sigma) were cut to desired length, immersed into 1L of 2% sodium bicarbonate/1mM EDTA in a 1L glass beaker, boiled for 10 min and rinsed with H_2O.

Tubings were subsequently immersed into 1L H_2O with 1mM EDTA and boiled for 10 min. After rinsing with water, tubings were immersed into 1L of 50% Ethanol containing 1mM EDTA and stored at 4°C. Tubing were rinsed with H_2O before their use, filled with the sample and immersed in the appropriate dialysis buffer. Samples were routinely dialysed O.N., then the dialysis buffer was exchanged with freshly prepared dialysis buffer and samples dialyzed for additional 24h. The volume of the dialysis buffer used in each step was at least 50-fold greater than the sample volume and dialysis was always performed at 4°C.

Fast protein liquid chromatography

Chromatography was performed on an ÄKTA purifier (GE Healthcare, Chalfont St. Giles, UK) following the manufacture's instructions.

Collection of root exudates

Roots from 2 weeks-old plants (approximately 150 plants) were washed carefully to remove the adhering vermiculite, placed in a 1 L beaker containing 500 ml sterile water and kept at 25ºC for 2 days. The collected root exudates were sterile-filtered through a 0.22-µm Millipore filter (Millipore) and stored at -20°C or lyophilized until use.

To obtain root exudates from plant seedlings, approximately ten seeds were surface sterilized using a 20% hypochlorite solution and left to germinate in a humid chamber for 2 days at 28ºC. When the roots reached 1 cm, seedlings were placed in a glass tube containing 10 ml of sterile water, incubated at 28°C and 170 rpm for two additional days and stored at -20°C or lyophilized until use.

Chemotropism assay

Quantification of directed hyphal growth was performed using a plate assay. It consists in filling a Petri dish with 4 ml of a 0.5% sterile water-agar solution (WA) supplemented with 2.5 x 10^6 spores/ml of the appropriate *F. oxysporum* strain. When

the media is solid, two wells are digged at 0.5 cm from a central line (named scoring line) using a P1000 pipette tip. One of the wells is filled with 40 µl of the chemoattractant compound and the other one is filled with the same volume of a solvent control (Figure 6). Plates are incubated at 28ºC for 13h and the number of germ tubes growing towards and away from the test compound are scored on the central line with an Olympus binocular microscope (200 x magnification). The chemotropic index is calculated as $[(H_{test} - H_{solv}) / H_{total}] \times 100$, where H_{test} is the number of hyphae growing towards the test compound, H_{solv} is the number of hyphae growing towards the solvent control, and H_{total} is the total number of hyphae counted. For each test compound a total of 500 hyphal tips were scored. All experiments were performed at least twice.

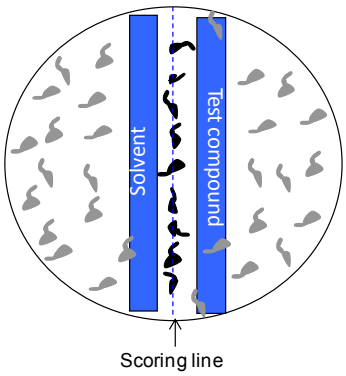

Figure 6. Plate assay for quantitative determination of directed hyphal growth. Schematic representation of the plate used for the chemotropism assay. A Petri dish is filled with 4 ml of 0.5% WA supplemented with 2.5 x 10^6 spores/ml. Test compound and solvent control are applied on either side of the scoring line at a distance of 0.5 mm.

Peroxidase enzymatic activity assays

Qualitative peroxidase assay

To visualize the enzymatic activity of secreted tomato root peroxidases, two weeks-old plants and four-days old seedlings were placed on a Petri dish containing 0.5% WA medium supplemented with 0.91 mM 2,2'-azino-bis(3-ethylbenzothiazoline-6-sulphonic acid (ABTS), 2.5 mM 3,3'-Diaminobenzidine (DAB) or 0.04 % guaiacol (Sigma) and 2.5 mM, 1 mM or 13.4 mM of H_2O_2 (J.T.Baker, Deventer, Holland). WA medium containing DAB was adjusted to pH 7.5. Plates were incubated for 13 h at 28°C and scanned.

To visualise peroxidase enzymatic activity directly on tomato roots, four-days old seedlings were placed in a Petri dish containing 0.5% WA medium supplemented with 0.91 mM ABTS and 2.5 mM H_2O_2, incubated 45 min at 28°C, transferred to a new Petri dish containing 0.5% agarose and imaged with a stereomicroscope (Stereo Lumar. V12 Zeiss).

Quantitative assay in microtiter plates

Peroxidase activity was quantified in 96-well microtiter plates. The reaction mixture contained 0.91 mM ABTS, 2.5 mM H_2O_2 in phosphate-citrate buffer (pH 5.6) and 0.0025 µM of HRP, 100 µl of tomato RE or 100 µl of wheat RE, in a final volume of 150 µl. If applicable, peroxidase inhibitors/scavengers were pre-incubated with the assay solution before the addition of ABTS and H_2O_2. Thiourea (TH), adenine (Ade), salicylhydroxamic acid (SH), sodium azide (NaN_3), sodium orthovanadate (Na_3VO_4) and sodium L-ascorbate (Asc) were used as peroxidase inhibitors at 1 mM. For each reaction, a negative control containing heat-inactivated (20 min boiling) HRP or RE was performed. Reactions were incubated at 28°C and the A_{405} nm was recorded every 30 min using a Spectrafluor Plus microplate reader (Tecan, Crailsheim, Germany). Peroxidase activity was calculated in units per ml, using the formula [(ΔA_{405nm}/min Test - ΔA_{405nm}/min Blank) x (total vol assay in ml) x (dilution factor)] / [(Millimolar extinction coefficient of oxidized ABTS at 405nm) x (vol enzyme used)]. The extinction factor of the oxidized ABTS at 405nm is equal to 36,8.

Generation of oxidized ABTS

Oxidized ABTS was generated by mixing 88 µM horseradish peroxidase (HRP, Sigma) with 20 mM ABTS and 10 mM H_2O_2 as substrates. The reaction was carried out in a final volume of 5 ml and incubation was performed O.N. at 28°C. H_2O_2 was used as limiting substrate. Oxidized ABTS was separated from the HRP enzyme by the use of a 3kDa MWCO Amicon Ultra-0.5 ml device (see section 4.4).

Quantification of *F. oxysporum* germ tubes producing bulged structures

Quantification of the number of *F. oxysporum* germ tubes undergoing the formation of bulged-like structures when growing in a gradient of oxidized ABTS was performed using a standard chemotropism plate assay. A total of 500 germlings was scored using an Olympus binocular microscope (200 x magnification). All experiments were performed at least twice.

H_2O_2 sensitivity assay

To determine H_2O_2 sensitivity, $1x10^6$ microconidia were evenly spread onto the surface of a SM plate (Table 8) and incubated O.N. at 28 °C before adding a filter paper disc imbibed with 5%, 10%, 15% and 20% H_2O_2 solution on top of the plate. Growth inhibition induced by H_2O_2 was determined after 3 days of growth at 28°C by assessing the size of the clear halo surrounding the filter paper disc (Rispail and Di Pietro 2010).

Tomato root infection assay

Tomato seeds were surface sterilized, grown for 2 days in a humid chamber at 28°C or for 1 month in a growth chamber (15/9 h light/dark cycle, 28°C), then transferred to a Petri dish containing a WA solution supplemented with $2.5x10^6$ microconidia/ml or to plastic bottles containing 50 ml dH_20 supplemented with $2.5x10^6$ microconidia/ml of *F. oxysporum*, respectively. In the latter case bottles were maintained in the growth chamber for 6h, 12h, 24h and 48h with shaking (80 rpm). For qRT-PCR experiments 3 plants per treatment were used and each treatment was repeated three times.

Identification of Fmk1-Regulated effector genes

To study the expression profile of putative Fmk1-regulated effector genes, $5x10^8$ freshly obtained microconidia were inoculated into 200 ml of PDB. After 15 h of incubation at 28ºC and 170 rpm, mycelia were harvested, washed twice with sterile minimal medium (Table 8), resuspended in 10 ml of MM, and transferred onto three MM agar plates or MM agar plates supplemented with NH_4NO_3. Plates were incubated for 4 h at 28ºC, mycelia were harvested, frozen in liquid nitrogen and stored at -80°C until RNA extraction (Perez-Nadales and Di Pietro 2011).

Expression and purification of peroxidases from *E. coli*

Cloning of TMP2, $TMP2_{R38S,H42E}$ and CEVI-1 into the pGEM®-T vector plasmid

cDNAs encompassing the entire open reading frame of *TMP2* and *CEVI-1* were RT-PCR amplified from total RNA extracted respectively from roots and wounded leaves of 2 weeks-old tomato plants (see section 2.3.1.), using the primer pairs Tap2_for1/Tap1/2_rev and Cevi1_for1/Cevi1_rev, respectively (Table 9). The obtained amplicons were cloned into the pGEM®-T plasmid (Table 7) and transformed into *E. coli* DH5α competent cells (Table 5).

Generation of $TMP2_{R38S,H42E}$ was performed by site-directed mutagenesis using the PCR fusion method (see section 3.8). First, plasmidic DNA was isolated from an *E. coli* DH5α clone carrying the pGEM-*TMP2* plasmid (Table 7). Second, two PCR amplifications were performed using the primer pairs Tap1/2_for/Tmp2FPCR-rev and Tmp2FPCR-rev/Tap1/2_rev and the pGEM-*TMP2* plasmid as a template (Table 9). The products of both PCR were, in turn, used as templates for a third PCR reaction using the Tap1/2_for and Tap1/2_rev primers. PCR products were further cloned in the pGEM®-T plasmid as mentioned above for *TMP2* and *CEVI-1* cDNAs. Finally, plasmidic DNA was isolated from *E. coli* DH5α transformants carrying the pGEM-$TMP2_{R38S,H42E}$ plasmid and the correctness of the mutations was confirmed by DNA sequencing.

Cloning of TMP2, $TMP2_{R38S,H42E}$ and CEVI-1 into the pET-28a expression vector

Plasmidic DNA was isolated from *E. coli* DH5α clones carrying the pGEM-*TMP2*, pGEM-$TMP2_{R38S,H42E}$ and pGEM-*CEVI-1* plasmids, and *Nde*1 and *Xho*1 digested. *TMP2*, $TMP2_{R38S,H42E}$ and *CEVI-1* fragments were purified by agarose gel electrophoresis and ligated into the *Nde*1 and *Xho*1 digested pET-28a(+) expression vector (Table 7) using the following formula: ng insert = [(ng vector x size insert) / size vector] x 5. pET28a-*TMP2*, pET28a-$TMP2_{R38S,H42E}$ and pET28a-*CEVI-1* ligation constructs were first transformed into *E. coli* DH5α competent cells, then purified and finally transformed into BL21 (DE3) competent cells. Plasmidic DNA extracted from antibiotic resistant clones was analyzed by PCR, restriction enzyme analysis and DNA sequencing.

Heterologous production of TMP2, $TMP2_{R38S,H42E}$ and CEVI-1 proteins in E. coli

A fresh single transformant colony was inoculated into 5 ml of LB containing 30 µg/ml kanamycin and 34 µg/ml chloramphenicol. Cultures were incubated O.N. at 37°C with 200 rpm shaking. The O.N. culture was inoculated into 500 ml of LB medium containing 30 µg/ml kanamycin and 34 µg/ml chloramphenicol and incubated at 37 °C, 200 rpm, until the OD_{600} reached 0.5-0.8. A 2 ml aliquot was taken as a control (without induction), centrifuged at 13000 g for 2 min and the pellet resuspended in 20 µl 1x protein loading buffer to be further analysed by SDS-PAGE gel. Expression of proteins was induced by adding isopropyl-1-thio-β-D-galactopyranoside (IPTG) to 1 mM in the culture followed by an incubation of 8h, 5h and 2h at 23°C, 28°C and 37°C, respectively. After induction, cells were collected by centrifugation at 7800 g for 15 min at 4°C, and the pellet frozen at -80 °C. The stored pellet was thawed and resuspended in 10 ml of sonication buffer (Table 8). Cells were disrupted by sonication and the soluble and insoluble fractions were seprated after centrifugation at 10000 g for 25 min. The expression level of the recombinant proteins in cell extracts, in the soluble and insoluble fractions and purity of protein samples were analyzed by SDS–PAGE

using a 10% polyacrylamide gel (Table 8) (Ponferrada-Marin, Roldan-Arjona et al. 2009).

Extraction of TMP2, TMP2$_{R38S,H42E}$ and CEVI-1 from E. coli *inclusion bodies*

The cell pellet collected by centrifugation after induction with IPTG at 37°C (see section above) was resuspended in lysis buffer (5 ml/g wet pellet, see Table 8) and disrupted by sonication. The lysate was centrifuged at 10000 g for 25 min at 4°C. (Ponferrada-Marin, Roldan-Arjona et al. 2009). The pellet was washed twice with buffer A (20 mM Tris-HCl pH 8.0, 1 mM EDTA), harvested and finally resuspend in 30 ml buffer A (Smith, Santama et al. 1990). To 10 ml of bacterial suspension 20 mg of lysozyme (Sigma), 100 pg of DNase I (Roche), phenylmethanesulfonyl fluoride to 0.5 mM, and EDTA to 10 mM were added. After 30 min on ice, lysed bacteria were sonicated. After centrifugation at 10 000 g for 30 min, the pellet was resuspended in 10 ml of Buffer A containing 2 M urea, homogenized, and re-sedimented at 10 000 g for 30 min. The pellet was washed two further times with Buffer A containing 2 M urea before finally being dissolved in 2 ml of Buffer A containing 8 M urea. The residual pellet was re-sedimented and extracted with a further 2 ml of 8 M urea buffer, centrifuged as above, and the two 8 M urea supernatants pooled (Smith, Santama et al. 1990).

Reduction of disulfide bonds and refolding of TMP2, TMP2$_{R38S,H42E}$ and CEVI-1 proteins

Peroxidases previously solubilized in 8 M urea were reduced by adding 30 mM Dithiothreitol (DTT) and incubating for 1h at 28°C. Then the enzyme solution was transferred into Buffer A containing 6 M urea and 1 mM DTT using 3 kDa MWCO Amicon Ultra-20 ml devices (Millipore). Samples were diluted 10-fold into the folding medium containing 50 mM Tris-HCl pH 8.0, 1 mM EDTA, 2 M urea, 5 mM $CaCl_2$, 5 µM bovine hemin, 0.7 mM oxidized glutathione, 100 µM reduced DTT (Table 8). After 24 h at 22°C, the folding medium was centrifuged (10000 g, 30 min) and soluble

peroxidases dialyzed against two changes of H_20. Precipitated peroxidases were removed by centrifugation, 30 min at 10000 g (Smith, Santama et al. 1990).

Purification of solubilized TMP2, TMP2^{R38S,H42E} and CEVI-1 proteins

Solubilized recombinant proteins were purified by immobilized-metal affinity chromatography (IMAC) using a 1 ml Ni–NTA column (GE Healthcare, Uppsala, Sweden) previously equilibrated with binding buffer (Table 8). After sample injection (500 µl loop), the column was washed with 15 ml of binding buffer and proteins were eluted with a 40 ml linear gradient of elution buffer and collected in 1.5 ml fractions. 20 µl of each fraction was analyzed by SDS-PAGE using a 10% polyacrylamide gel and those containing a single band of the overexpressed protein were pooled (Ponferrada-Marin, Roldan-Arjona et al. 2009). Buffer was exchanged by dialysis to H_2O and concentrated using PEG 35000 (polyethylene glycol). Protein concentrations were determined on the SDS-PAGE gel using the Muti Gauge software (Table 10) using known concentrations of BSA as a reference.

Virus-induced gene silencing

Cloning of the TMP, CEVI-1 and AP PCR amplicons into the pTRV2 vector

Amplification and cloning of *CEVI-1* and *TMP2* cDNA fragments in the pGEM®-T plasmid was explained previously in section 13.1.

pTRV2-*CEVI* plasmid was used to silence the *CEVI-1* gene. It was generated by cloning a 328-bp *CEVI-1* cDNA fragment [corresponding to bases 406-692, and obtained by PCR amplification using the primers CEVI-1_for and CEVI-1_rev (Table 9)] into the EcoRI-XhoI-cut pTRV2 plasmid.

pTRV2-*TMP* plasmid was used to silence both the *TMP1* and *TMP2* genes. It was generated by cloning a 307-bp *TMP2* cDNA fragment [corresponding to bases 533-798,

and obtained by PCR amplification using the primers TMP1-2_for and TMP1-2_rev (Table 9)] into the EcoRI-XhoI-cut pTRV2 plasmid.

pTRV2-*AP* plasmid was used to silence simultaneously utmost class III peroxidase genes.It was generated by cloning a 388-bp*CEVI-1* cDNA fragment (corresponding to bases 533-798, and obtained by PCR amplification using the primers CEVI-1_for and CEVI-1_rev (Table 9)) into the EcoRI-XhoI-cut pTRV2 plasmid.

The VIGS tool software (Table 10) was used to select the best target region of tomato peroxidase genes to be silenced using the VIGS approach. Oligonucleotides used in qRT-PCR to measure the expression level of *TMP1*, *TMP2* and *CEVI-1* genes were designed outside the region targeted by the silencing constructs to ensure the quantification of plant gene transcripts only (Table 10).

Microscopy

Light and fluorescence microscopy low-resolution imaging was performed with a SteReo Lumar.V12 fluorescence stereomicroscope (Zeiss). Wide-field fluorescence imaging was performed with a Leica DMR epifluorescence microscope or a Zeiss Axio Imager M2 microscope equipped with a Photometrics Evolve EMCCD camera, using the 63X oil objective. To visualise colonization of tomato roots by *F. oxysporum*, tomato seeds were germinated in a humid chamber (see section 2.3.1), transferred 1 day to water-agar containing 2.5 x 10^6 microconidia/ml of the *F. oxysporum* wt-GFP strain (Di Pietro, Garcia-MacEira et al. 2001) and incubated at 28°C for 2 days before microscopic examination. For the visualization of morphological changes occurring in *F. oxysporum* germ tubes when grown in presence of oxidized ABTS, 0.5 % water-agarose containing 2.5 x 10^6 microconidia/ml of the *F. oxysporum* wt strain were incubated 13h in presence of a gradient of oxidized ABTS as in a chemotropism plate assay. Different concentrations of oxidized ABTS from 8 µM to 1.5 mM were used.

Bioinformatic prediction and phylogenetic analysis

Genomic and protein sequences retrieval

The genomic sequences of *tkl2*, *ssa4*, *htb2*, *dhh1*, *car2*, *rpn12*, *grr1*, *rnr1*, *sfp1* and *yps1* were retrieved from the *Saccharomyces* Genome Database (SGD) (http://www.yeastgenome.org/). Sequences of their *F. oxysporum* orthologues and of the *fpr1* gene were obtained from the Fusarium Comparative database (www.broadinstitute.org). Gene and protein sequences of TMP1, TMP2 and CEVI-1 were retrieved from the NCBI genome Database and the UniProt Knowledgebase, respectively (Table 10). Protein alignment was performed using BioEdit and the presence of a signal peptide was determined with SignalP-4.1 using a standardized threshold value of 0.5 (Table 10).

Identification, sequence analysis and mapping of S. lycopersicum *peroxidase genes.*

Seventy protein sequences of tomato class III peroxidases were retrieved from the Peroxibase (Table 10). Among them, 33 sequences were completely annotated and 41 were partially annotated. The full-length sequences of the truncated proteins were obtained by screening the tomato plant protein database [Sol Genomics Network Database; ITAG Release 2.3 predicted proteins (SL2.40)]. For each sequence, the outputs generating an E. value = 0 were selected. Then the mRNA sequences, the protein sequences and the coordinates of the genes on the chromosomes were retrieved. Of the 41 initially partially annotated sequences, 36 full sequences were obtained, however the remaining five (P33, P41, P43, P51 and P52) remained incomplete. The full-length protein sequences of P33, P41, P43, P51 were obtained by screening the nucleotide collection database (nr/nt) from NCBI using the incomplete mRNA sequences. The output sequence generating 100% of identity with the incomplete mRNA sequences was chosen and its protein sequence was used for further analysis. The protein sequence P52 remained incomplete since unretrivable from any of the three databases used.

Phylogeny.fr web service was used to make an alignment of the deduced amino acid sequences and to build a phylogenetic tree.

Softwares and online tools

Data management and processing was performed using softwares and online programs listed in Table 10.

Table 10. Softwares and online programs used in this study.

Program	Application
Office software	
Microsoft Office	Word: Word processing PowerPoint: Image presentation and processing Excel: Data processing
Adobe Photoshop	Elements/images processing
Adobe Illustrator	Elements/images processing
Image J	Elements/images processing
BioEdit	Multiple sequence alignment
LaserGene (DNA-Star)	Sequence editor
Oligo 6	Synthetic oligonucleotides design
Kodak 1D Image Analysis	Edition and analysis of DNA and RNA gel
Espson Scan	Image scanning
Bio-Rad iQ5	Obtaining and analysis of real time RT-PCR data
Endnote	Reference and bibliography editing
Carl Zeiss Vision (AxioVision 4.7)	Imaging and image analysis
AxioVision	Edition and analysis of binocular and microscope images
UNICORN	Control every stage of your purification process on ÄKTA systems

Multi Gauge	Protein quantification software
Online program	
NCBI http://www.ncbi.nlm.nih.gov/	BLAST: Sequence alignment Genome Database: Retrieval of gene and protein sequences
Clustal Omega http://www.ebi.ac.uk/Tools/msa/clustalo/	Multiple sequence alignment
Phylogeny http://www.phylogeny.fr	Obtaining phylogeny tree
Peroxibase www.peroxibase.toulouse.inra.fr	Retrieval of classIII peroxidase protein sequences from tomato and *Arabidopsis thaliana*.
Solgenomics Network Database http://solgenomics.net/	Retrieval of tomato classIII peroxidase gene and protein sequences.
SignalP-4.1 http://www.cbs.dtu.dk/services/SignalP/	Prediction of signal peptides
UniProt Knowledgebase www. uniprot.org	Retrieval of protein sequences
NEBcutter V2.0 nc2.neb.com/NEBcutter2/	Find cutting sites for restriction enzymes
http://vigs.solgenomics.net/	Find the best target region for VIGS

Results

1. Identification of the genes regulated by the Fmk1 MAPK pathway

To date, Western blot analysis with phospho-specific antibodies is used to detect the state of phosphorylation of the Fmk1 MAPK. Although very informative, this technique is laborious and expensive, and therefore difficult to be used routinely (Perez-Nadales and Di Pietro 2014).

Other methods used to quantify activation of the Fmk1 cascade are based on phenotypic characterization of knock-out mutant strains. These include the capacity for plant and fruit infection, root adhesion and cellophane penetration assays, where *fmk1Δ* mutants, but not *mpk1Δ* or *hog1Δ* mutants show clear phenotypes compared to the wt strain (Di Pietro, Garcia-MacEira et al. 2001; Prados Rosales and Di Pietro 2008). However, despite providing valuable insights on pathway function, phenotyic observation remains a qualitative and time-consuming method that cannot be used in high throughput functional screens.

In this section, our purpose was to develop a simple and reproducible method to measure activation of the Fmk1 pathway and to identify genes acting downstream of this cascade. Our approach consisted in using quantitative real time PCR to validate candidate genes, which are differentially expressed between Fmk1 MAPK cascade mutants and the wt strain (Figure 7).

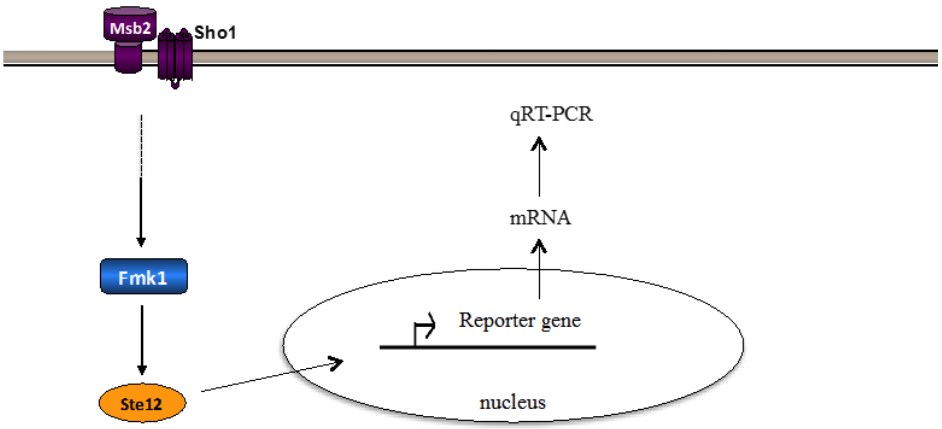

Figure 7. Use of downstream genes as readouts of the Fmk1 pathway. Transcript levels of downstream genes are measured by qRT-PCR in mutant strains of the Fmk1 cascade and compared to those of the wt strain.

1.1. Selection of candidate genes putatively regulated by the Fmk1 MAPK pathway

Downstream genes regulated by the Kss1 pathway in *S. cerevisiae* are well-characterized. We took advantage of two studies where an exhaustive list of genes downregulated in mutants of the Kss1 pathway was reported (Madhani, Galitski et al. 1999; Prinz, Avila-Campillo et al. 2004). Predicted gene orthologs in *F. oxysporum* were identified by searching the Fusarium Comparative Database (www.broadinstitue.org). Among a hundred analyzed genes, nine were selected based on two criteria: (1) percentage of identity between *S. cerevisiae* and *F. oxysporum* gene greater than or equal to 30%; (2) blast search with the *S. cerevisiae* genomic sequence in the *F. oxysporum* database gives only one significant hit. The selected genes are listed in Table 11.

Table 11. Selected *S. cerevisiae* genes regulated by the kss1 pathway and respective *F. oxysporum* orthologs.

Standard name in *S. cerevisiae*	Function in *S. cerevisiae*	Ortholog in *F. oxysporum*	Identity (%)	Function in *F. oxysporum*
TKL2 [1]	Transketolase	FOXG_05349.3	65%	Transketolase
SSA4 [1]	Stress-Seventy subfamily A	FOXG_00795.3	62%	Hsp70-like protein
HTB2 [1]	Histone H2B	FOXG_08172.3	70%	Histone H2B
DHH1 [1]	DEAD box Helicase Homolog	FOXG_12722.3	67%	ATP-dependant RNA helicase DHH1
CAR2 [1]	Catabolism of Arginine	FOXG_09346.3	64%	Ornithine aminotransferase
RPN12 [2]	Regulatory Particle Non-ATPase	FOXG_03730.3	33%	26S proteasome regulatory particle subunit N12
GRR1 [2]	Glucose Repression-Resistant	FOXG_04438.3	37%	F-box and leucine-rich repeat protein GRR1
RNR1 [1]	Ribonucleotide reductase	FOXG_07921.3	65%	Hypothetical protein with domains found in ribonucleotide reductases
SFP1 [1]	Split finger protein	FOXG_00980.3	66%	Hypothetical protein (no protein domain found)
YPS1 [1]	YaPSin family of protease	FOXG_09428.3	30%	Hypothetical protein with an eukaryotic aspartyl protease domain

TKL2 encodes a transketalose whose activity is necessary for the biosynthesis of the aromatic amino acids. *SSA4* encodes a chaperone protein of the SSA subfamily of cytosolic Hsp70 proteins. SSA4 is a cytoplasmic protein that concentrates in the nucleus upon starvation. *HTB2* encodes the histone H2B, the core histone protein required for chromatin assembly and chromosome function. The gene exists in several copies in the genome. *DHH1* encodes a highly conserved DEAD-box RNA helicase that associates with components of RNA decapping, deadenylation and transcription complexes. *CAR2* encodes an L-ornithine transaminase, which catalyzes the second step of arginine degradation. *RNP12* encodes a subunit of the 19S regulatory particle of the 26S proteasome lid. *GRR1* encodes an F-box protein of an SCF ubiquitin-ligase complex, a central component of the glucose signal transduction mechanism. It is also required for degradation of the G1 cyclins Cln1 and Cln2, providing a mechanism for coupling nutrient availability to gene expression and cell cycle regulation. *RNR1* encodes the regulatory subunit of the ribonuleotide reductase, whose activity is essential for the progression through the cell cycle by catalyzing the rate-limiting step for the production of deoxyribonucleotides needed for DNA synthesis. *SFP1* encodes a unique member of the Cys2His2 zinc-finger family of DNA-binding proteins. Finally,

YPS1 encodes an aspartic protease of the yapsin family, involved in nutrient limitation-induced cleavage of the signaling mucin Msb2p, resulting in the activation of the filamentous growth MAPK pathway (Vadaie, Dionne et al. 2008).

We used the qRT-PCR to measure the transcript levels of the candidate genes in *F. oxysporum* wt and *fmk1*Δ mutant strains. The *fpr1* gene encoding a secreted PR1-like protein with an SCP-PR-1-like domain was included in our analysis as a positive control, since previous work demonstrated that its expression was reduced in the *fmk1*Δ, *msb2*Δ and *fmk1*Δ/*msb2*Δ mutants (Perez-Nadales and Di Pietro 2011; Prados-Rosales, Roldan-Rodriguez et al. 2012). Unexpectedly, besides *fpr1*, none of the selected genes was down-regulated in the *fmk1*Δ mutant (Figure 8). *CAR2* and *GRR1* were overexpressed in the *msb2*Δ and *fmk1*Δ mutants in comparison to the wt strain.

Previous work showed that Msb2 is required for transient phosphorylation of Fmk1 upon transfer to plates with sodium nitrate as the nitrogen source (Perez-Nadales and Di Pietro 2011). We therefore analysed the expression level of seven candidate genes (*rnr1*, *sfp1*, *tkl2*, *yps1*, *ssa4* and *car2*) in the *msb2*Δ mutant under the conditions described previously. All genes showed a similar expression profile in the *msb2*Δ and the *fmk1*Δ mutants suggesting that Msb2 and Fmk1 act in the same pathway to regulate the expression of the selected genes (Figure 8).

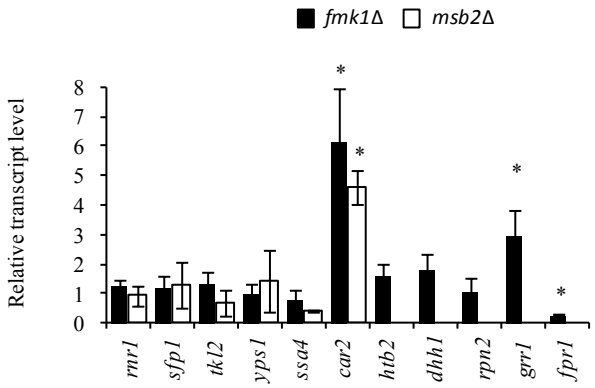

Figure 8. Expression levels of different candidate genes in the *fmk1*Δ and *msb2*Δ mutants. Transcript levels of the indicated candidate genes were measured by qRT-PCR in the wt strain and the *fmk1*Δ and *msb2*Δ mutants 4 hours after transfer to MM plates containing $NaNO_3$ as nitrogen source. Relative transcript levels represent mean cycle threshold values normalized to actin gene transcript level and expressed relative to those of the wt strain. Data shown are from two independent experiments with at least two technical replicates each. Error bars, s.e.m. $P < 0.02$.

1.2. *Fpr1* transcript levels are regulated by both the Fmk1 and the Mpk1 pathways

To test whether the *fpr1* gene is specifically regulated by the Fmk1 MAPK pathway or also by other MAPK pathways, transcript levels were determined in different Fmk1 and Mpk1 pathway mutants. The gene knock-out strains used were *msb2*Δ, *sho1*Δ, *fmk1*Δ, *ste12*Δ, *msb2*Δ*sho1*Δ, *msb2*Δ*fmk1*Δ and *ste2*Δ and *mpk1*Δ, whose genes code for components of the Fmk1 and Mpk1 pathway, respectively. Additionally, we used the *fmk1*Δ*mpk1*Δ double mutant, which is impaired in both MAPK cascades.

When transcript levels of *fpr1* were compared between the wt strain and the mutants under nitrogen-limiting conditions (sodium nitrate), a significant down-regulation was observed in the *msb2*Δ (11 times), *fmk1*Δ (13 times), *ste12*Δ (16 times), *msb2*Δ*sho1*Δ (16 times) and *msb2*Δ*fmk1*Δ (24 times) mutants (Figure 9). A slighter and not statistically significant reduction was observed for *sho1*Δ (6 times), *ste2*Δ (4 times) and *mpk1*Δ (3 times) mutants. A drastic reduction in *fpr1* expression was observed in the double mutant *fmk1*Δ*mpk1*Δ (approximately 40 times). These results demonstrate that the expression of *fpr1* is positively regulated by Msb2, Fmk1 and Ste12, while Sho1, Ste2 and Mpk1 play a minor role. Interestingly, deletion of both Fmk1 and Mpk1 lead to a more drastic phenotype than that of the single mutants, confirming that Mpk1partially contributes to activation of *fpr1*expression.

It was previously reported that fungal pathogens fail to undergo invasive growth in the presence of rich nitrogen sources such as ammonium since the genes related to this process are down-regulated (Madhani, Galitski et al. 1999). To understand whether nitrogen sources have an impact on *fpr1* expression, we measured its expression in presence of ammonium. *Fpr1* transcript levels in the wt strain were three times lower in the presence of ammonium compared to nitrate (Figure 9). In the *msb2*Δ, *fmk1*Δ and *msb2*Δ*fmk1*Δ mutants, an 11-, 12- and 9-fold reduction in *fpr1*expression, respectively, was observed in relation to the wt. No reduction was detected in *sho1*Δ and in *ste12*Δ, while a 5- to 6-fold reduction was observed in the double *msb2*Δ*sho1*Δ and *fmk1*Δ*mpk1*Δ mutants. No reduction in *fpr1* expression was observed for *ste2*Δ and *mpk1*Δ mutants suggesting that *fpr1* regulation is independent of Ste2 and Mpk1 under rich nitrogen conditions, further supported by the finding that the *fmk1*Δ*mpk1*Δ mutant showed a level of reduction similar to the one observed in the *fmk1*Δmutant (Figure 9).

In view of these results, we conclude that both Fmk1 and Mpk1 pathways contribute positively to the expression of *fpr1* in the presence of invasive growth-inducing conditions (sodium nitrate). However, *fpr1* expression is independent of the Mpk1 pathway in penetration-repressive conditions (ammonium nitrate).

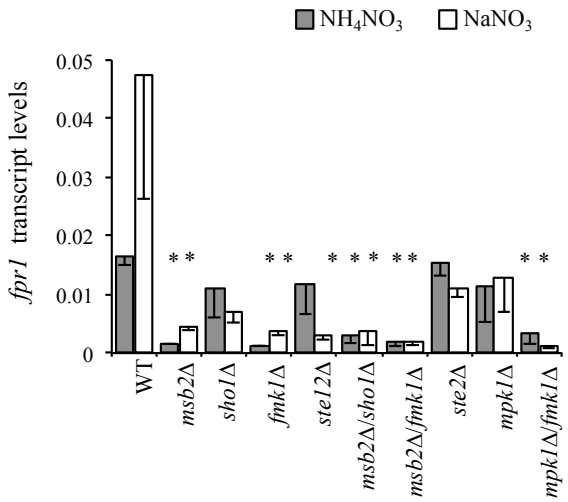

Figure 9. *Fpr1* expression depends both on the Fmk1 and the Mpk1 pathway. Transcript levels of *fpr1* were measured by qRT-PCR in the wt strain and in the *msb2*Δ, *sho1*Δ, *fmk1*Δ, *ste12*Δ, *ste2*Δ, *mpk1*Δ, *msb2*Δ/*sho1*Δ, *msb2*Δ/*fmk1*Δ and *mpk1*Δ/*fmk1*Δ mutant strains 4 hours after transfer to MM plates supplemented either with $NaNO_3$ (white bars) or NH_4NO_3 (grey bars). Relative transcript levels represent mean cycle threshold values normalized to actin transcript levels. Data shown are from two independent experiments with at least two technical replicates each. Error bars, s.e.m. *, $P < 0.05$, versus wt.

2. Identification of the compounds secreted from tomato roots that elicit chemotropic growth in *F. oxysporum*

Evidence for directed hyphal growth during infection of *F. oxysporum* - Previous studies suggested that *F. oxysporum* penetrates tomato roots by growing towards natural openings at the junction of epidermal cells (Perez-Nadales and Di Pietro 2011), indicating that it might be chemotropically attracted by substances secreted from tomato roots (Figure 10A). In order to identify the chemoattractant compound(s) and the underlying mechanisms, a quantitative plate assay was developed in our laboratory that allows to measure directed hyphal growth of *F. oxysporum* towards a chemical gradient (Turrà, El Ghalid et al. 2015). In this experimental setup, positive chemotropism results in a higher number of germ tubes pointing towards the chemoattractant than towards the solvent control (Figure 10B).

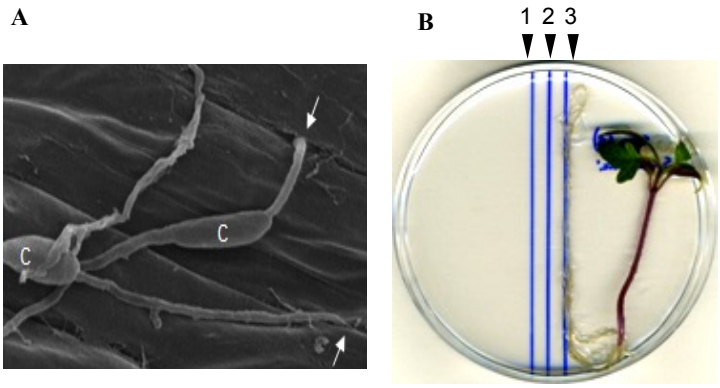

Figure 10. Directed growth of *F. oxysporum* towards tomato roots. A. Scanning electron microscopy analysis of tomato roots, 24 h after inoculation with microconidia of *F. oxysporum*. Fungal hyphae enter the root through natural openings at intercellular junctions. Arrows point to penetration events. c, conidium (Perez-Nadales and Di Pietro 2011). **B.** Chemotropism plate assay for measuring directed growth of *F. oxysporum* germ tubes towards tomato roots. Microconidia are spread evenly on the plate, and a tomato root (or root exudate), or water (solvent control) are applied at 5 mm distance from the central scoring line. 1, solvent application line; 2, scoring line; 3, compound application line. After 14 h the direction of individual germ tubes is determined along the scoring line (Turrà, El Ghalid et al. 2015).

Using this plate assay, it was previously shown that *F. oxysporum* can redirect hyphal growth rapidly and specifically towards gradients of different chemoattractants, including sugars, amino acids, mating pheromones or tomato root exudate (Turrà, El Ghalid et al. 2015). The chemotropic sensitivity differed depending on the compound tested. For example, a concentration of 378 µM was sufficient to trigger a maximum chemotropic response towards α-pheromone, whereas a 1000-fold higher concentration was required for chemoattraction by glutamate. Furthermore, not all carbon or nitrogen sources induced chemotropic response. Whereas glutamate, aspartate, glucose, cellulose and pectin elicited a positive response, glutamine, methionine, ammonium, galactose or glycerol did not (Turrà, El Ghalid et al. 2015). All compounds tested exhibited a bell-shaped dose-response curve with a peak and a gradual decrease at higher concentrations, indicative of receptor saturation (Figure 11).

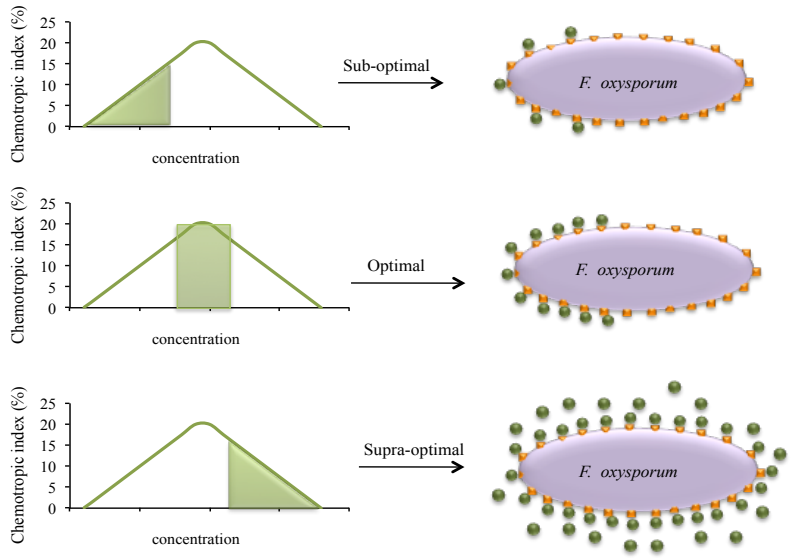

Figure 11. Chemotropic response to increasing concentrations of a chemoattractant. A. A sub-optimal dose of chemoattractant binds only a minor fraction of the putative cell receptor, resulting in weak downstream signaling and chemotropism. **B.** An optimal chemoattractant concentration binds to most of the receptors located on the proximal side of the cell, causing maximal activation of the signaling pathway and chemotropism. **C.** Supra-optimal concentrations of chemoattractants lead to saturation of all the receptors resulting in loss of directional signaling and chemotropism. Green

circles and orange squares represent the chemoattractant and cell receptor, respectively.

Differential role of MAPK signaling cascades in chemotropic sensing - The use of different *F. oxysporum* deletion mutants demonstrated that chemotropism towards different types of compounds is governed by distinct signaling pathways (Turrà, El Ghalid et al. 2015). Chemotropic response to nutrient sources such as sugars or amino acids requires the Fmk1 MAPK module Ste11-Ste7-Fmk1-Ste12. The upstream sensors acting in this pathway are currently unknown. By contrast, sensing of *F. oxysporum* α-pheromone or tomato root signals is mediated by the cell wall integrity MAPK cascade module Rho1-Bck1-Mkk2-Mpk1 and the α-pheromone receptor Ste2 (Figure 12). Interestingly, the *F. oxysporum ste2Δ* mutants showed a reduction in virulence on tomato plants, indicating that chemotropic sensing of root compounds is important for the infection process.

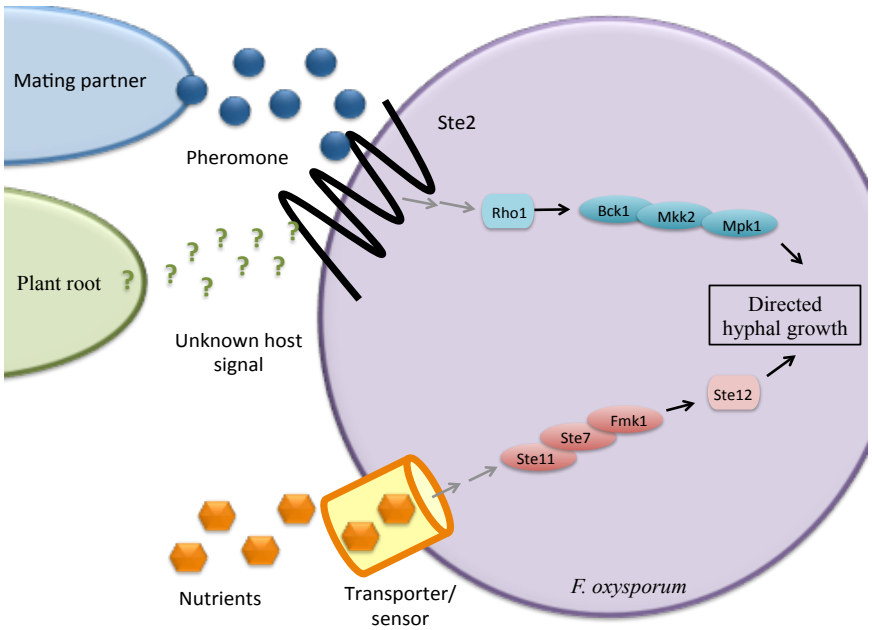

Figure 12. Perception of different classes of chemoattractants in *F. oxysporum*. Directed growth towards a gradient of nutrients is mediated by the invasive growth MAPK module composed by the MAPKKK Ste11, the MAPKK Ste7, the MAPK Fmk1 and the homeodomain transcription factor Ste12, via an unknown sensing mechanism. By contrast, chemotropism towards peptide mating pheromones or plant root signals is governed by the cell wall integrity MAPK module composed of Rho1, Bck1, Mkk2 and Mpk1, and requires the

seven-pass transmembrane protein Ste2 (Turra and Di Pietro 2015; Turrà, El Ghalid et al. 2015).

Here we set out to identify the chemoattractants secreted by tomato roots that elicit directed hyphal growth in *F. oxysporum* and to identify the underlying mechanims.

2.1. Selection of candidate genes putatively regulated by the Fmk1 MAPK pathway

To investigate the nature of the compounds secreted by tomato roots that trigger chemotropism in *F. oxysporum,* we performed chemotropic plate assays with different root exudate fractions. Throughout these assays the *ste12*Δ strain was used, since previous work demonstrated that the Fmk1-Ste12 pathway is specifically required for the chemotropic response to nutrients, but dispensable for directed growth towards tomato roots. The use of the *ste12*Δ mutant strain in chemotropic assays allowed us to avoid possible collateral effects due to the release of nutrients (sugars, amino acids) from dead or wounded plant cells. Root exudates obtained from 2 weeks-old tomato plants elicited a robust chemotropic reponse (chemotropic index 16,71%) (Figure 13A). The response was abolished after root exudate treatment with proteinase K (-0,56%) or boiling (-0,52%), suggesting that the chemoattractants are proteins. When, root exudates were fractionated by ethyl acetate partitioning, the chemotropic response towards the water fraction (WF) was significantly (13,84%) whereas it was null towards the ethyl acetate fraction (EAF) (Figure 13A). To determine the molecular size of the chemoattractant compound(s), the water fraction (WF) was further partitioned into three fractions by centrifugal ultrafiltration: (1) <30 kDa, (2) 30-50 kDa, and (3) >50 kDa. While the <30 kDa and the >50 kDafractions did not elicit significant chemotropic activity, the 30-50 kDa fraction induced a robust chemotropic response (12,66 %) (Figure 13B). Collectively, these results suggested that the chemotropic activity of tomato root exudate resides predominantly in the molecular weight fraction between 30 and 50 kDa and originates from one or several proteins.

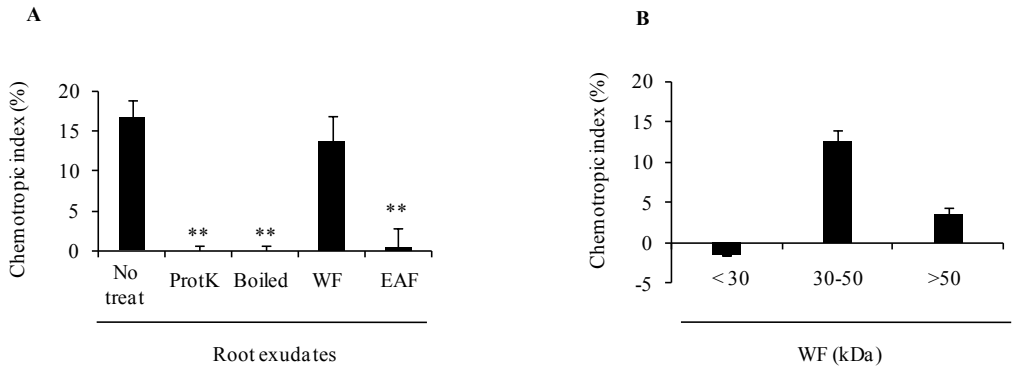

Figure 13. Secreted root chemoattractants are relatively large proteins. A. Chemotropic growth of germ tubes of the *F. oxysporum ste12*Δ strain towards a gradient of tomato root exudate either untreated (no treat); treated with 1 mg/ml proteinase K for 30 min at 37ºC (ProtK); heat treated (10 min at 100ºC, boiled); extracted to obtain an ethyl acetate fraction (EAF) and a water fraction (WF), (**, $P < 0.0001$, versus no treat). **B.** Chemotropic growth of germ tubes of the *F. oxysporum ste12*Δ strain towards the WF separated by centrifugal ultra-filtration (MWCO 30 and 50 kDa) in fractions <30 kDa, 30-50 kDa, and >50 kDa. Mean values were calculated from two independent experiments, each with 500 germlings scored.

2.2. Purification of chemoattractant proteins fronm tomato root exudate

The 30-50 kDa WF was fractionated by Fast Protein Liquid Chromatography (FPLC) using an anion exchange column. On the resulting chromatogram, eight protein peaks (A280 nm) were distinguished (Figure 14A). Three peaks corresponded to the flowthrough (FT), while the other five were retained and eluted at different times from the column. After elution, each peak was brought to its initial volume and tested for the ability to elicit chemotropism. Peaks P1 through P4, but not P5, triggered a significant chemotropic response (Figure 14B).

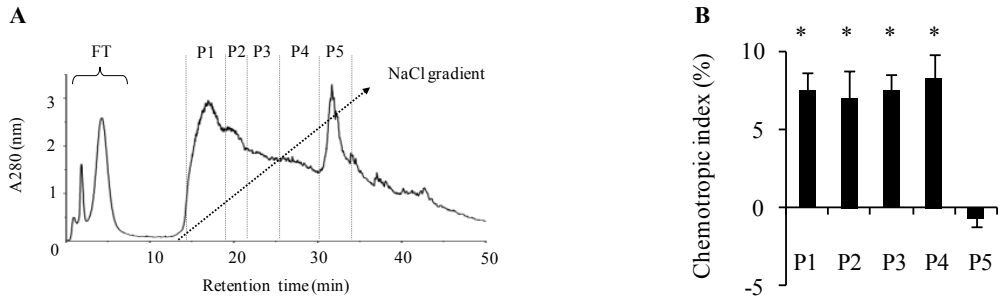

Figure 14. Purification of chemoattractant compounds from the 30-50 kDa WF of tomato root exudate. A. Anion exchange chromatography elution profile of the 30-50 kDa WF. Five hundred µl of the 30-50 kDa WF were applied onto a pre-equilibrated anion-exchange chromatography column washed with 10 ml of 20 mM Tris-HCl buffer pH 8.0. The fraction was then eluted using 40 ml of 0-1M NaCl linear gradient with a flow rate of 1 ml/min. Absorption was monitored at 280 nm. Fractions corresponding to individual peaks (separated with dotted lines) were pooled and named P1 through P5. **B.** Chemotropic growth of germ tubes of the *ste12*Δ strain towards the different fractions, desalted by centrifugal ultra-filtration (MWCO 3 kDa) and reconstituted to the initial volume (500 µl) with water. Mean values were calculated from two independent experiments, each with 500 germlings scored. Error bars, s.d. (*, $P < 0.0001$, versus H_2O).

Next, the proteins in the biologically active fractions P1, P2, P3, P4 and P5 were further separated by sodium dodecyl sulfate polyacrylamide gel electrophoresis (SDS-PAGE) under mildly denaturing conditions (2 min at 100°C). To obtain the minimum amount of protein required for detection in a SDS-PAGE-Coomassie-stained gel, 22 rounds of FPLC were performed as previously described. Fractions from each run corresponding to the same peak were pooled. Moreover, P3 and P4 were joined since no differential chromatographic peaks were detected between these two sets of fractions (Figure 15A), and the resulting fraction was called P3/4. Separation by SDS-PAGE identified five protein bands (named B1 through B5) that were present in the biologically active fractions P1, P2 and P3/4, but absent from the inactive fraction P5 (Figure 15B). When bands B1 through B5 were excised, eluted from the gel and tested in the chemotropic plate assay, only B2 and B3 elicited a positive chemotropic response (Figure 17B). B2 was 4.5 times more active than B3 and produced a very high chemotropic response (29,61%).

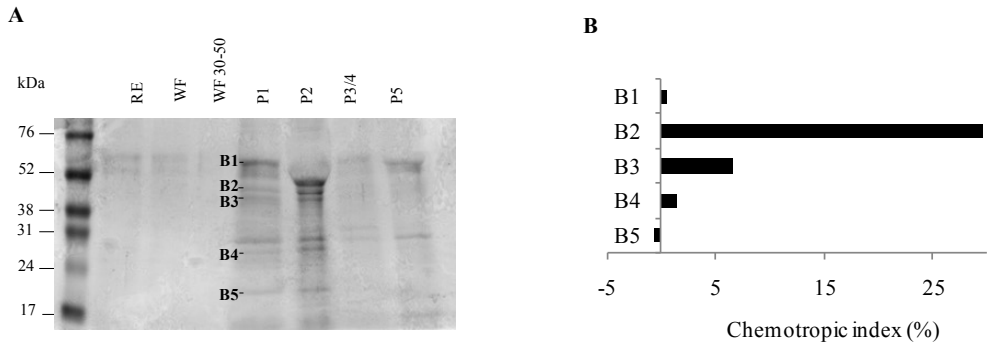

Figure 15. Protein bands B2 and B3 elicit a positive chemotropic response. A. SDS-PAGE analysis of proteins present in the tomato root exudate (RE), WF, 30-50 kDa WF and in peaks P1, P2, P3/4 and P5 obtained by anion exchange chromatography. Twenty five µl from each sample were subjected to SDS-PAGE and stained with Coomassie blue. Protein size markers labeled with their respective molecular weights in kDa are shown in the first lane. Protein bands present in the biologically active fraction P1 but absent in P5 are named B1 through B5. **B.** Chemotropic growth of germ tubes of the *ste12*Δ strain towards protein bands B1 through B5 after excision and elution from the SDS-PAGE gel.

2.3. Chemoattractants secreted by tomato roots are class III peroxidases

The biologically active protein bands P2 and P3 were subjected to in-gel tryptic digestion followed by liquid chromatography electrospray ionization tandem mass spectrometry (LC-ESI-MS/MS) (Table 12). This led to the identification of three tomato proteins: suberization associated anionic peroxidase 1 (TMP1), suberization associated anionic peroxidase 2 (TMP2), and citrus exocortis viroid induced protein 1 (CEVI-1). All three proteins belong to the family of secreted heme-containing oxido-reductases also called class III peroxidases. TMP1 and CEVI-1 were identified both in B2 and B3, while TMP2 was only identified in B2. Peptides identified for each peroxidase were absent from the two other peroxidases, confirming that distinct peroxidases were present in each protein band. Although the coverage was relatively low due to the low amount of protein in the samples, the results were considered reliable, based on the value "high" assigned in the confidence icon column (probability

of positive identification>99%). Importantly, the experimental masses of the identified peptides perfectly matched the predicted values (Table 12).

Protein identification	Protein abbreviation	Uniprot accesion number	Gel protein Band	Sequences of peptides analyzed [a]	Total protein coverage (%)	Confidence Icon [b]	Experimental mass of peptides analyzed	Theoretical massof peptides analyzed
Suberization-associated anionic peroxidase 1	TMP1	P15003	2/3	EMVALAGAHTVGFAR AVVDSAIDAETR	7,42/7,42	High/High	1,545.63/1529,55 1,246.51/1246,43	1,528.78 1,245.62
Citrus exocortis viroid induced 1	CEVI-1	Q9LWA2	2/3	YASSQSQFFDDFASSMIK LGNIGVLTGTNGEIR **DAASNVGAGGFDIVDDIK**	10,15/**11,08**	High/**High**	2,074.83/**2,058.67** 1,513.79 **1,763.79**	2,057.90 1,512.83 **1,762.84**
Suberization-associated anionic peroxidase 2	TMP2	P15004	2	EMVALAGAHTVGFAR LGGQTYTVALGR	7,44	High	1,545.6 1,235.4	1,528.78 1,234.67

Table 12. Liquid chromatography-electrospray ionization tandem mass spectrometry (LC-ESI/MS/MS) analysis of protein B2 and B3. [a] Peptide sequences from tryptic digest of B2 and B3 analyzed by LC-ESI-MS/MS. In italic, peptides identified in band 2 and 3; highlighted, peptides exclusively analyzed in band 2 and in bold, peptides and informations about peptides exclusively obtained from B3. [b] "High" in confidence icon represents the probability for a positive result is grater than 99%. Theoretical masses (Da) were calculated with Expasy Compute pI/Mw using monoisotopic masses of the occurring amino acid residues and giving peptide masses as [MH].

CEVI-1 was originally identified as a gene induced during infection of tomato plants by citrus exocortis viroid (CEV) (Gadea, Mayda et al. 1996). *CEVI-1* is also transcriptionally activated by other pathogens such as the fungus *Rhizoctonia solani* (Taheri and Tarighi 2011). *CEVI-1* expression correlates with lignin biosynthesis and is also induced by mechanical stress such as wounding (Mayda, Marques et al. 2000).

TMP1 and *TMP2* (Suberization-associated anionic peroxidases 1 and 2) are two tandemly oriented genes encoding anionic tomato peroxidases, which most likely evolved from a gene duplication event (Roberts, Kutchan et al. 1988; Roberts and

Kolattukudy 1989). While the exons are highly conserved between the two genes (90% identity), the introns show lower sequence identity even though their position isconserved. Interestingly, *TMP1* and *TMP2*have different signal peptides which may reflect different locations in the cell wall (Roberts and Kolattukudy 1989). While the stimuli that trigger expression of *TMP2* are yet unknown, expression of *TMP1* is upregulated in the periderm of 3-day-wound-healed tomato fruits or upon treatment with abscisic acid (ABA) (Roberts, Kutchan et al. 1988; Roberts and Kolattukudy 1989). TMP1 is thought to be involved in polymerizing phenolic monomers to generate the aromatic matrix of suberin (Borchert 1978; Kolattukudy 1980; Cottle and Kolattukudy 1982).

The differences in the chemotropic response elicited by B2 and B3 could be due either to the additional presence of TMP2 in B2 or to post-translational modifications of peroxidase isoforms in B2 and B3 explaining the different migration pattern of the same proteins in two bands.

The fact that the chemoattractants are class III peroxidases, a class of enzymes known for their robustness and stability at high temperatures, explains our finding that they still remained biologically active after a mild denaturation process (2 min at 100°C before separation by SDS-PAGE). This property allows peroxidases to be used commercially as an indicator of blanching efficiency. For example, peroxidases from corn or broccoli plants are inactivated only after 8 min of steam blanchin treatment (Barrett, Garcia et al. 2000).

3. Role of class III peroxidases in chemoattraction of *F. oxysporum*

The class III peroxidase family - Heme peroxidases catalyze the oxido-reduction between H_2O_2 and various reductants according to the equation $H_2O_2 + 2AH_2 \rightarrow 2H2O + 2A_2\bullet$, where AH_2 and $A_2\bullet$ represent a reducing substrate and its oxidized radical product, respectively (Hiraga, Sasaki et al. 2001). They fall into two major families, animal peroxidases and non-animal peroxidases which are found in plants, fungi, bacteria and protists (Figure 16). Non-animal peroxidases are further sub-divided into four classes (Koua, Cerutti et al. 2009). Class I includes intracellular peroxidases such as catalase peroxidases, ascorbate peroxidases and cytochrome c peroxidases. Class II includes secreted fungal peroxidases, class III secreted plant peroxidases and a separate group includes all the other non-animal peroxidases.

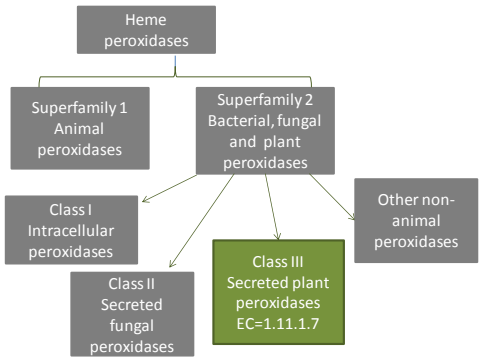

Figure 16. Classification of heme peroxidases. Heme peroxidases are subdivided into two superfamilies, animal peroxidases and non-animal peroxidases. The latter, in turn, are subdivided into four classes: intracellular peroxidases (class I), fungal secreted peroxidases (class II), plant secreted peroxidases (class III), and other non-animal peroxidases. Modified from (Koua, Cerutti et al. 2009).

Class III peroxidases, also called plant oxidoreductases (POXs; EC1.11.1.7), exist in all land plants (Vitali, Botta et al. 1998) and are encoded by large multigene families. For example, the *A. thaliana* genome encodes more than 70 class III peroxidases (Tognolli, Penel et al. 2002). Although different class III peroxidases of a given plant species can be highly diverse, showing amino acid sequence identities of less than 35%, a high degree of identity is usually observed between orthologs in different plants species.This suggests that different plant species possess a common set of POXs with similar characteristics among each species (Kjaersgard, Jespersen et al. 1997).

Structure and functions of class III peroxidases - POXs have highly variable molecular weights (ranging between 28 and 60 kDa) and isoelectric points (from 3 to 9). However, all contain three highly conserved domains, a distal heme-binding domain, a central conserved domain of unknown function and a proximal heme-binding domain, whose position and order is strictly conserved. Figure 17 shows the structure of horseradish peroxidase (HRP) isoenzyme C (HRP-C), the best studied class III peroxidase, which is secreted by roots of*Armoracia rusticana* (Veitch 2004). An iron (III) protoporphyrin IX group, also called heme group, is located between the 'distal' (above the heme) and the 'proximal' (below the heme) domains. Other structural elements conserved among class III peroxidases are four disulfide bridges, a buried salt bridge motif and sites of N-glycosylation. The enzyme is mostly shaped by α-helices, although it also contains a small β-sheet region (Figure 17).

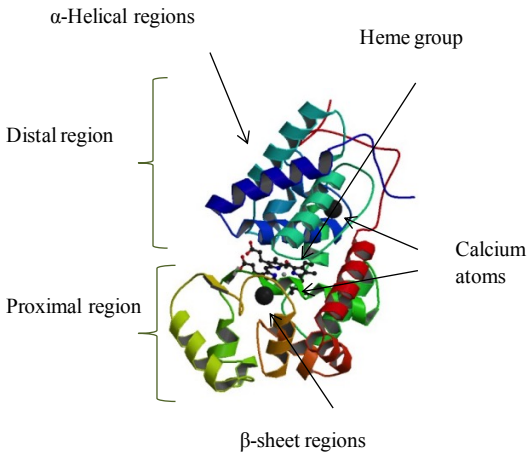

Figure 17. Schematic representation of the three-dimensional structure of HRP-C.3D representation of the X-ray crystal structure of HRP-C. The heme group in red is located between the distal and proximal domains which each contain one calcium atom (shown as blue spheres). α-helical and β-sheet regions of the enzyme are shown in purple and yellow, respectively. From (Veitch 2004).

Although class III peroxidases were first described in the 19th century, their purification was only achieved a century later (Theorell 1950). They are mainly involved in developmental processes such as cell elongation, auxin metabolism, wound-healing and defense against pathogens. Class III peroxidases play a crucial role in the formation of radical products that serve in the cross-linking reaction such as the formation of diferulate linkages from polymer-attached ferulate groups of polysachharides or pectins, the cross-linking of phenolic monomers in the formation of suberin, and the oxidative coupling of phenolic compounds for the synthesis of lignin. Wounding is a potent inducer ofPOX gene expression in horseradish (Kawaoka, Kawamoto et al.

1994), rice (Hiraga, Yamamoto et al. 2000; Ito, Hiraga et al. 2000; Sasaki, Matsumoto et al. 2002), tobacco (Sasaki, Matsumoto et al. 2002) and tomato (Mohan, Vijayan et al. 1993)and others plants.

POXs are also induced in response to pathogen attack and are included among the pathogenesis-related proteins (PR) as PR-9 group. *POX* gene expression is triggered by different plant pathogens such as fungi (Harrison, Curtis et al. 1995; Curtis, Rae et al. 1997), bacteria (Young, Guo et al. 1995; Bestwick, Brown et al. 1998), viruses (Lagrimini and Rothstein 1987; Harrison, Curtis et al. 1995; Hiraga, Ito et al. 2000) and viroids (Vera, Tornero et al. 1993). For example, POX activity increases in rice plants after infection by *M. oryzae* (Sasaki, Iwai et al. 2004), and transcript levels of *POX8.1* and *POX22.3* genes increased upon infection with Xanthomonas *oryzae*pv. *Oryza* (Chittoor, Leach et al. 1997).

Generally, class III peroxidases do not exhibit a strict specificity for reductants, and some isoenzymes canalso catalyze H_2O_2 independent oxido-reduction (Hinman and Lang 1965; Mader, Ungemach et al. 1980; Dayan, Rimando et al. 1999). Additionally, it is difficult to define specific functions for individual POXs, due to their functional redundancy, and because purified POX preparations generally catalyze a broad range of reductants *in vitro* and comprise several isoenzymes (Kjaersgard, Jespersen et al. 1997; Bernards, Fleming et al. 1999; de Marco, Guzzardi et al. 1999). As a result, the function of individual POXs cannot be defined only on the basis of their *in vitro* catalytic properties. Rather, a combination of *in vitro* studies, tissue localization and gene expression profiles is required.

Expression profiles of POX genes suggest possible functions of these enzymes in several biological processes. Lagrimini and Rothstein (1987) reported organ-specific and stress response-related differences in the expression of 12 tobacco *POXs*. In rice and *Stylosanthes humilis*, POX genes responded differentially to pathogen infection and wounding (Harrison, Curtis et al. 1995; Chittoor, Leach et al. 1997). In rice, 21 *POX*genes were differentially expressed in different organs and induced in response to distinct environmental stimuli (Hiraga, Yamamoto et al. 2000).

Chittoor et al, (Chittoor, Leach et al. 1997) proposed a correlation between primary structure and physiological function of class III peroxidases based on the analysis of the region between the proximal heme-binding site and the 7th conserved cysteine residue (Figure 20). This region is divergent in length and sequence among POXs, and is part of the substrate access channel in peanut and horseradish POXs (Schuller, Ban et al. 1996; Gajhede, Schuller et al. 1997). Therefore, it has been suggested that it could reflect the biological function of a given POX.

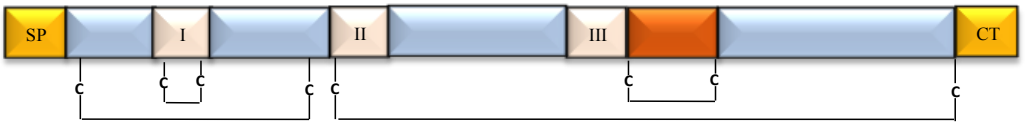

Figure 18. Schematic representation of the primary structure of class III peroxidases. The highly conserved domains I, II, and III correspond to the distal heme-binding domain, a conserved domain of unknown function and the proximal heme-binding domain, respectively. The orange box corresponds to a putative variable domain responsible for catalytic specificity. The signal peptide (SP) and C-terminal extension (CT) are highly variable in length and amino acid composition. From (Cosio and Dunand 2009).

As mentioned previoulsy, POXs are large multigenic familes required for multiple physiological processes such as plant growth and defense. The existence of many isoenzymes in a plant genome could have evolved from gene duplication events coupled with structural modification of one or more ancestral genes. This process would allow for protection against accidental loss of essential POX functions. In rice, approximately 130 POX genes are scattered across all the 12 chromosomes (Sasaki, Matsumoto et al. 2002). However, such redundancy makes it difficult to conclusively determine the functions of individual POXs.

The aim if this section was to unravel the mechanism by which class III peroxidases elicit chemotropism in *F. oxysporum*. We initially proposed three hypothetical mechanisms (Figure 19): (1) peroxidases activate a cognate fungal receptor through direct binding; (2) peroxidases activate a fungal receptor through enzymatic oxidation;

(3) peroxidases oxidize intermediate substrate(s), which in turn activate a fungal receptor. In the first hypothesis, the peroxidase protein structure should be essential for activation of the chemotropic response, while in the second and third hypotheses peroxidase enzymatic activity should be required for the chemotropic response.

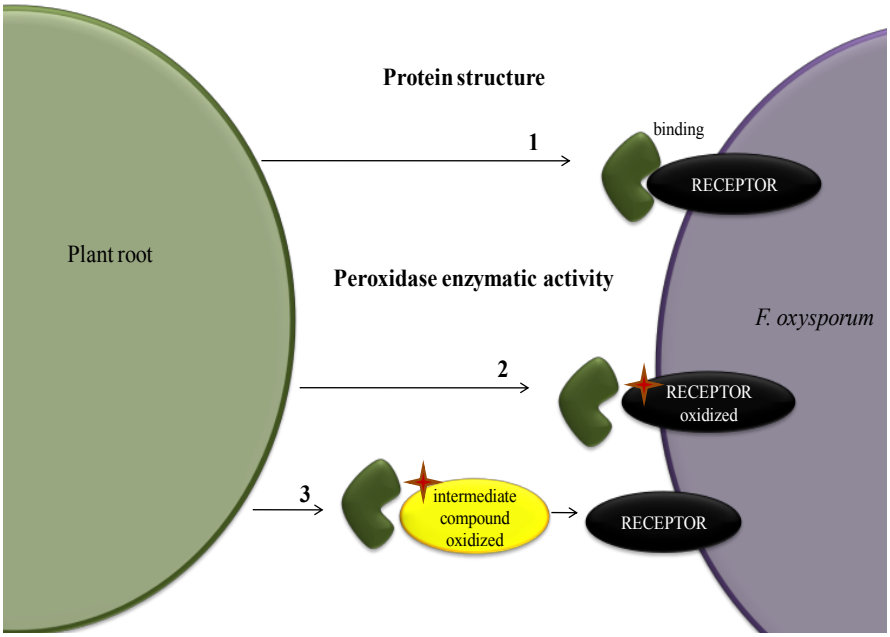

Figure 19. Schematic model illustrating the three different postulated mechanisms for activation of hyphal chemotropism by class III peroxidases. (1)Peroxidases activate a specific fungal receptor through direct binding; (2) peroxidases activate a specific fungal receptor through enzymatic oxidation; (3) peroxidases oxidize intermediate substrates which in turn activate a fungal receptor. Green structure, peroxidase; red star, oxidized residue; yellow oval, intermediate compound; black oval, fungal receptor.

4.1 Homology analysis of the identified tomato class III peroxidases

To identify the regions of similarity between the different peroxidases, a protein alignment with TMP1 (Uniprot accesion number P15003), TMP2 (P15004), CEVI-1 (Q9LWA2) and HRP-C (K7ZWW6) was performed, including HRP-C as a model class III peroxidase. TMP1, TMP2, CEVI-1 and HRP-C all contained the three conserved

domains characteristic of class III peroxidases (Figure 20). CEVI-1 displayed a higher percentage of amino acid sequence identity with HRP-C (49%) than with TMP1 and TMP2 (32% and 31%, respectively). In TMP1 and TMP2, the sequence between the 6th and the 7th conserved cysteine residues, corresponding to the variable domain responsible for catalytic specificity was identical, suggesting that both enzymes could catalyse the oxidation of the same or a similar substrate. However, no significant identity in this region was found between TMP1/TMP2 and CEVI-1 or HRP-C, while in the latter two the identity was 57%. While this region TMP1/2 was constituted by 16 amino acids, it was about twice the size in CEVI-1 and HRP-C (31 amino acids). Also the N-terminal and C-terminal regions were highly divergent between TMP1/2 proteins and CEVI-1. Whereas TMP1 and TMP2 signal peptides presented 85% identity, no significant identity was found with CEVI-1, HRP-C, or between the latter two. The same holds true for the C-terminal extensions that were also highly variable in length and amino acid composition.

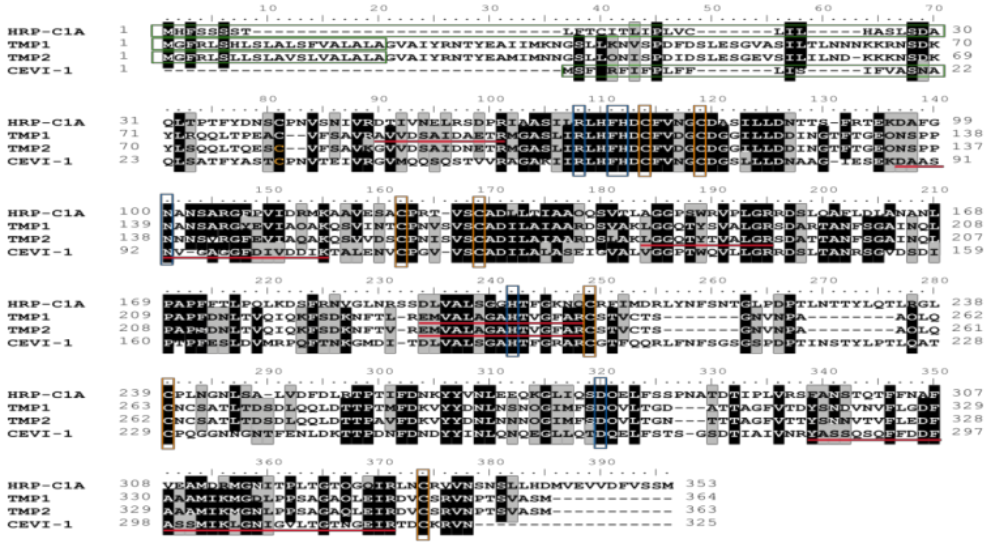

Figure 20. Amino acid sequence alignement of the three identified peroxidases with the HRP-C. TMP1, TMP2, CEVI-1 and horseradish peroxidase isoenzyme C (HRP_C1A) Uniprot accession numbers are P15003, P15004, Q9LWA2 and K7ZWW6, respectively. The peptides identified by LC-ESI-MS/MS in TMP1, TMP2 and CEVI-1 are underlined in red. Predicted signal peptides (according to SignalP-4.1 (www.cbs.dtu.dk/services/SignalP/)) are

framed by green boxes. Conserved residues important for catalytic activity are represented by blue boxes and conserved cysteine residues forming disulfure bridges by orange ones. Conserved amino acids are highlighted on a shaded background. Residues conserved in at least 3 of the 4 proteins are shaded in black. Dashes indicate gaps in the alignments.

3.2 The tomato genome encodes 70 predicted class III peroxidases

We took advantage of the complete *Solanum lycopersicum* genome sequence to compile a list of the predicted tomato class III peroxidase genes. *POXs* gene sequences were retrieved using the Sol Genomics Network (www.solgenomics.net) and the NCBI database (www.ncbi.nlm.nih.gov). This information was combined with that available in Peroxibase (www.peroxibase.toulouse.inra.fr) (Fawal, Li et al. 2013). Certain partial gene sequences in PeroxiBase, which had been named differentially (eg. LePrx24, LePrx68 and LePrx69) turned out to match to the same gene and were thus joined. Collectively, the information in Peroxibase and our annotation studies identified a total of 70 predicted *POX* genes in the tomato genome (Table 13).

The peroxidase genes were distributed across the 12 tomato chromosomes and did not form apparent clusters (Table 13). However, a more detailed analysis of gene coordinates and their homology suggested the presence of adjacent *POX* genes (≤ 10000 bp) that could have evolved from tandem duplications. For example, the genes encoding P16-P18, P48-P51 or TMP1-TMP2 (P22-P23) are highly conserved and each pair is separated by less than 5000 bp (Table 13 and Figure 23).

Table 13. Accession numbers and coordinates of the 70 predicted POX genes in tomato (*S. lycopersicum*). Accession numbers starting with LePrx, Solyc and XM were retrieved from PeroxiBase (www.peroxibase.toulouse.inra.fr), Sol Genomics Network (www.solgenomics.net) and NCBI (www.ncbi.nlm.nih.gov), respectively. The protein sequence of P52 was not found in any database. Coordinates of the genes correspond to the position of each gene on the respective chromosome (Chr).

Reference	Accesion number	Chr	Coordinates of the gene
P1	LePrx22	unpositioned scaffold	14657444/14656061
P2	LePrx05	1	891747/888896
P3	LePrx06	1	93354312/93356101
P4	LePrx28	1	884779/887621
P5	LePrx31	1	95673715/95675247
P6	LePrx43	1	90909753/90910895
P7	LePrx49	1	66807766/66806122
P8	LePrx55	1	2143061/2134714
P9	LePrx64	1	76839927/76841525
P10	LePrx64	1	76860512/76862172
P11	LePrx03	2	46872102/46873459
P12	LePrx08	2	53629631/53627090
P13	LePrx14	2	49665501/49666487
P14	LePrx17/62	2	44741297/44739605
P15	LePrx23	2	45815385/45813165
P16	LePrx24/68/69	2	47882432/47880732
P17	LePrx38	2	54788317/54789985
P18	LePrx40/70	2	47876593/47874773
P19	LePrx57	2	48699854/48703424
P20	LePrx65	2	36095618/36097543
P21	LePrx67	2	34204123/34201832
P22	LePrx75	2	44046955/44044563
P23	LePrx76	2	44042618/44040159
P24	Solyc02g084800.2.1	2	47889825/47888460
P25	LePrx21	3	1262506/1259766
P26	LePrx29/37	3	8098828/8096015
P27	LePrx32	3	52050347/52051941
P28	LePrx66	3	5315137/5318145
P29	LePrx72	3	2813769/2816283

P30	LePrx07	4	64859239/64857005
P31	LePrx09	4	58913334/58915438
P32	LePrx16	4	58919910/58922921
P33	XM_004238556	4	64553548/64554942
P34	LePrx41	4	65731641/65729103
P35	LePrx73	4	61652559/61649557
P36	LePrx11	5	62562832/62559763
P37	LePrx12/33	5	58103304/58104907
P38	LePrx46	5	58037266/58039451
P39	LePrx50	5	4476583/4479812
P40	LePrx60/71	5	61092909/61090944
P41	XM_004239674	5	65001185/65002725
P42	Solyc05g046010.2.1	5	58049383/58047387
P43	XM_004240093	5	58128352/58129954
P44	LePrx20	6	47594316/47592055
P45	LePrx25	6	33054091/33051778
P46	LePrx01	7	61020110/61021912
P47	LePrx02	7	59520799/59522115
P48	LePrx15	7	61035832/61037571
P49	LePrx48	7	8263025/8260969
P50	LePrx51	7	61020180/61021604
P51	XM_004243410	7	61029695/61031406
P52	/	7	58951739/58953436
P53	Solyc07g052550.1.1	7	61042290/61043801
P54	LePrx04/18	8	59920913/59922336
P55	LePrx42	8	1709615/1708656
P56	LePrx52	8	58125521/58127215
P57	LePrx58/74	8	3406620/3401624
P58	LePrx19	9	65314163/65312183
P59	LePrx30	9	1099568/1092950
P60	LePrx10	10	59084119/59082990
P61	LePrx13	10	59055612/59054478
P62	LePrx35/44/45	10	60552219/60554250
P63	Solyc10g076220.1.1	10	59060961/59059828
P64	LePrx26/27/63	11	9598442/9597159
P65	LePrx39	11	1629588/1628496
P66	LePrx47	11	3243624/3246066
P67	LePrx54	11	56078850/56077525
P68	LePrx39	11	1634249/1633156
P69	LePrx56	12	65413887/65410423
P70	Solyc12g005790.1.1	12	442920/440801

To obtain a general view of the evolutionary history of *S. lycopersici* POXs, a phylogenetic tree based on the alignment of all amino acid sequences was constructed, including the calculated evolutionary distances between the different peroxidases (Figure 23). Besides a single POX (P32), all remaining POXs clustered into five main groups named Gr1 through Gr5, each organized into several subclusters. This organization is supported by specific amino acid variations within each group. For example, TMP1/2 and CEVI-1 belong to the same group (Gr-5), but within different subclusters. A similar clustering of class III peroxidases was reported for *A. thaliana* (Tognolli, Penel et al. 2002) indicating that these two plants have evolved to create a similar set of class III peroxidases.

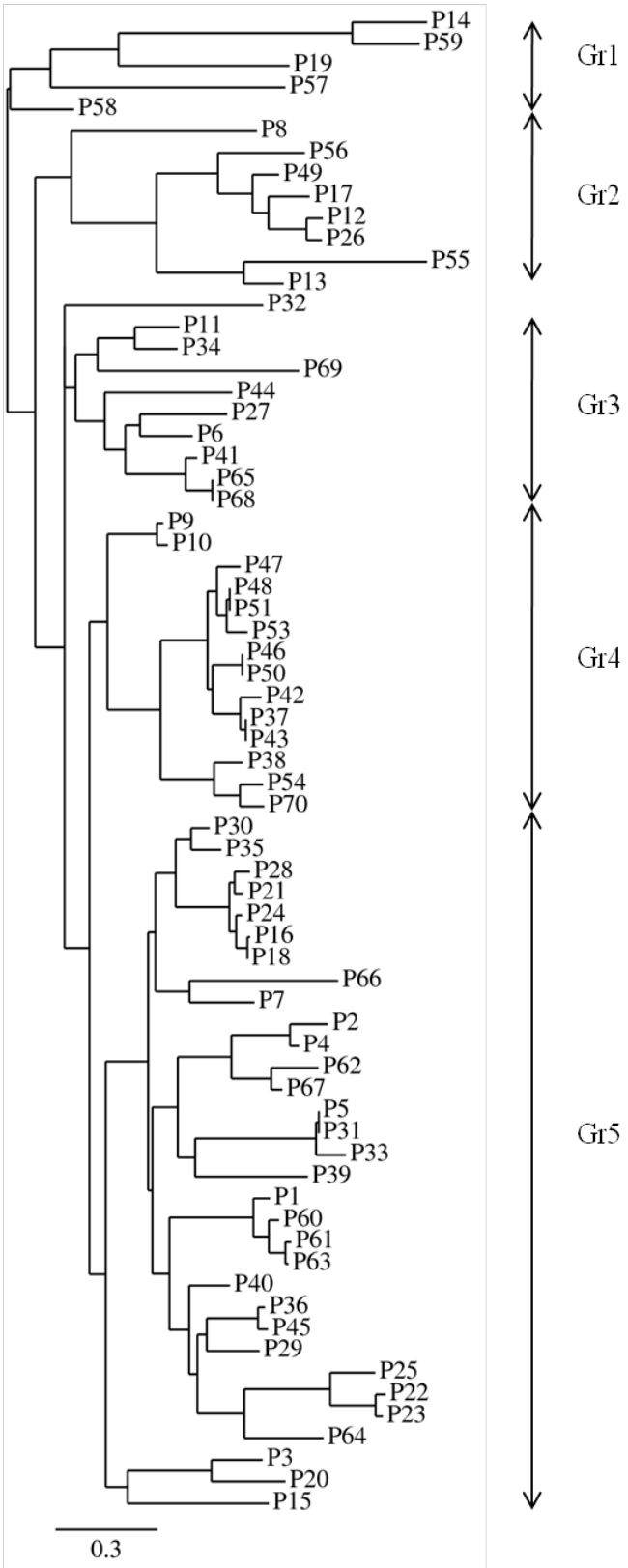

Figure 21. Phylogenetic relationships of tomato (*S. lycopersicum*) class III peroxidases based on sequence alignment of the complete predicted proteins. For references of sequences used to establish the phylogenetic tree, see. **Table 13.** P52 was not included. The tree was generated using www.phylogeny.fr. The five main groupings are indicated (Gr1-Gr5). Branch length scale bar at the bottom represents amino acid substitions per site.

3.3 *TMP1*, *TMP2* and *CEVI-1* are expressed in tomato roots and upregulated during infection in *F. oxysporum*

To confirm that *TMP1*, *TMP2* and *CEVI-1* are expressed, transcript levels of the three genes in tomato roots were measured by qRT-PCR. *CEVI-1* presented the highest transcript level, which was 100 and 6 times higher than of *TMP1* and *TMP2*, respectively (Figure 22A). It is important to note that the mean cycle threshold values were low, indicate that under these conditions the three genes are expressed at low levels in the roots.

We next asked whether peroxidases are secreted from tomato roots. Exudates obtained from roots of 4 day-old seedlings (RE 1) and 2 week-old plants (RE 2) and tested for peroxidase enzymatic activity, using 2,2′-azinobis-(3-ethylbenzothiazoline-6-sulfonic acid) (ABTS) as a chromogenic substrate. Commercial HRP was used as a positive control. These assays detected significant peroxidase activity in the tomato root exudates, confirming the secretion of peroxidases (Figure 22B).

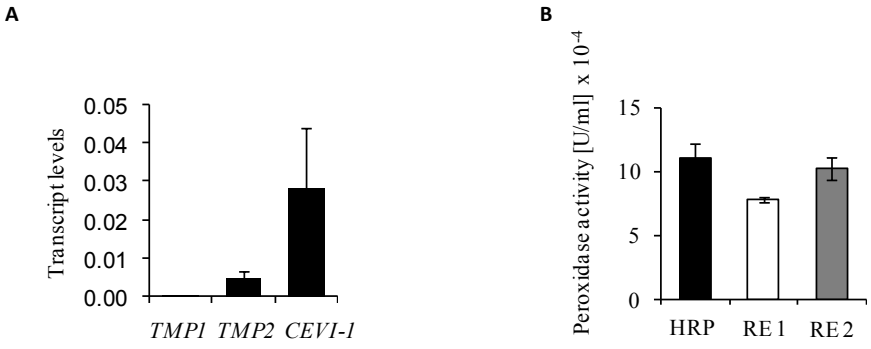

Figure 22. Expression of *TMP1*, *TMP2* and *CEVI-1* genes and secretion of peroxidases in tomato roots. A. *TMP1*, *TMP2* and *CEVI-1* transcript levels were measured in roots of 2 week-old tomato plants using qRT-PCR. Transcript levels are expressed relative to those of the *EF1-α* gene. For each experiment, roots of three plants were pooled. Data show the means from three independent experiments with three technical replicates each. Error bars, s.d. **B.** Peroxidase enzymatic activity was measured from 0.0025 μM HRP or from 100 μl of root exudate from 2 week-old plants (RE1) or from 4 day-old plants (RE2), using 0.91 mM ABTS and 0.0025 mM H_2O_2 as substrates. RE1 and RE2 represent root exudates obtained from roots of 2 week-ols plants and

4 day-old seedlings, respectively. Activity is expressed as units/ml (U/ml). Error bars represent s.d. from two technical replicates.

Since certain class III peroxidases are induced upon pathogen infection, *TMP1*, *TMP2* and *CEVI-1* transcript levels were measured in roots of tomato plants inoculated with a suspension of *F. oxysporum* microconidia as a positive control, PR1 (Pathogenesis-Related protein 1), a known defense gene reported as a molecular marker for plant defense responses was used. qRT-PCR analysis revealed that *TMP1* and *CEVI-1* transcript levels were dramatically upregulated in roots inoculated with *F. oxysporum* (Figure 23) .Increased levels of both transcripts were detectable after 24h and reached a maximum level at 48h after inoculation. The induction of *TMP1* and *CEVI-1* (one hundred and one thousand times, respectively, compared to the uninoculated control) was much higher than that of *PR-1*. Conversely, *TMP2* transcript levels remained stable over the entire experiment. While *TMP1* and *TMP2* expression did not vary significantly in the uninoculated control plants, *CEVI-1* expression fluctuated over the same time period being up-regulated from 0h to 12h, down-regulated from 12h to 24h and again up-regulated to reach its maximal expression at 48h (Figure 23). Consistent with previous studies (Mayda, Marques et al. 2000), our results suggest that *CEVI-1* expression could also be induced by stimuli other than pathogen attack reflecting putative function in the regulation of endogenous plant physiological processes.

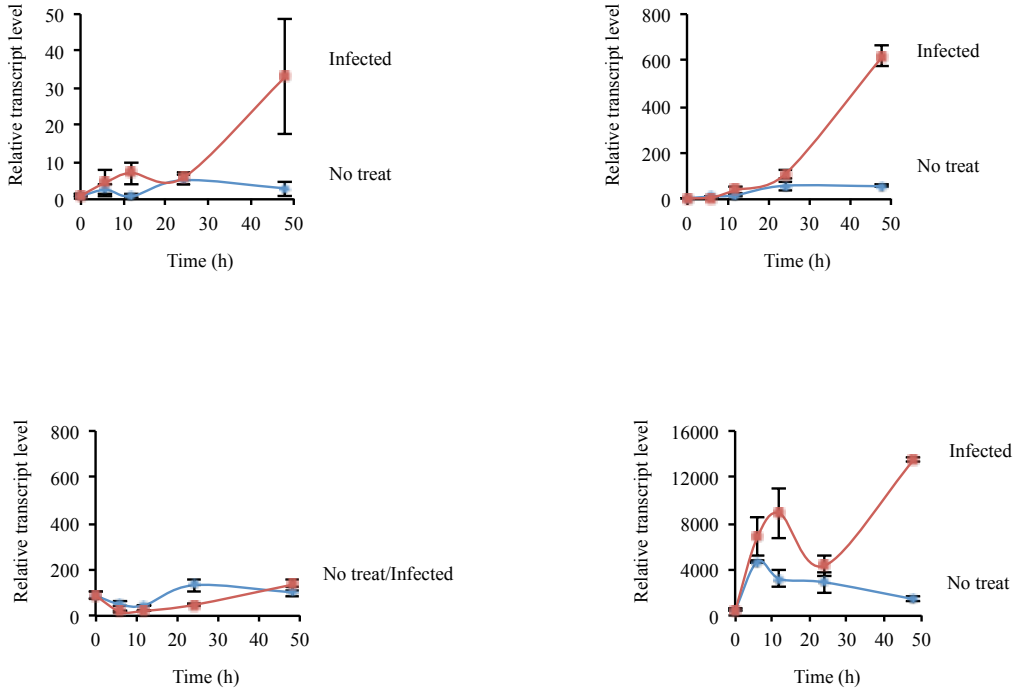

Figure 23. Time course of *PR-1, TMP1, TMP2 and CEVI-1* gene expression in tomato roots infected with *F. oxysporum*. Transcript levels of the indicated genes in tomato roots were measured by qRT-PCR at the indicated times after submerging the roots in water (No treat) or in a suspension of *F. oxysporum* microconidia (Infected). Transcript levels are expressed relative to those of the *EF1-α* gene and are normalized to *PR-1* transcript levels at t=0h. For each experiment, roots of three plants were pooled. Data shown are from three independent experiments with three technical replicates each. Error bars, s.d.

3.4 Regions of tomato roots enriched in peroxidase activity are preferentially colonized by *F. oxysporum*

We next undertook a comparative study of the localization of *F. oxysporum* mycelium using a GFP-labelled fungal strain, and of root peroxidase activity, using the chromogenic substrate ABTS. The highest peroxidase activity was detected in the root hair region, whereas the root tip was largely devoid of activity (Figure 24A,B). Interestingly, the highest density of *F. oxysporum* mycelium was found in the root

region with the highest peroxidase enzymatic activity (Figure 26C,D). By contrast, *F. oxysporum* hyphae did not accumulate at the root tip.

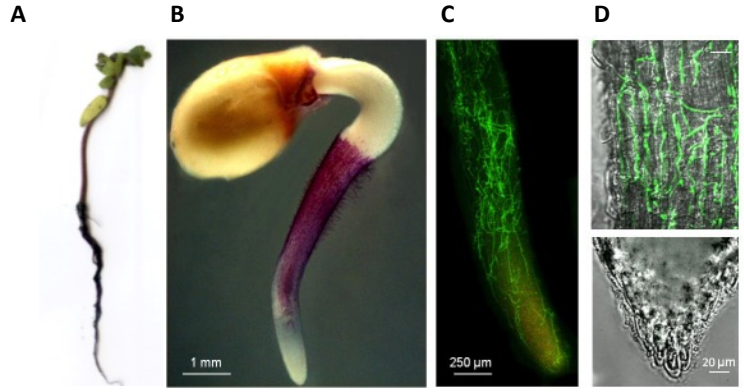

Figure 24. Tomato root regions displaying high peroxidase activity are preferentially colonized by *F. oxysporum*. A. Distribution of peroxidase enzymatic activity on 2 weeks-old plants. **B.** Distribution of peroxidase enzymatic activity on 4 days-old germlings visualized with a stereomicroscope. Size bar, 1 mm. **C** and **D.** Colonization of tomato roots by a *F. oxysporum* strain expressing green fluorescent protein (GFP), at 2 days after inoculation. Size bar, 250 µm and 20 µm. Experiments were performed four times with similar results.

3.5 Commercial horseradish peroxidase elicits a chemotropic response in *F. oxysporum*

To confirm that class III peroxidases function as general chemoattractants for *F. oxysporum*, the chemotropic response of germ tubes towards increasing concentrations of commercial HRP was tested. We observed a bell-shaped chemotropic dose-response curve towards HRP, with a maximum at concentrations between 2 µM and 8 µM (Figure 25). The finding that a class III peroxidases from a non-host plant species can trigger chemotropismin *F. oxysporum* f. sp. *lycopersici* is important, since it suggests that POXs function as general chemoattractants for this fungal pathogen.

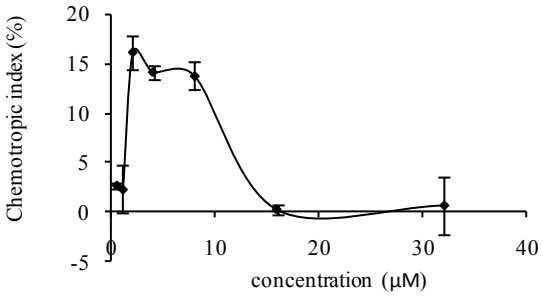

Figure 27. Commercial HRP triggers a strong chemotropic response in *F. oxysporum*. Chemotropic response of *F. oxysporum* towards increasing concentrations of HRP (from 0.5 µM to 32 µM). Mean values were calculated from two independent experiments, each with 500 germlings scored. Error bars, s.d. (experimental data obtained by Dr. David Turra)

3.6 Enzymatic activity of class III peroxidases is required for chemoattraction of *F. oxysporum*

To elucidate the mechanism by which class III peroxidases trigger directed hyphal growth in *F. oxysporum* we asked whether protein structure and/or enzymatic activity is required for the response. To this aim, commercial HRP and tomato root exudate were subjected either to denaturalization by boiling, or applied in the presence of specific peroxidase inhibitors or ROS scavengers.

Among the different chemicals described to inhibit peroxidase activity, we tested thiourea (TH), adenine (Ade), salicylhydroxamic acid (SH), NaN_3, Na_3VO_4 and sodium L-ascorbate (Asc). Quantification of HRP enzymatic activity in presence of 1 mM of each compound revealed that the peroxidase substrate scavenger TH, the specific peroxidase inhibitor SH and the oxygen radical scavenger Asc were the most efficient inhibitors, besides boiling (Figure 26A). Unexpectedly, adenine, which was reported as a peroxidase inhibitor, increased enzymatic activity. We next determined the minimum inhibitory concentration (MIC) of TH, SH and Asc that abolishes the enzymatic activity of 0.0025 µM HRP, the quantity used in our chemotropism assay. We found that HRP activity was totally inhibited in the presence of 75 µM TH or SH, and by 250 µM of Asc (Figure 26B).

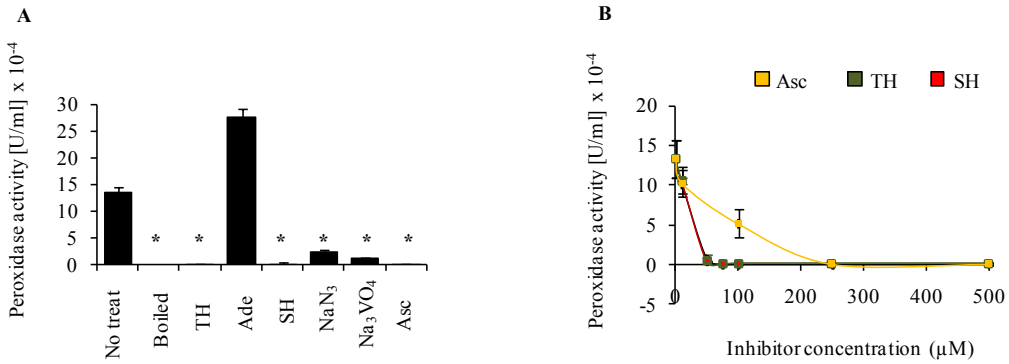

Figure 26. TH, SH, and Asc are efficient inhibitors of HRP enzymatic activity. A. Peroxidase activity was quantitied for HRP (No treat), heat-inactivated HRP (boiled), or HRP incubated 10 min with 1 mM of the following inhibitors: thiourea (TH), adenine (Ade), SHAM (SH), NaN_3, Na_3VO_4 and sodium ascorbate (Asc). *, $P < 0.001$ according to unpaired *t* test. **B.** Dose inhibition curves of HRP activity in the presence of increasing concentrations of TH, SH and Asc. Enzymatic activity was quantified for 0.0025 µM HRP using 0.91 mM ABTS and 0.0025 mM H_2O_2 as substrates and expressed in units/ml (U/ml). Error bars represent s.d. from three technical replicates.

We next tested the effect of the inhibitor treatments on root exudates of 4 day-old seedlings (RE 1) and 2 week-old plants (RE 2), both of which were previously shown to exhibit significant peroxidase activity (Figure 22B). When these samples where boiled or treated with 75 µM TH and, 75 µM SH or 250 µM Asc, enzymatic activity was drastically reduced or completely abolished (Figure 27A). These results confirm that class III peroxidases are the major oxido-reductases present in tomato root exudate. Importantly, elimination of peroxidase enzymatic activity by either boiling or treatment with inhibitors/scavengers caused a significant reduction of their chemoattractant effect on *F. oxysporum* (Figure 29B). However, neither SH nor Asc affected directed growth towards glucose or α-pheromone, indicating that these compounds are not general inhibitors of chemotropism (Turra, El Ghalid et al. 2015). These results suggest that the enzymatic activity of class III peroxidases is an essential component of the mechanism that triggers directed hyphal growth in *F. oxysporum*.

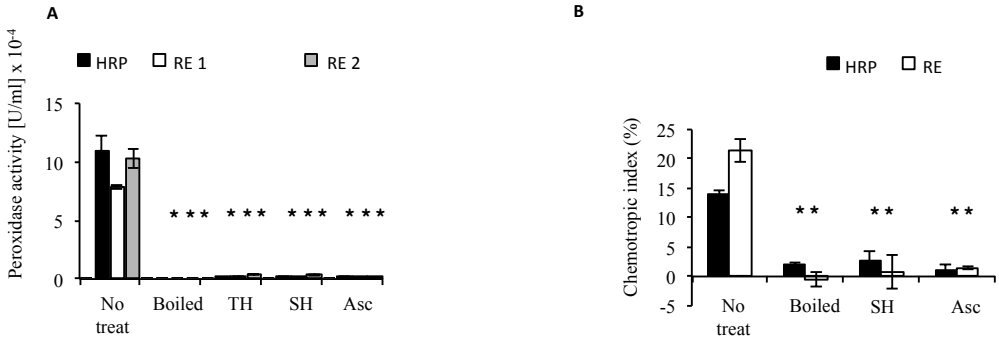

Figure 27. Enzymatic activity of secreted root peroxidases is required to elicit a chemotropic response in *F. oxysporum*. A. Peroxidase enzymatic activity was quantified for 0.0025 µM HRP or 100 µl RE obtained from 4-day-old tomato seedlings (RE 1) or 2-week-old plants (RE 2), using 0.91 mM ABTS and 0.0025 mM H_2O_2 as substrates. Samples were either untreated (No treat) or subjected to heat treatment (boiled) or incubation with 75 µM TH, 75 µM SH or 250 µM Asc. Activity is expressed in units/ml (U/ml). *, $P \leq 0.0002$ according to unpaired *t* test. Error bars represent s.d. from two technical replicates. **B.** Chemotropic response of *F. oxysporum* towards a gradient of 4 µM HRP or RE. Samples were either untreated (No treat) or subjected to heat treatment (boiled) or incubation with 60 mM SH or 160 mM Asc. *, $P < 0.0001$, versus no treat for a given compound. Mean values were calculated from two independent experiments, each with 500 germlings scored. Error bars, s.d (Chemotropism assays were performed by Dr. David Turrà).

3.7 Secreted root peroxidases generate diffusible radical products

The above findings suggest that class III peroxidases exert their chemoattractant effect through their enzymatic activity, either by direct oxididation of a putative fungal receptor or by oxidation of an intermediate substrate that acts as the chemotropic signal. To investigate the second hypothesis, we attempted to visualize the secretion of radical compounds generated by peroxidase enzymatic activity of 2-week-old tomato plants or 4-day-old germlings roots using three different chromogenic substrates: ABTS, 3, 3'-Diaminobenzidine (DAB) and guaiacol. In presence of H_2O_2, these substrates are converted into radicalized products staining, respectively, in green, brown or red. Only when ABTS was used as a substrate, a gradient of radicalized compounds was observed (Figure 28). In the case of adult plants, the gradient of radicalized products reached the scoring line after 12h, which is approximately the incubation time used in our

chemotropism assay. Oxidized ABTS was described as a water-soluble product of the peroxidase reaction, whereas DAB and guaiacol radicals are insoluble (Kricka 1995). These characteristics might explain the absence of a visible gradient in the case of DAB and guaiacol.

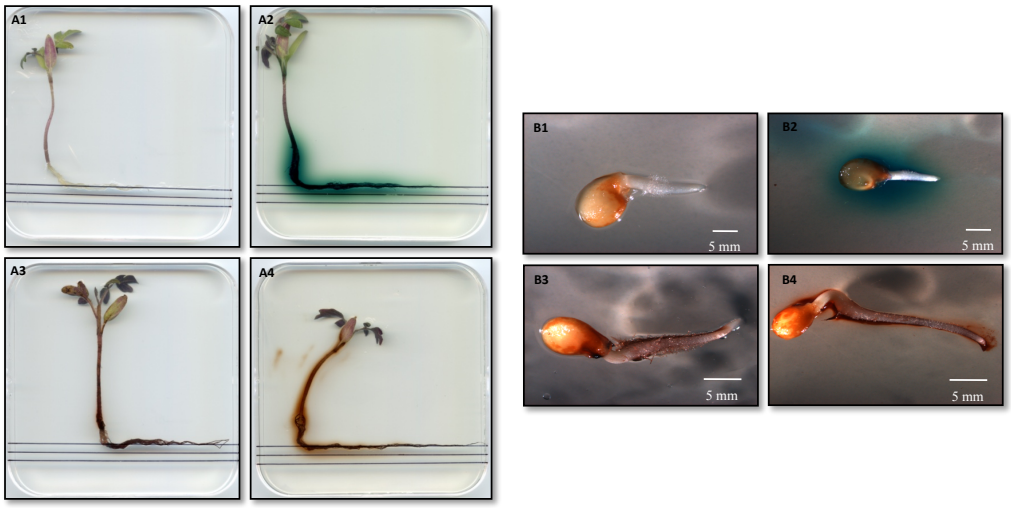

Figure 28. Diffusion of radical products of peroxidase activity from tomato roots. Radical products generated by root peroxidases of 2-week-old plants and 4-day-old seedlings was visualized 12h and 45 min, respectively, after addition of water (A1, B1), or the chromogenic substrates ABTS (A2, B2), DAB (A3, B3) or guaiacol (A4, B4). Size bar, 5 mm.

3.8 The oxidized substrate ABTS functions as a chemoattractant

As previously shown, peroxidase enzymatic activity is required to elicit a significant chemotropic response in *F. oxysporum*. To investigate if the oxidation of a specific fungal compound could be involved in this process, we tested the chemotropic response of *F. oxysporum* germlings towards increasing concentrations of oxidized ABTS, a non-specific oxidant. Oxidized ABTS was obtained by co-incubating commercial ABTS with HRP and H_2O_2. H_2O_2 was added as the limitant substrate and at the end of the reaction the HRP was separacted from the oxidized ABTS using ultra-centrifugation columns of 3-kDa cut-off (see Materials and Methods for details). Oxidized ABTS elicited a significant chemotropic response in *F. oxysporum* (Figure 29). Interestingly,

the dose-response curve was similar to that obtained with HRP and both compounds triggered a maximum response at 4 µM (see Figure 29). These results indicate that non-specific oxidation products of peroxidase enzymatic activity could be responsible for the chemotropic response elicited by tomato root exudates.

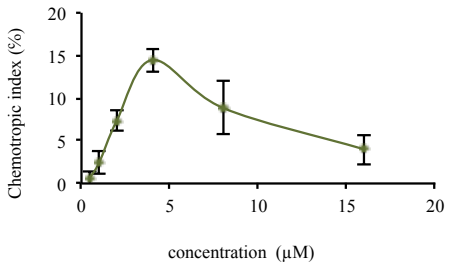

Figure 29. Oxidized ABTS functions as chemoattractant. Chemotropic response of *F. oxysporum* wt strain towards increasing concentrations of oxidized ABTS (from 0.5 µM to 16 µM). Mean values were calculated from two independent experiments, each with 500 germlings scored. Error bars, s.d.

3.9 Oxidized ABTS is modified by *F. oxysporum*

To understand how the oxidized ABTS products may trigger a chemotropic response in *F. oxysporum*, we followed the oxidation of ABTS substrate by a gradient of HRP or by secreted root peroxidases over a period of 40h. HRP or tomato roots were applied on the central scoring line of plates containing water-agar supplemented with ABTS, either in the absence or in the presence of *F. oxysporum*. While in the absence of the fungus the green color of oxidized ABTS persisted over a time, in the presence of *F. oxysporum* the color faded from 24h and completely disappeared at 40h of incubation (Figure 32). We envisage three different explanations for this observation: (1) Secreted root peroxidases are degraded or internalized by the fungus leading to a gradual decrease in oxidation of ABTS; (2) Oxidized ABTS is degraded or internalized by the fungus; (3) Oxidized ABTS is reducedby the fungus.

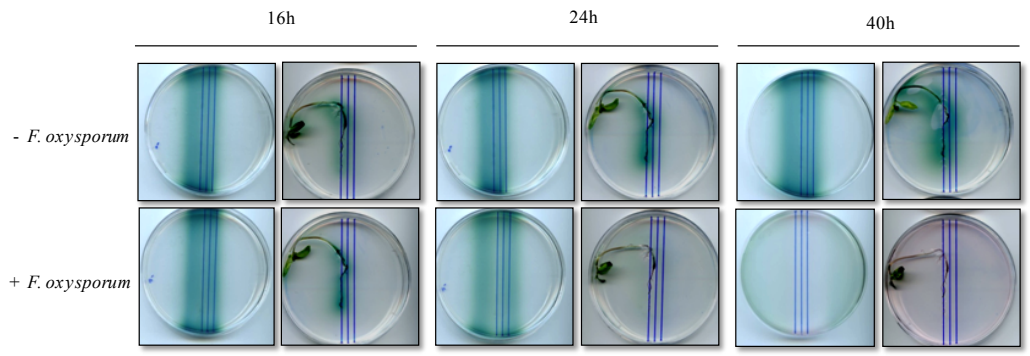

Figure 30. Oxidized ABTS generated by a gradient of class III peroxidases is modified in presence of *F. oxyporum*. Oxidation of ABTS by a gradient of 4 µM HRP (left plates) or tomato root peroxidases (right plates) was visualized in the presence or absence of *F. oxysporum* after the indicated times of incubation at 28°C. Three technical replicates were performed.

3.10 The H_2O_2 is a chemoattractant

Our previous results showed that oxidized products from ABTS generated by peroxidase activity elicit chemotropism in *F. oxysporum*. These products belong to the family of Reactive Oxygen Species (ROS) which comprises highly reactive free oxygen radicals such as the superoxide anion $O_2^{\cdot -}$, the hydroxyl radical OH^- and the stable non-radical oxidants. H_2O_2 is the best studied ROS (Gough and Cotter 2011). We therefore wondered whether this molecule by itself could act as a chemoattractant. Indeed, we found that H_2O_2 elicited a strong chemotropic response in *F. oxysporum* (Figure 30). Unlike all other chemoattractants tested so far, H_2O_2 was active over a wide range of concentrations ranging fromthe nanomolar to the millimolar scale (50 nM to 2.5 mM). This led to an atypical chemotropic dose-response curve which does not present a bell-shaped form. To our knowledge, H_2O_2 is the first described compound which is chemotropically active over 6 magnitude orders of concentrations.

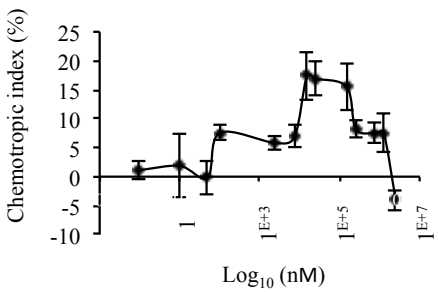

Figure 31. H_2O_2 functions as a chemoattractant. Chemotropic response of *F. oxysporum* wt strain towards increasing concentrations of H_2O_2 (from 1 nM to 2.5 mM). Mean values were calculated from two independent experiments, each with 500 germlings scored. Error bars, s.d.

Additive chemoattractant effect of HRP, oxidized ABTS and H_2O_2

We next tested the combined effect of HRP, oxidized ABTS and H_2O_2 on the chemotropic response of *F. oxysporum*, using all possible combinations between these compounds. Two concentrations for each compound were tested either individually or in combination: sub-optimal (0.5 µM HRP, 0.5 µM oxidized ABTS and 1 nM H_2O_2) and optimal (4 µM HRP, 4 µM oxidized ABTS and 25 µM H_2O_2).

When sub-optimal concentrations were applied individually, the chemotropic response of *F. oxysporum* was almost null as observed previously (Figure 31, see also Figures 25, 29 and 30). However, combinations of these compounds at sub-optimal concentrations elicited a significant response suggesting that they could act either additively or synergically (Figure 31A). When optimal concentrations were used individually, the chemotropic response was positive (Figure 31B). However, when used in double combination sat optimal concentrations, they triggered either no (HRP + ABTS and HRP +H_2O_2) or only a very weak (ABTS + H_2O_2) chemotropic response, possibly due to a confusion effect due to receptor saturation. The triple combination between HRP, ABTS and H_2O_2 even significant negative response (-7,75 %), suggesting that high concentrations of ROS could induce negativechemotropism in the fungus.

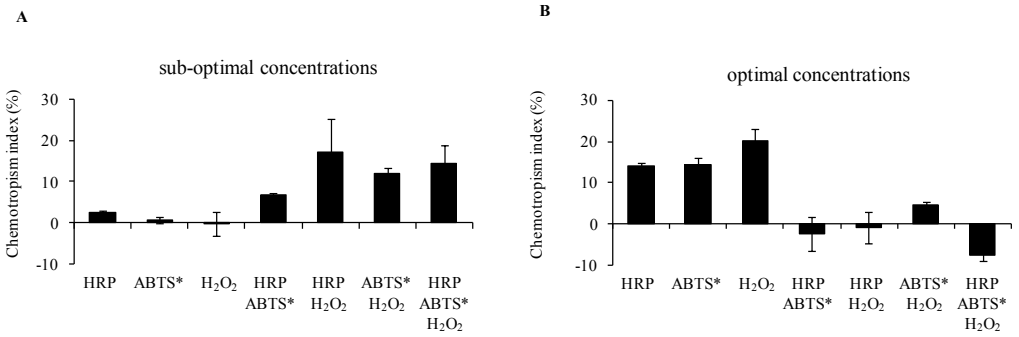

Figure 32. HRP, oxidized ABTS and H_2O_2 have additive or synergic effects on *F. oxysporum* directed hyplal growth. **A, B.** Directed growth of *F. oxysporum* germ tubes towards the indicated concentrations of HRP, oxidized ABTS (ABTS*) or H_2O_2, or different combinaisons of these compounds. **A.** Sub-optimal concentrations (0.5 µM HRP, 0.5 µM oxidized ABTS, 1 nM H_2O_2) were used. **B.** Optimal concentrations (4 µM HRP, 4 µM oxidized ABTS, 25 µM H_2O_2) were used. Mean values were calculated from two independent experiments, each with 500 germlings scored. Error bars, s.d.

3.11 Hyphal chemotropism induced by ROS requires the seven transmembrane receptor Ste2 and the MAPK Mpk1

Previous studies demonstrated that the chemotropic response of *F. oxysporum* towards tomato roots and root exudates requires the α-pheromone receptor Ste2 and the MAPK Mpk1 (Turrà, El Ghalid et al. 2015). To test if Ste2 and Mpk1 are aslo required for the chemotropic response to ROS we tested the ability of the *ste2*Δ and *mpk1*Δmutant strains to grow towards a gradient of 4 µM HRP or 4 µM oxidized ABTS. In both mutants their chemotropic response towards the peroxidase and the radical product was impaired (Figure 32). For HRP, the response was fully restored in the *ste2*Δ+*ste2* and *mpk1*Δ+*mpk1* complemented strains. However, in presence of oxidized ABTS, only the *mpk1*Δ+*mpk1* fully recovered the wt phenotype whereas *ste2*Δ+*ste2* did it partially. Since the wt phenotype is not always fully restored in all complemented strains, an additional *ste2*Δ+*ste2* strain should be tested to confirm these results.

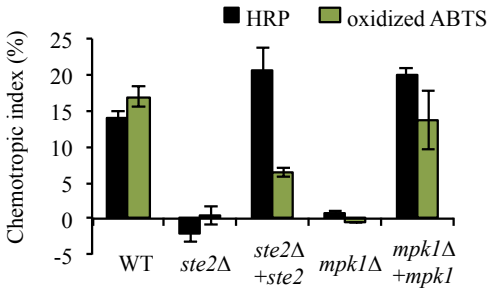

Figure 33. HRP and oxidized ABTS function as a chemoattractants via the Ste2 receptor and the Mpk1 kinase. Chemotropic response of *ste2*Δ and *mpk1*Δ mutant strains and their respective complemented strains (*ste2*Δ+*ste2* and *mpk1*Δ+*mpk1*) towards 4 µM of HRP and 4 µM oxidized ABTS. Mean values were calculated from two independent experiments, each with 500 germlings scored. Error bars, s.d. (experimental data for HRP obtained by Dr. David Turra)

Ste2 was also essential for the chemotropic response to a gradient of 25 µM of H_2O_2 (optimal concentration) (Figure 35). However, at a supra-optimal concentration of 1.25 mM H_2O_2, chemotropism was not affected in the *ste2*Δ mutant. This suggests the presence of a Ste2-independent mechanism for H_2O_2-triggered chemotropic growth at high concentrations of this compound.

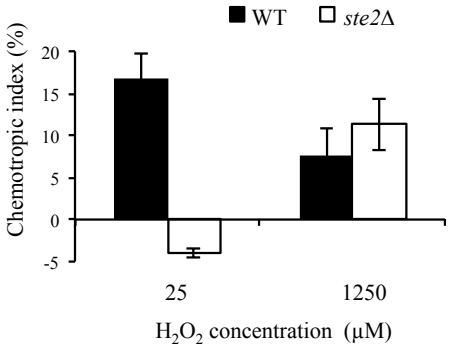

Figure 34. At low concentration, H_2O_2 triggers chemotropism in *F. oxysporum* via the Ste2 receptor. Directed growth of germ tubes of *F. oxysporum* wt and *ste2*Δ mutant strains towards 25 µM and 1250 µM of H_2O_2. Mean values were calculated from two independent experiments, each with 500 germlings scored. Error bars, s.d.

Taken together, these results suggest that the seven transmembrane receptor Ste2 is involved in chemotropic sensing of different types of reactive oxygen species including chemically reactive radicals and nonradical oxygen derivatives.

3.12 Ste2 has no role in the oxidative stress response

We next asked whether Ste2 might have a role in the response of *F. oxysporum* to oxidative stress. To this aim, we tested the effect of 5%, 10%, 15% and 20 % H_2O_2 (1.63 M, 3.26 M, 4,89 M and 6,52 M, respectively) on the growth of the *F. oxysporum* wt strain, the *ste2*Δ mutant and its complemented strain *ste2*Δ+*ste2*. No significant differences were detected between the strains in colony morphology or diameter in the presence of different concentrations of H_2O_2. Thus, Ste2 is not required for the oxidative stress response and acts essentially in chemotropic sensing of ROS.

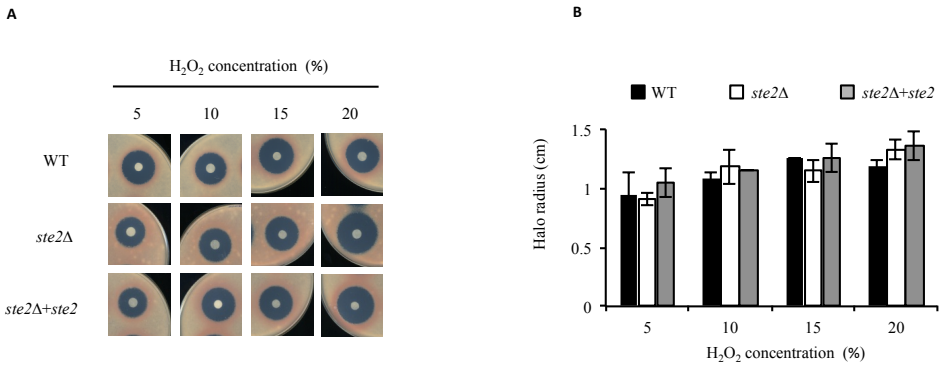

Figure 35. Ste2 has no role in the oxidative stress response. A. wt, *ste2*Δ and *ste2*Δ+*ste2* conidia were spread onto SM plates and grown for 1 day at 28 °C before placing a filter disc saturated with 5%, 10%, 15% and 20% of H_2O_2 solution (v/v) at the centre of the plates, followed by growth for 3 additional days at 28°C. **B.** Growth inhibition was quantified by measuring the radius of the clear halo surrounding the filter disc. Mean values were calculated from at least two technical repeats. Error bars, s.d.

3.13 Evidence for a role of NADPH oxidases in the chemotropism of *F. oxysporum*

NADPH oxidases (NOX) are the only known family of enzymes whose sole function is the production of ROS (Foreman, Demidchik et al. 2003). Therefore, we were interested in a possible role if the NOX complex in chemotropic sensing of *F. oxysporum*. To test this idea, we used DPI (diphenylene iodonium), a known selective inhibitor of NOX activity. Initial assays revealed an inhibitory effect of 25 µM DPI on

the germination rate of *F. oxysporum* microconidia, while 10 µM DPI had no inhibitory effect (data not shown). We therefore used a concentration of 10 µM in DPI in the chemotropism experiements. We next tested the effect of DPI on the chemotropic response of *F. oxysporum* against a gradient of 378 µM α-pehromone or 2.95 mM sodium glutamate, which are known to trigger chemotropism through the Fmk1 and the Mpk1 pathway, respectively (Turrà, El Ghalid et al. 2015). In the presence of DPI, chemotropic sensing of both chemoattractants was drastically reduced (Figure 37). This indicates that NADPH oxidases may be involved in the chemotropic sensing of *F. oxysporum*.

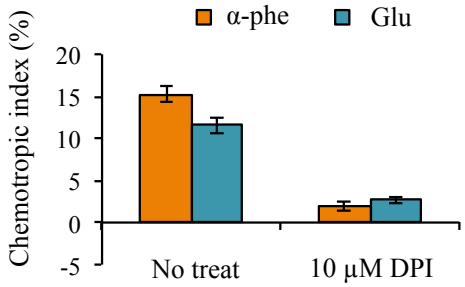

Figure 36. Specific inhibitor of NAPDH oxidases (DPI) blocks chemotropic response of *F. oxysporum* towards the α-pheromone and the sodium glutamate. Directed hyphal growth of *F. oxysporum* wt strain germ tubes towards 378 µM α-pheromone and 2.95 mM sodium glutamate; untreated and in presence of 10 µM DPI. Mean values were calculated from two independent experiments, each with 500 germlings scored. Error bars, s.d.

3.14 Peroxidase activity elicits developmental changes in *F. oxysporum*

Besides its chemoattractant properties, we investigated the possibility of additional effects of oxidized ABTS on *F. oxysporum*. Strinkingly, we found that germlings exposed to a gradient of oxidized ABTS formed characteristic bulges that were not observed in the water control (Figure 37A). The percentage of fungal cells presenting the bulge phenotype increased linearly with the concentration of oxidized ABTS until reaching a maximum of 80 % at 500 µM (Figure 37B). Interestingly, the morphological effect was observed at concentrations of oxidized ABTS that were well above those eliciting maximum chemotropism (Figure 37B). At concentrations higher than 500 µM, a decrease in the percentage of a germlings presenting this phenotype was observed.

Even at these high concentrations, the germlings did not present any symptoms of stress or dead cells.

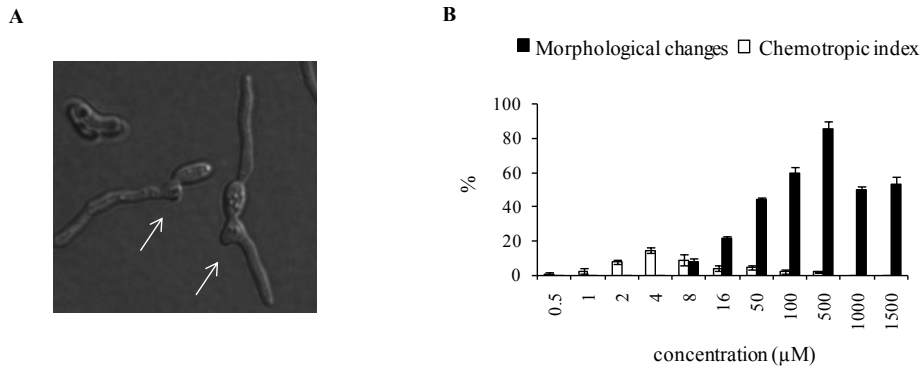

Figure 37. Peroxidase activity elicits morphological changes in *F. oxysporum*. A. Morphological changes seen in *F. oxysporum* wt germlings in presence of a gradient of 500 μM oxidized ABTS. Arrows point to the bulge-like structures. **B.** Chemotropic response of *F. oxysporum* (empty bars) and percentage of germlings displaying morphological changes (black bars) in the presence of increasing concentrations of oxidized ABTS. Germlings were observed and scored on the central line. Mean values were calculated from two independent experiments, each with 500 germlings scored. Error bars, s.d.

3.15 Evidence for a conserved role of secreted plant root peroxidases as fungal chemoattractants

Our previous results showing that commercial peroxidase from the non-host plant horseradish can trigger a chemotropic response in *F. oxysporum* f. sp. *Lycopersici* suggest that the role of class III peroxidases as chemoattractants of root-infecting fungi could be broadly conserved. To test this idea, we measured directed growth of *F. oxysporum* towards the root exudates of wheat (a monocot) and *A. thaliana* (a dicot). We observed a significant chemotropic response towards the wheat root exudate (12,13%), which also exhibited a detectable enzymatic activity in the peroxidase assay (Figure 38). Chemotropic response and enzymatic activity were drastically reduced after boiling or in the presence the peroxidase inhibitor SH. Interestingly, in presence of the wheat root exudates several germ tubes displayed a bulge phenotype previously observed in the presence of oxidized ABTS (data not shown).

By contrast, no chemotropic response was detected towards *A. thaliana* root exudates possibly because these root exudates did not display significant peroxidase enzymatic activity (Figure 38). When *A. thaliana* root exudates were concentrated 10 times (RE 10X), a chemotropic response was detected. This response was not abolished with two concentrations of SH (60 mM, normally used and 92 mM, the maximum solubility in water) (Figure 40B). However the slight reduction obtained in presence of both inhibitor concentrations suggest that the concentrations of inhibitors used may be too low to fully abolish peroxidase enzymatic activity in the RE 10X. Alternatively, we cannot exclude that additional components of the RE such as concentrated nutrients may contribute to the chemotropic response. Using a nutrient-insensitive strain such as the *fmk1*Δ mutant should allow to dicriminate between the two hypotheses.

These results point towards a general rather than a host plant-specific role of secreted root peroxidases in chemoattraction of *F. oxysporum* f. sp. *lycopersici*. Therefore host-specific interactions leading to compatibility or incompatibility between the fungus and the plant are likely to be established at later stages of the infection process.

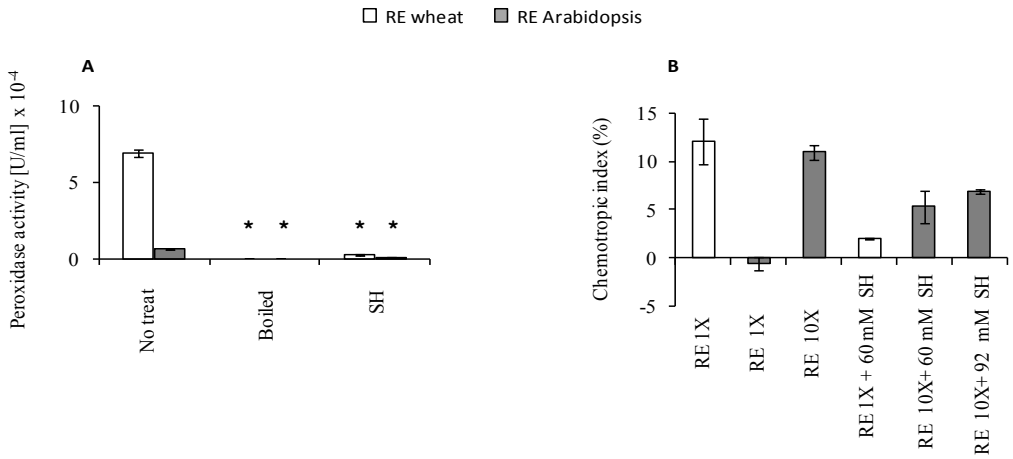

Figure 38. Root exudates from wheat and *Arabidopsis thaliana* trigger chemotropism in *F. oxysporum* through peroxidase activity. A. Peroxidase activities were determined in root exudates obtained from 4 days-old seedlings of wheat (white bars) or *A. thaliana* (grey bars), either untreated (No treat), boiled or in presence of 75 μM SH. Enzymatic activity is expressed as units/ml (U/ml). *, P≤0.0005 according to an unpaired *t* test. Error bars represent s.d. from three technical replicates. **B.** Directed hyphal growth of *F.*

oxysporum towards a gradient of root exudates from wheat (white bars) or *A. thaliana* (grey bars). Root exudates were applied either at a concentration of 1X or 10X, in the absence or presence of 60 mM or 92 mM SH. Mean values were calculated from two independent experiments, each with 500 germlings scored. Error bars, s.d.

4. Virus-induced gene silencing of *TMP1*, *TMP2* and *CEVI1* genes in tomato plants

Gene silencing in plants - The results obtained in the previous sections provide strong evidence suggesting that *F. oxysporum* is attracted towards plant roots through the activity of secreted class III peroxidases. To further substantiate these results, and to understand how they relate to the disease process itself, we aimed to obtain functional evidence from the plant side by silencing the expression of specific class III peroxidase genes in tomato plants.

T-DNA integration (Azpiroz-Leehan and Feldmann 1997) and transposons based insertional inactivation (Martienssen 1998; Parinov, Sevugan et al. 1999; Speulman, Metz et al. 1999; Tissier, Marillonnet et al. 1999) have been traditionally used as genetic tools to inactivate genes in plants for functional analysis. However, these techniques present several drawbacks, such as the impossibility to disrupt certain genes, loss of non-viable insertion mutants, gene target bias, and the abscence of a phenotype in the case of duplicated genes in the plant genome.

More recently, double-stranded RNA interference (dsRNAi) and variants thereof have been used for gene silencing in plants. The dsRNAi method is based on post-transcriptional gene silencing (PTGS) (Baulcombe 1999; Dinesh-Kumar, Anandalakshmi et al. 2003). PTGS does not affect transcription of the target gene, but rather its transcript levels because mRNA molecules become unstable. The process of RNA-mediated systemic silencing mechanism was first described in the fungus *Neurospora crassa* as quelling (Romano and Macino 1992) and subsequently in mammals as RNA interference (Fire, Xu et al. 1998). It involves the generation of double stranded RNA, of small (21 to 25 nucleotide) interfering RNAs (siRNAs) that mediate specific cleavage of the target mRNAs (Klahre, Crete et al. 2002).SiRNAs are processed from long double-stranded RNAs (dsRNA) by the RNAse-like enzyme

DICER, prior to their incorporation into the RNA-induced silencing complex (RISC). The complex targets specific mRNA transcripts exhibiting sequence complementarity with the specific siRNA, inducing its degradation (Bartel 2004) (Figure 39).

Virus-Induced Gene Silencing (VIGS) - Even though efficient in generating silenced transgenic lines, the initial dsRNAi methods in plants required the generation of stable plant transformants, which prevented their use for large scale screening studies in most plant species.

Virus-Induced Gene Silencing (VIGS) provides a reliable, cost-efficient and straight forward method for the rapid generation of a phenotype without the need to obtain stable transformants. VIGS is induced by the presence of a recombinant viral genomic RNA carrying a partial sequence of the target plant gene. As the virus replicates and spreads throughout the plant, the endogenous gene transcripts which are homologous to the insert in the viral vector are degraded. Historically, the term VIGS was first used to describe siRNA-based resistance against viral infection (Kammen 1997). Plants infected viruses induce RNA-mediated defense which targets viral RNAs and any transgene RNA products inserted into it (Voinnet 2001).

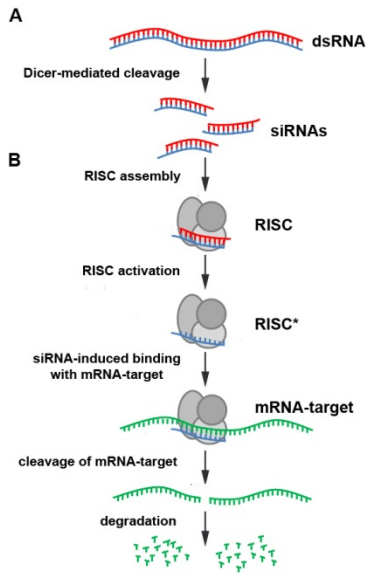

Figure 39. Mechanisms of post-transcriptional gene silencing (PTGS). A. SiRNAs are processed from long double-stranded RNAs (dsRNA) by DICER **B.** SiRNAs were then incorporated into the RNA-induced silencing complex (RISC). Activated RISC (RISC*) unwinds the siRNAs and targets specific mRNA transcripts sharing sequence complementarity, leading to their selective degradation (Petrova, Zenkova et al. 2013)

Vectors for VIGS - For use in VIGS, around ten plant host-specific viruses have been genetically modified for silencing genes of interest (Unver and Budak 2009). In our study, we used the tobacco rattle virus (TRV)-derived vector which has been widely used in various plant species including Arabidopsis, different Solanaceous species, opium poppy and *Aquilegia vulgaris*, among others (Dalmay, Hamilton et al. 2000; Liu, Schiff et al. 2002; Ekengren, Liu et al. 2003). An advantage of this vector in Solanaceous is the ease of introduction into plants. Additionally, TRV spreads efficiently throughout the entire plant, including the meristematic tissue and the infection symptoms are mild (Ratcliff, Martin-Hernandez et al. 2001). Liu *et al.,* were the first to use this vector in tomato plants, demonstrating its efficiency in inducing silencing of the *PDS*, *CTR1* and *CTR2* genes encoding Raf-like MAPKKKs (Liu, Schiff et al. 2002).

TRV is a bipartite, positive-strand RNA virus consisting of the TRV1 and TRV2 genomes. TRV1 encodes two replicase proteins of 134 and 194 kDa from the genomic RNA, a 29 kDa movement protein and a 16 kDa cysteine-rich protein from the subgeV 35S promotor and a nopaline synthase terminator (NOSt) and cloned into an *Agrobacterium* T-DNA vector. In the TRV2 cDNA construct, non-essential structural genes were replaced with a multiple cloning site (MCS) for insertion of the target gene sequences. Addtionally, a self-cleaving ribozyme site was included at the 3' end of TRV2. To induce VIGS silencing, the modified TRV2 and TRV1 are introduce into the plant by agroinoculation (Senthil-Kumar and Mysore 2014).

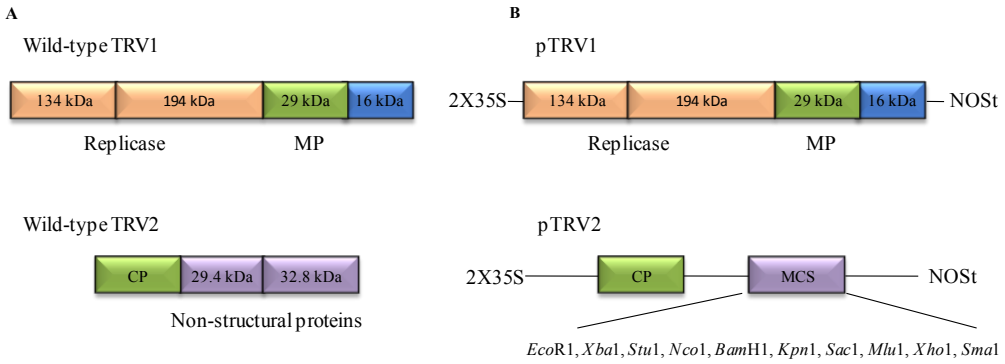

Figure 40. TRV1 and TRV2 constructs for VIGS. A. Tobacco rattle virus (TRV) is a bipartite, positive-sense RNA virus. TRV1 encodes 134 and 194 kDa replicase proteins, 29 kDa movement protein (MP), and 16 kDa cysteine-rich protein from. TRV2 encodes coat protein (CP) and two nonstructural proteins. **B.** To construct the TRV-based VIGS vector, a cDNA clone of TRV1 or TRV2 was placed between a duplicated CaMV 35S promoter and nopaline synthase terminator (NOSt) in an *Agrobacterium* T-DNA vector. In the TRV2 cDNA construct, nonessential structural genes were replaced with a multiple cloning site (MCS).

Our aim was to use the VIGS silencing method to knock down the expression of the class III peroxidase genes *TMP1*, *TMP2* and *CEVI-1* in tomato plants, in order to corroborate the role of these enzymes in chemotropic hyphal growth of *F. oxysporum* towards the plant roots.

4.1 Construction of VIGS vectors and Agrobacterium-mediated transformation of tomato plants

We used a TRV-based VIGS vector to corroborate the function of root secreted tomato peroxidases on the chemotropic response of *F. oxysporum*. A mixture of *Agrobacterium* cultures containing pTRV-*RNA1* andpTRV-*RNA2* T-DNA constructs (pTRV-*RNA2*::*TMP*, pTRV-*RNA2*::*CEVI* and pTRV-*RNA2*::*AP*) was infiltrated onto the lower leaves of 3 weeks-old tomato plants.

pTRV-*RNA2*::*CEVI*, also called pTRV2-*CEVI* plasmid, was used to silence the *CEVI-1* gene. A fragment of *CEVI-1* cDNA, corresponding to bases 406-692, which has low homology with *TMP1* and *TMP2* cDNA (< 30%) was cloned into pTRV2 plasmid. The best target region, which generally corresponds to a sequence < 400 bp that has no or low homology with other mRNA sequences, was choosen using the VIGS tool software (http://vigs.solgenomics.net/, Table 11). pTRV-*RNA2*::*TMP* plasmid (pTRV2-*TMP*) was used to silence both the *TMP1* and *TMP2* genes. A 307-bp fragment of *TMP2* cDNA, corresponding to bases 533-798, was used as a template and cloned into pTRV2 plasmid. The selected region was highly conserved between *TMP1* and *TMP2* and presented low homology with *CEVI-1* (< 30%). Finally, pTRV-*RNA2*::*AP* (pTRV2-*AP*)

plasmid was used to silence simultaneously utmost class III peroxidase genes by a region, which is conserved among most of the peroxidases. *CEVI-1* cDNA was used as a template since it presented homology with a higher number of sequences when compared to *TMP1* or *TMP2*. A 388-bp *CEVI-1* cDNA fragment (corresponding to bases 533-798) was cloned into pTRV2.

Agro-infiltrated plants were grown in a growth chamber (15/9 h light/dark photoperiod, 28°C). Four weeks after infiltration, nine plants presented VIGS symptoms named a growth delay and characteristic spots and lighter zones on leaves were selected for each conditions and total RNA was prepared from the roots. The transcript level of *TMP1*, *TMP2* and *CEVI-1* were measured for tomato infiltrated with pTRV-*RNA1* and the three different pTRV-*RNA2* derivative plasmids and compared with their transcription levels in non-silenced tomato plants grown under the same conditions.

4.2 *CEVI-1* transcript levels were reduced in silenced plants

Transcript levels of *CEVI-1* in roots of plants transformed with pTRV2-*CEVI* were generally lower than in those transformed with the control construct pTRV2-*GFP*, as determined by qRT-PCR (Figure 41A). The average *CEVI-1* transcript level calculated from the nine analyzed pTRV2-*CEVI* plants was reduced by 33% compared to that of the pTRV2-*GFP* plants (Figure 41C). Moreover, in each individual pTRV2-*CEVI* plant, the *CEVI-1* transcript level was lower than the average transcript level in the control plants (Figure 41C). These results suggest that the VIGS strategy with the pTRV2-*CEVI-1* construct was moderately successful.

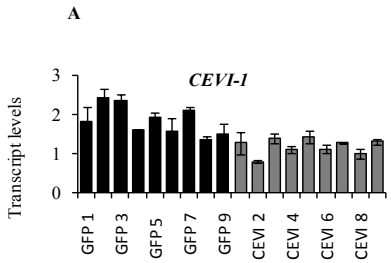

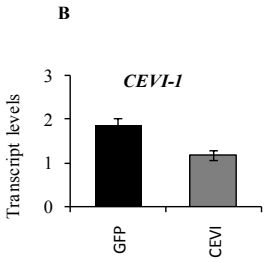

C

plant	% of silencing
CEVI 1	28.85
CEVI 2	55.14
CEVI 3	21.48
CEVI 4	38.41
CEVI 5	20.79
CEVI 6	37.59
CEVI 7	28.38
CEVI 8	43.38
CEVI 9	26.81

Figure 41. VIGS of *CEVI-1* leads to moderately reduced transcript levels in tomato roots. A, B. *CEVI-1* transcript levels were measured by qRT-PCR in roots of nine individual tomato plants infected with pTRV2-*CEVI* (grey bars) or with the negative control pTRV2-*GFP* (black bars). Transcript levels are expressed relative to those of the *EF1-α* gene. Error bars represent s.d. from three technical replicates. A. *CEVI-1* transcript levels in nine individual plants from each treatment (numbered from #1 through #9). **B.** Average *CEVI-1* transcript levels calculated from the nine plants per treatment shown in A. **C.** Percentage of reduction of *CEVI-1* transcript levels in nine individual plants infected with pTRV2-*CEVI* relative to the average *CEVI-1* transcript level calculated from nine plants infected with pTRV2-*GFP*. Percentages were obtained using the following formula: 100 - ((relative transcript level in individual plant infected with pTRV2-*CEVI* * 100) / average relative transcript level calculated from nine plants infected with pTRV2-*GFP*).

4.3 VIGS of *CEVI-1* affects *TMP1* and *TMP2* transcript levels

To ask whether partial silencing of *CEVI-1* had an effect on transcript levels of *TMP1* and *TMP2*, we quantified transcripts of *TMP1* and *TMP2* in plants inoculated with pTRV2-*CEVI* and compared them to those in the negative control. Although the average transcript level of *TMP1* in *CEVI-1* silenced plants was similar to that of the negative control (Figure 42B), a high heterogeneity among individual plants was observed (Figure 42A). Thus, *TMP1* transcript levels were strongly upregulated in 3 of the 9 plants analyzed, but downregulated in the remaining ones (Figure 42A and C). Interestingly, in control plants *TMP1* transcript levels did not display such variations (Figure 42A). These results suggest that silencing of *CEVI-1* might affect transcript levels of *TMP1* in a stochastic manner.

By contrast, *TMP2* transcript levels in plants inoculated with pTRV2-*CEVI* were reduced by 37% in average compared to those in the negative control (Figure 42E), and except for a single individual (plant CEVI-4), they were below the average in all plants (Figure 42D and F).

These results suggest that the VIGS-mediated silencing of a peroxidase gene may result in changes in transcript levels of other peroxidases genes, although in this case the variations did not always present the same pattern. While *TMP1* transcript levels were

randomly deregulated in *CEVI-1* silenced plants, *TMP2* transcript levels were generally reduced. In further experiments, it would be interesting to investigate if expression of certain peroxidase genes could be upregulated in these plants to compensate for the loss of CEVI-1 function.

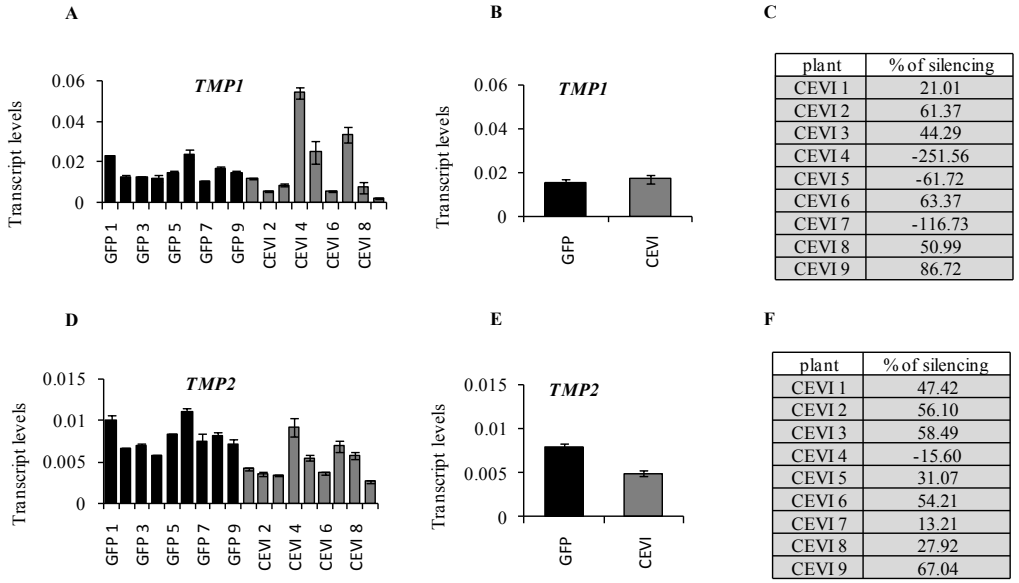

plant	% of silencing
CEVI 1	21.01
CEVI 2	61.37
CEVI 3	44.29
CEVI 4	-251.56
CEVI 5	-61.72
CEVI 6	63.37
CEVI 7	-116.73
CEVI 8	50.99
CEVI 9	86.72

plant	% of silencing
CEVI 1	47.42
CEVI 2	56.10
CEVI 3	58.49
CEVI 4	-15.60
CEVI 5	31.07
CEVI 6	54.21
CEVI 7	13.21
CEVI 8	27.92
CEVI 9	67.04

Figure 42. VIGS of *CEVI-1* results in changes in *TMP1* and *TMP2* transcript levels. A, B, D and **E.** *TMP2* and *TMP1* transcript levels were measured by qRT-PCR in roots of nine individual tomato plants infected with pTRV2-*CEVI* (grey bars) or with the negative control pTRV2-*GFP* (black bars). Transcript levels are expressed relative to those of the *EF1-α* gene. Error bars represent s.d. from three technical replicates. **A, D.** *TMP2* or *TMP1* transcript levels in nine individual plants from each treatment. **B, E.** Average *TMP2* or *TMP1* transcript levels calculated from the nine plants per treatment. C, F. Percentage of reduction of *TMP2* or *TMP1* transcript levels in nine individual plants infected with pTRV2-*CEVI* relative to the average of *TMP2* or *TMP1* transcript levels in plants infected with pTRV2-*GFP*.

4.4 VIGS of *TMP1* and *TMP2* leads to increased transcript levels of both genes

We next quantified *TMP1* and *TMP2* transcript levels in nine plants inoculated with pTRV2-*TMP*, a construct carrying a conserved region designed to silence both genes simultaneously (see Materials and Methods). Unexpectedly, transcript levels of both genes were significantly upregulated in these plants, with an average increase around 45% (Figure 43B and E). Except for individuals TMP4 and TMP6 in the case of *TMP1* and individuals TMP7 and TMP8 in the case of *TMP2,* all the plants showed an increase in transcript levels of the two genes (Figure 43A, C, D and F).

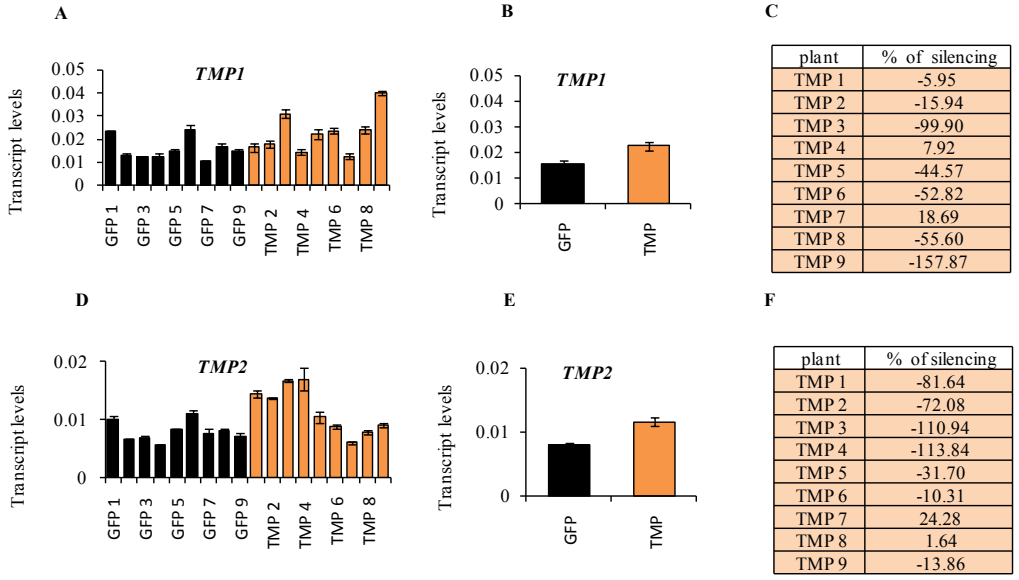

plant	% of silencing
TMP 1	-5.95
TMP 2	-15.94
TMP 3	-99.90
TMP 4	7.92
TMP 5	-44.57
TMP 6	-52.82
TMP 7	18.69
TMP 8	-55.60
TMP 9	-157.87

plant	% of silencing
TMP 1	-81.64
TMP 2	-72.08
TMP 3	-110.94
TMP 4	-113.84
TMP 5	-31.70
TMP 6	-10.31
TMP 7	24.28
TMP 8	1.64
TMP 9	-13.86

Figure 43. Simultaneous VIGS of *TMP1* and *TMP2* leads to an increase in the transcipt levels of both genes. A, B, D and **E.** *TMP2* and *TMP1* transcript levels were measured by qRT-PCR in roots of nine individual tomato plants infected with pTRV2-*TMP* (orange bars) or with the negative control pTRV2-*GFP* (black bars). Transcript levels are expressed relative to those of the *EF1-α* gene. Error bars represent s.d. from three technical replicates. **A, D.** *TMP2* or *TMP1* transcript levels in nine individual plants from each treatment. **B, E.** Average *TMP2* or *TMP1* transcript levels calculated from the nine plants per treatment. **C, F.** Percentage of reduction of *TMP2* or *TMP1* transcript levels in nine individual plants infected with pTRV2-*TMP* relative to the average of *TMP2* or *TMP1* transcript levels in plants infected with pTRV2-*GFP*.

VIGS with a general construct targeting class III peroxidase genes has no detectable effect on *TMP1*, *TMP2* and *CEVI-1* transcript levels

4.5 VIGS with a general construct targeting class III peroxidase genes has no detectable effect on *TMP1*, *TMP2* and *CEVI-1* transcript levels

In an attempt to target a large number of peroxidase genes, we designed the pTRV2-AP construct carrying a sequence corresponding to a region highly conserved in class III peroxidases (see Materials and Methods). In plants carrying this construct, *TMP1* and *TMP2* transcript levels did not differ significantly from those of the control plants (Figure 44A-F). By contrast, *CEVI-1* transcript levels showed a significant increase in 8 of the 9 plants analyzed (Figure 44G-I).

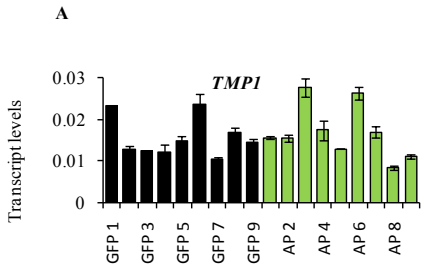

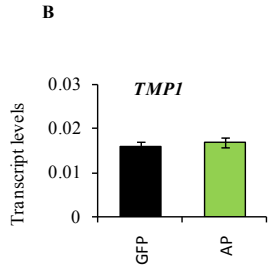

C

plant	% of silencing
AP 1	-1.30
AP 2	0.37
AP 3	78.75-
AP 4	12.59-
AP 5	15.91
AP 6	70.75-
AP 7	9.81-
AP 8	45.58
AP 9	28.17

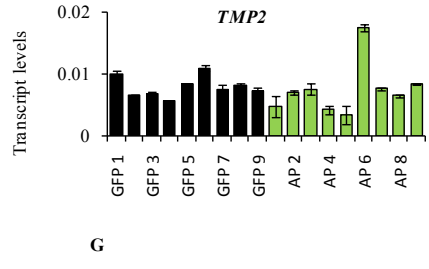

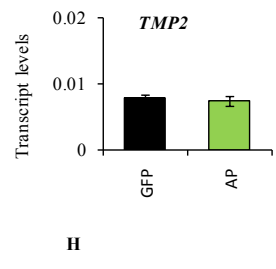

F

plant	% of silencing
AP 1	40.38
AP 2	11.70
AP 3	4.78
AP 4	47.17
AP 5	57.23
AP 6	119.75-
AP 7	4.28
AP 8	18.36
AP 9	4.53-

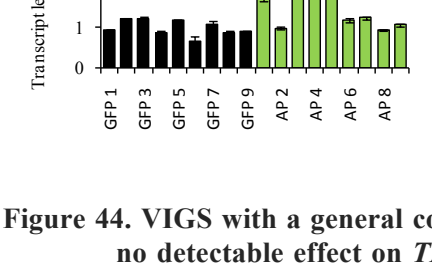

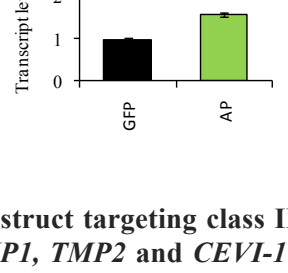

I

plant	% of silencing
AP 1	-80.88
AP 2	-3.92
AP 3	112.65-
AP 4	157.13-
AP 5	184.41-
AP 6	24.82-
AP 7	30.19-
AP 8	0.97
AP 9	11.86-

Figure 44. VIGS with a general construct targeting class III peroxidase genes has no detectable effect on *TMP1, TMP2* and *CEVI-1* transcript levels. A, B, D, E, G and H. *TMP1, TMP2,* and *CEVI-1* transcript levels were measured by qRT-PCR in roots of nine individual tomato plants infected with pTRV2-*AP* (green bars) or with the negative control pTRV2-*GFP* (black bars). Transcript levels are expressed relative to those of the *EF1-α* gene. **B, E** and **H.** Average *TMP1* or *TMP2* or *CEVI-1* transcript levels calculated from the nine plants per treatment. **C, F** and **I.** Percentage of reduction of *TMP1* or *TMP2* or *CEVI-1* transcript levels in nine individual plants infected with pTRV2-*AP* relative to the average of *TMP1*, *TMP2* or *CEVI-1* transcript levels in plants infected with pTRV2-*GFP*.

A summary of transcript levels of *TMP1*, *TMP2*, and *CEVI-1* in plants inoculated with pTRV2-*TMP*, pTRV2-*CEVI*, and pTRV2-*AP* is given in the table below. In summary, only the expression of *CEVI-1* was successfully knocked-down by VIGS, although the silencing was only partial.

Table 14. Summary table showing the average percentage of the *TMP1*, TMP2 and *CEVI-1* transcript levels in tomato plants infected with pTRV2-*TMP*, pTRV2-*CEVI* and pTRV2-*AP* in relation to the control plants infected with pTRV2-*GFP*, where 100% means that there is neither silencing nor increase in transcripts.

Gene/Construct	pTRV2-*TMP*	pTRV2-*CEVI*	pTRV2-*AP*
TMP1	143,03 %	109,79 %	107,69 %
TMP2	146,01 %	62,45 %	93,84 %
CEVI-1	Not checked	63,95 %	159,15 %

4.6 *TMP1*, *TMP2* and *CEVI-1* transcript levels in individual tomato plants do not correlate with peroxidase enzymatic activity in root exudates

To study the contribution of *TMP1*, *TMP2* and *CEVI-1* transcript levels to total peroxidase activity in the tomato root exudate, peroxidase activity was measured in root exudates obtained from individual plants inoculated carrying pTRV2-*GFP*, pTRV2-*CEVI*, pTRV2-*TMP* or pTRV2-*AP*. We failed to detect a correlation between peroxidase gene transcript levels of individual plants and secreted peroxidase activity in their root exudate (Figure 45). For example, although the *CEVI-1* transcript level in plant CEVI 1 was higher than those in plant CEVI 2 plant, peroxidase activities in root exudates of the two plants plants were similar (Figure 45 A and D). As another example, plant CEVI 3 presents a slightly higher transcription level of *CEVI-1* compared to CEVI 4, while the peroxidase activity of CEVI 3 is considerably higher than that of CEVI 4. Interestingly, *TMP1* and *TMP2* where both significantly more expressed in CEVI 3 than in CEVI 4 (Figure 45A-D).

An absence of correlation was observed in plants inoculated with the other vectors. For example, *CEVI-1* transcript levels in GFP 1 and GFP 3 plants do not match with peroxidase activities in these plants, and similar observations were made regarding *TMP1*, *TMP2* and *CEVI-1* transcript levels and peroxidases activities in plants

inoculated with pTRV2-*AP* (Figure 45). Collectively, these results suggest that the levels of peroxidase enzymatic activity in the root exudates cannot be solely explained by the transcript levels of *CEVI-1*, *TMP1* and *TMP2*, suggesting that additional class III peroxidase genes must contribute to this activity.

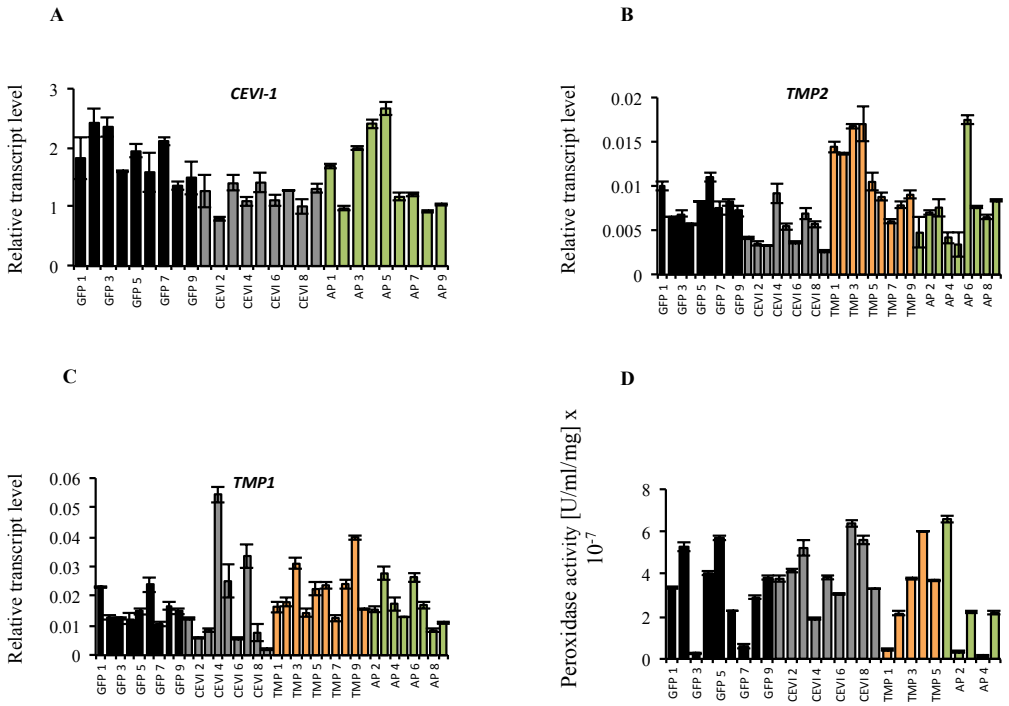

Figure 45. Absence of correlation between *TMP1*, *TMP2* and *CEVI-1* transcript levels and peroxidase enzymatic activity in root exudates of individual tomato plants. A, B, C. Transcription levels of *CEVI-1* (A), *TMP2* (B) and *TMP1* (C) in roots of individual tomato plants *Agro*-infiltrated with pTRV2-*GFP* (named from GFP 1 to GFP 9), pTRV2-*CEVI-1* (named from CEVI 1 to CEVI 9), pTRV2-*TMP* (named from TMP 1 to TMP 9) and pTRV2-*AP* (named from AP 1 to AP 9). Transcript levels were quantified by qRT-PCR and are expressed relative to those of the *EF1-α* gene. **D**. Peroxidase activities in root exudates obtained from individual tomato plants infected with pTRV2-*GFP* (named from GFP 1 to GFP 9), pTRV2-*CEVI* (named from CEVI 1 to CEVI 9), pTRV2-*TMP* (named from TMP 1 to TMP 5) and pTRV2-*AP* (named from AP1 to AP5). Enzymatic activity is expressed as units/ml per mg fresh root weight (U/ml/mg). Error bars represent s.d. from three technical replicates.

An important finding derived from these experiments was that peroxidase enzymatic activity in root exudates may differ considerably between individual tomato plants, even when normalized to root biomass. To corroborate this finding, we measured peroxidase activity in root exudates of untransformed tomato plants, and also found large differences between different individuals (Figure 46A). This natural variation most likely reflects the multiplicity and complex temporal and spatial regulation of class III peroxidase genes. To exploit this natural variation for further strengthening the functional link between secreted root peroxidase activity and fungal chemoattraction on the plant side, we determined the effect of the root exudates on directed hyphal growth of *F. oxysporum*. We observed a significant correlation between secreted peroxidase activity in root exudates of individual plants and their chemoattractant activity towards the fungus (Figure 46B).

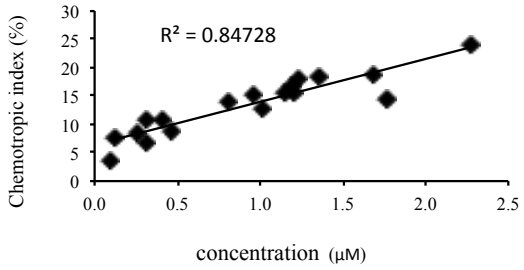

Figure 46. Relationship between peroxidase enzymatic activity of REs and the elicited chemotropic response. Each dot represents a RE sample obtained from an individual tomato plant (n = 18). Linear regression (solid line) and 95% mean prediction interval (dashed lines) indicate that the twovariables are linearly correlated ($P < 0.001$, chemotropism assay performed by Dr. David Turra).

5. Fungal chemoattraction by purified recombinant TMP2 and CEVI-1 proteins requires an intact catalytic site.

Insights into catalytic properties of horseradish peroxidase from site-directed mutagenesis - As previously mentioned, the reaction catalysed by the majortity of class III plant peroxidases can be summaried by the equation $H_2O_2 + 2\ AH_2 \rightarrow 2H_2O + 2A_2\bullet$. This reaction is divided into three main steps, as shown below(Veitch 2004).

$$E(Fe^{III}, R) + H_2O_2 \xrightarrow{k_1} E(Fe^{IV}=O, R^{\cdot+}) + H_2O$$

compound I

$$E(Fe^{IV}=O, R^{\cdot+}) + AH_2 \xrightarrow{k_2} E(Fe^{IV}=O, R) + AH^{\cdot}$$

compound II

$$E(Fe^{IV}=O, R) + AH_2 \xrightarrow{k_3} E(Fe^{III}, R) + AH^{\cdot} + H_2O$$

$$2AH^{\cdot} \longrightarrow A_2H_2$$

1) The first step is the reaction between the H_2O_2 and the resting state of the enzyme, represented by equation. E represents the enzyme for which the oxidation state of the heme-iron atom and the status of the porphyrin are indicated in parenthesis. This generates a high oxidation state intermediate known as compound I, which is considered to be two oxidizing equivalents above the Fe (III) resting state of the enzyme. This intermediate comprises an iron (IV) oxoferryl centre and a porphyrin-based cation radical.

2) Step 2 consists of the first of two subsequent one-electron reduction steps. Compound I is reduced to compound II, and the reducing substrate AH_2 is oxidized to radical product $AH^{\cdot}$. Compound II, a second iron (IV) oxoferryl species, is one oxidizing equivalent above the Fe(III) resting state of the enzyme.

3) The reaction cycle is completed by the second one-electron reduction step shown in the last equation. Another molecule of reducing substrate is oxidized to the

corresponding radical product. The mechanism of each of these three steps has been investigated in detail, and can best be considered in two parts: the formation of compound I and the reduction of compounds I and II.

Purification of secreted peroxidases from plants is a laborious and time-consuming process with low yield, besides the difficulty of isoenzyme separation (Duarte-Vazquez, Garcia-Almendarez et al. 2001). As an alternative, heterologous expression systems have been used for the production and analysis of recombinant class III peroxidases (Howes, Veitch et al. 2001). The availability of the three-dimensional structure of the catalytic intermediates and of site-directed mutantsof HRP-C has provided detailed insights into the role of specific amino acid residues and structural features in class III peroxidase enzymatic activity (Berglund, Carlsson et al. 2002). Thus, His42 and Arg38 play a crucial role in the catalysis of hydrogen peroxide and are essentially invariant among all plant peroxidases (Poulos and Kraut 1980). His42 acts as a proton acceptor when peroxide binds to the heme iron. Arg38 plays a significant role in controlling the positioning and ionization state of His42 and the stabilization of the substrate in the active site, by creating hydrogen-bond interactions (Henriksen, Smith et al. 1999; Meno, Jennings et al. 2002) (Figure 47A).

Analysis of different site-directed mutants revealed that $HRP_{R38S,H42E}$ mutant enzyme exhibits a reduction estimated in 6 orders of magnitude in the activity constant k_1 for the formation of coumpound I (Figure 47B) (Meno, Jennings et al. 2002). Generally, mutants affected in His42 showed a stronger decrease in k_1 than Arg38 mutants (Rodriguez-Lopez, Smith et al. 1996; Savenkova, Newmyer et al. 1996).

Other amino acids surrounding Arg38 and His42 also play an important role in the enzymatic activity of peroxidases. Pro139 is conserved in all plant peroxidases and is directly involved in substrate binding and oxidation; Phe41 presents the substrate access to the ferryl oxygen of compound I; and Asn70 maintains the basicity of His42 by forming a hydrogen bond. On the opposite side of the heme, the most important amino acid residues of the proximal heme binding domain are His170 and Asp247 which,

respectively, form a coordinate bond with the heme iron atom and contribute to the stability of His170 (Figure 47B).

A

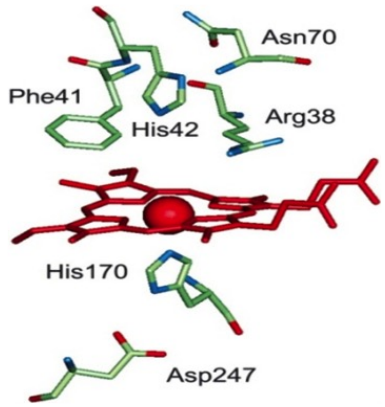

B

HRP C	K_1 (M^{-1} s^{-1})	HRP C	K_1 (M^{-1} s^{-1})
WT	1.7×10^7	H42L	1.4×10^2
R38A	8.0×10^4	H42Q	9.6×10^1
R38H	1.3×10^6	H42D	1.3×10^3
R38K	4.0×10^4	E64G	4.3×10^5
R38L	1.1×10^4	E64P	4.4×10^5
F41V	2.1×10^6	E64S	4.3×10^5
H42A	**1.9×10^1**	N70D	1.5×10^6
H42A:F41H	3.0×10^4	N70V	6.0×10^5
H42A:N70D	3.7×10^1	H42E	4.9×10^3
H42V:R38H	1.6×10^3	F221W	1.5×10^7
H170A	**1.6×10^1**	F172Y	1.6×10^7
H42E:R38S	**3.2×10^1**		

Figure 47. Essential residues of horseradish peroxidase isoenzyme C (HRP-C). A. Key amino acid residues in the heme-binding region of HRP-C (Veitch 2004). **B.** Summary of the rate constant associated with the formation of compound I (k_1) in wild-type HRP-C and selected site-directed mutants (Howes, Veitch et al. 2001). Green boxes show those mutants with the lowest k_1.

Heterologous expression of tomato class III peroxidases as a strategy to investigate their role in fungal chemotropism - We previously found that the VIGS gene silencing approach was unsuccessful for functional analysis of a large and functionally redundant gene family such as class III plant peroxidases (see previous chapter). We reasoned that an alternative proof-of-concept approach would consist in expressing TMP2 and CEVI-1, the two major tomato peroxidases identified in root exudates in a heterologous organism such as *E. coli* to confirm their chemoattractant activity against *F. oxysporum*. Additionaly, we decided to test a catalytically inactive TMP2 version obtained by site-directed mutagenesis of the essential residues Arg38 and the His42. Although active recombinant peroxidases have been produced in a number of heterologous systems such as baculovirus (Hartmann and Ortiz de Montellano 1992), *S.*

cerevisiae (Morawski, Lin et al. 2000) or *Pichia pastoris* (Morawski, Lin et al. 2000), *E. coli* remains the most attractive due to low cost, high productivity and rapid growth, well-characterized genetics and availability of efficient cloning vectors and expression strains (Smith, Santama et al. 1990; Terpe 2006)**.**

The aim of this section was to use heterologous expression in *E. coli* to obtain purified recombinant tomato peroxidases CEVI-1 and TMP2 and to test their chemoattractant activity against *F. oxysporum*. Moreover, we decided to generate $TMP2_{R38S,H42E}$ mutant protein where the Arg38 and His42 which were previously shown to be essential for the catalytic activity of class III peroxidases (Meno, Jennings et al. 2002) had been replaced, respectively, by aserine and a glutamic acid.

5.1 Generation of pET28-*TMP2*, pET28-$TMP2_{R38S,H42E}$ and pET28-*CEVI* constructs

To heterologously produce TMP2 and CEVI-1 in *E. coli*, respective cDNAs were amplified from RNA extracted from 2 weeks-old tomato plants. We previously demonstrated that the expression levels of both genes are very low in tomato roots (Figure 22A). Using a strategy to discriminate between *TMP1* and *TMP2* cDNAs based on a two rounds PCR amplification, *TMP2* cDNA could successfully be amplified for tomato roots. This strategy consists in using for the first PCR, a gene-specific forward primer that anneal exclusively to the 5'UTR region of *TMP2* and not to *TMP1*, then a forward primer that anneal to a conserved region between *TMP1* and *TMP2*. The products of the first PCR were used as templates for the second one. The first PCR was necessary since the 5' region of *TMP1* and *TMP2* coding sequences, which is required for the production of the recombinant peroxidases, is conserved between both cDNAs.

A different strategy was used to amplify *CEVI-1*. Mayda et al, reported that the expression of *CEVI-1* was induced by stresses such as wounding (Mayda, Marques et al. 2000). We, therefore, performed wounds using a scalpel in leaves of 2 weeks-old

plants and kept them in a growth chamber during 55h (15/9 h light/dark photoperiod, 28°C, see Materials and Methods). In such condition, *CEVI-1* RNA were isolated successfully. *CEVI-1* and *TMP2* cDNAs were further cloned into pGEMT.

TMP2$_{R38S,H42E}$ was generated by site-directed mutation using the fusion PCR method and pGEM-*TMP2* plasmid as a template. For *R38S* mutation, the first cytosine in nucleotide triplet encoding R38 was substituted by an adenine. For *H42E* mutation,the first cytosine and the third thymine in the nucleotide triplet encoding H42 were both substituted by guanine.

Finally, *TMP2, TMP2*$_{R38S,H42E}$ and *TMP2*$_{R38S,H42E}$ cDNAs were excised from pGEMT and cloned into the expression vector pET-28a(+).

5.2 Heterologous production of TMP2, TMP2$_{R38S,H42E}$ and CEVI-1 constructs in *E. coli*

E. coli BL21 (DE3) CodonPlus strains carrying *TMP2, TMP2*$_{R38S,H42E}$ or *CEVI-1* cDNAs were initially grown at three different temperatures (23, 28 and 37°C) in order to optimize expression of the heterologous protein (Figure 48A and C). Total protein extracts obtained at the three different temperatures, either before or after induction with isopropyl-beta-D-thiogalactopyranoside (IPTG) were analyzed by SDS-PAGE. Extracts from bacterial cells grown in the presence of IPTG contained a differential protein band of approximately 45 kDa, which is consistent with the predicted molecular size of His$_6$-tagged recombinant proteins TMP2, TMP2$_{R38S,H42E}$ and CEVI-1 (Figure 48B and D). In aggrement with previous studies on HRP (Meno, Jennings et al. 2002), the recombinant tomato peroxidases were insoluble and trapped in the bacterial inclusion bodies (Figure 48B and D). Attempts to obtain soluble protein by using lower temperatures (23°C and 28°C) were unsuccessful. We therefore decided to use 37°C in the subsequent experiments, since the amount of recombinant protein was highest at this temperature. Recombinant peroxidases were further purified from the insoluble fraction by Immobilized-Metal Affinity Chromatography (IMAC) (Figure 48B and D).

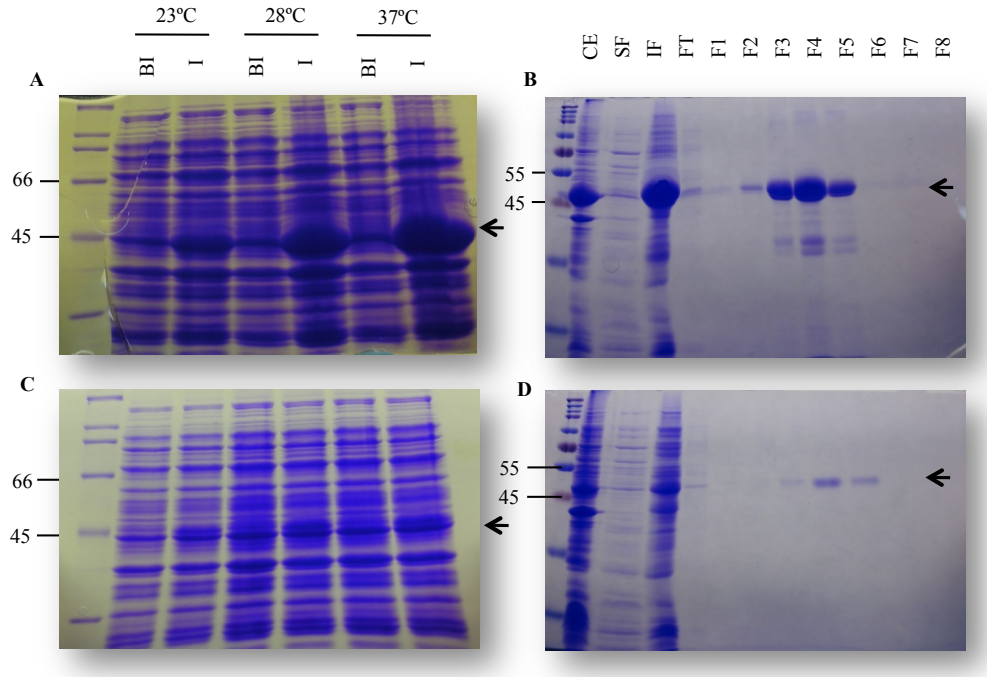

Figure 48. Heterologous expression and purification of TMP2 and CEVI-1 from *E. coli.* A. C. *E. coli* strains BL21(+)pET28a-*TMP2* (A) and BL21(+)pET28a-*CEVI-1* (B) were grown at 23ºC, 28ºC or 37ºC in the absence (BI) or presence (I) of 0.5 mM IPTG. **B. D.** Cultures of BL21(+)pET28a-*TMP2* (B) or BL21(+)pET28a-*CEVI-1* (D) induced with 0.5 mM IPTG at 37ºC were harvested (CE; cell extract), cells were were lysed and the soluble (SF) and insoluble fraction (IF) were separated by centrifugation. Recombinant TMP2 and CEVI-1 proteins were purified from the IF by IMAC and eluted from the column using a linear gradient from 5 to 500 mM imidazole with a flow rate of 1 ml min^{-1} to collect 1.5 ml fractions F1 through F8. U.V absorption at 280 nm was monitored. Twenty µl of each fraction was analyzed by SDS-PAGE. Arrows point to recombinant proteins.

5.3 Recombinant TMP2 and CEVI-1, but not $TMP2_{R38S,H42E}$ display peroxidase enzymatic activity and elicit chemotropic growth in *F. oxysporum*

To determine the peroxidase enzymatic and the chemotropic activities of recombinant tomato proteins TMP2, $TMP2_{R38S,H42E}$ and CEVI-1, a large-scale purification followed by refolding and solubilization of the proteinswas performed (see Materials and

Methods for details). Analysis of the obtained recombinant proteins by SDS-PAGE revealed TMP2, $TMP2_{R38S,H42E}$ and CEVI-1 were successfully produced in *E. coli*. (Figure 49A).

Recombinant TMP2 and CEVI-1 proteins displayed significant peroxidase enzymatic activity (Figure 49B). Moreover, both proteins elicited a robust chemotropic response in *F. oxysporum* (Figure 49C). Interestingly, the point mutations introduced in the catalytic residues of $TMP2_{R38S,H42E}$ abolished both enzymatic and chemoattractant activities. This result confirms that peroxidase enzymatic activity is essential for the chemoattractant property of TMP2 towards *F. oxysporum*. Interestingly, 170 nM of TMP2 and CEVI-1 triggered a chemotropic response whose extent was similar to that elicited by 4 µM of HRP. This indicates that the two tomato peroxidases are more active chemoattractants than HRP, possibly because they exhibit a higher specificity for the putative substrate.

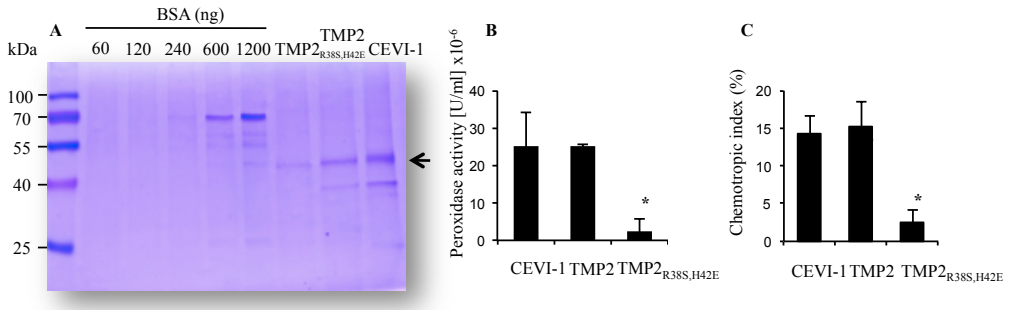

Figure 49. Recombinant TMP2 and CEVI-1, but not $TMP2_{R38S,H42E}$, display peroxidase enzymatic activity and elicit chemotropic growth in *F. oxysporum*. **A.** SDS-PAGE of heterologously expressed and purified tomato peroxidases CEVI-1, TMP2 and $TMP2_{R38S,H42E}$. Thirty µl of purified peroxidase sample and the indicated amounts of BSA (in ng) were loaded on the gel. **B.** Peroxidase enzymaticactivity of 56,3 nM of purified peroxidases CEVI-1, TMP2 or $TMP2_{R38S,H42E}$ was measured and expressed as units/ml (U/ml). Error bars represent s.d. from two technical replicates. (*,versus TMP2, $P < 0.005$) **C.** Directed growth of *F. oxysporum* towards a gradient of 169 nM recombinant CEVI-1, TMP2 or $TMP2_{R38S,H42E}$ (*,versus TMP2, $P < 0.0001$). Error bars, s.d.

Discussion

F. oxysporum Fmk1 and Mpk1 pathways contribute positively to the expression of *fpr1* in the presence of invasive growth-inducing conditions

In *S. cerevisiae,* the *rnr1*, *sfp1*, *tkl2*, *yps1*, *ssa4, htb2, dhh1* and *rpn12* genes were shown to be positively regulated by the Kss1 cascade. In this work we tested whether the *F. oxysporum* orthologs of these genes are differentially regulated in the *fmk1*Δ and/or *msb2*Δ mutants. Unexpectedly, none of them showed a differential expression pattern between the wt strain and these mutants. To explain the results, two hypotheses can be drawn.

(1) Gene regulation by the orthologous Fmk1/Kss1 pathways is not conserved between *Fusarium* and *Saccharomyces*. It is known that genes of the same functional family can function in distinct cellular processes. For example, in *S. cerevisae* the CLN1 cyclin is a morphogenetic regulator essential for pseudohyphal growth, whereas the close homolog CLN2 is dispensable for development (Hadwiger, Wittenberg et al. 1989). Thus, functional divergence might have occurred at the transcriptional regulation level between *F. oxysporum* and *S. cerevisae* downstream of the conserved MAPK modules.

(2) Regulation in the two species requires different stimuli and consequently different experimental conditions.

(3) Other genes regulated by the Fmk1 pathway might have functionally replaced the selected genes in *F. oxysporum*.

Together with previous studies (Perez-Nadales and Di Pietro 2011; Prados-Rosales, Roldan-Rodriguez et al. 2012), our data suggest that *fpr1* is an interesting candidate to monitor the activation status of the Fmk1 pathway, since its expression was strongly reduced in the *fmk1*Δ, *msb2*Δ, *ste12*Δ, *fmk1*Δ/*msb2*Δ and *msb2*Δ/*sho1*Δ mutants. However, the results obtained with the *mpk1*Δ mutants suggest that regulation of *frp1* relies both on the Fmk1 and the Mpk1 pathways. In agreement, *fpr1* showed intermediate expression levels in the two individual MAPK mutants, and was further reduced in the *fmk1*Δ*/mpk1*Δ double mutant. Cross talk between distinct MAPK signaling pathways is a well-characterized phenomenon and enables further complex

signaling behaviours. Therefore, we predict that it will difficult to identify a gene that is exclusively regulated by a single pathway such as the Fmk1 cascade. In *S. cerevisae,* expression of the cell-surface glycoprotein Flo11p, the best-characterized downstream effector of the filamentous growth pathway (Gagiano et al., 1999; Guo et al., Gagiano et al., 1999; Guo et al., 2000) is regulated both by the Kss1 and the PKA pathway (Lo and Dranginis 1996; Lo and Dranginis 1998). Our data suggest that *fpr1* regulation by the Fmk1 pathway is independent of the nitrogen-source used, while Mpk1-regulated *fpr1* induction is only functional under nitrogen-poor conditions.

We found that individual components of the Fmk1 pathway contribute differently to the regulation of *fpr1*expression. For example, *fpr1* transcript levels were not significantly reduced in the *sho1*Δ mutant. This is in agreed agreement with previous results (Perez-Nadales and Di Pietro 2014) showing that *fpr1* transcript levels were less reduced in the *sho1*Δ mutant in comparison to the *msb2*Δ and *msb2*Δ*sho1*Δ mutants during growth on solid medium. In *F. oxysporum*, the transmembrane protein Sho1 cooperates with the Msb2 receptor to regulate only a subset of the Fmk1-dependent functions, suggesting that the regulation of *fpr1* might be independent of this protein (Perez-Nadales and Di Pietro 2015). In other organisms such as the aerial plant pathogens *Ustilago maydis* and *Magnaporthe oryzae*, it was also shown that Sho1 and Msb2 play distinct and overlapping functions in recognition of plant surface signals, activation of Kss1 MAPK orthologs, appressorium formation and virulence (Lanver, Mendoza-Mendoza et al. 2010; Liu, Zhou et al. 2011).

In summary, our strategy failed to identify a gene that is exclusively regulated by the Fmk1 pathway. Therefore, additional genes should be tested. *ChsV*, encoding a class V chitin synthase, and *pl1*encoding the cell wall degrading enzyme pectate lyase, are interesting candidates (Huertas-Gonzalez, Ruiz-Roldan et al. 1999)Madrid et al., 2003.since their expression was found to be down-regulated in the *fmk1*Δmutant (Di Pietro et al. 2001; Pérez-Nadales & Di Pietro 2011). However, it might be more advantageous to use high throughput methods such as comparative microarray analysis between the wild-type and key MAPK pathway mutants such as *fmk1Δ*, *mpk1Δ*, *hog1Δ* to screen simultaneously for a large number of downstream effectors.

MAPK cascades are well conserved among fungi (Turra, Segorbe et al. 2014). However the signal inputs as well as the downstream genes and biological processes can vary between different species. In particular, the characterization of the upstream signals is essential to understand the specific mechanisms activating the infection program in each species. In this chapter, we did not find an appropriate downstream effector gene for the Fmk1 pathway. We next decided to redirect our work towards deciphering the plant signals that elicit directed hyphal growth in *F. oxysporum*. Host-induced chemotropism represents a crucial process for the onset of virulence, which requires different MAPK signaling pathways (Turrà, El Ghalid et al. 2015).

Enzymatic activity of root secreted peroxidases and ROS trigger chemotropism in *F. oxysporum* via the α-pheromone receptor Ste2 and the MAPK Mpk1

Root secreted peroxidases function as chemoattractants for F. oxysporum

Although directed hyphal growth of filamentous pathogens and symbionts towards plant roots has been reported previously, the nature of the chemical signals has so far remained elusive (Turrà & Di Pietro 2015). Identifcation of these compounds has been hampered mainly by methodological difficulties as well as by the low concentrations secreted by roots. Only few studies have reported chemotropism towards plant roots in fungal pathogens, and in none of these the chemoattractant compound(s) was identified. Germ tubes of the nematode-trapping fungus *Arthrobotrys oligospora*were attracted by roots of different plants species, but not by a nylon string used as a control (Bordallo, Lopez-Llorca et al. 2002). Moreover, *Cochliobolus sativus* hyphae grew towards barley roots and root exudates (Jansson, Johansson et al. 1988).

However, other studies reported an absence of chemotropic response of the fungus towards the host. Particularly relevant to the present work are the results from Steinberg et al., who failed to observe a chemotropic response of *F.oxysporum* towards tomato

roots (Steinberg, Whipps et al. 1999a). The discrepancy between this earlier report and our results reflect the historical controversy between those researchers affirming the existence of chemoattraction of the fungi towards the host organism and those denying such a response. We suggest that the main cause of controversy has been the lack of reliable methods to quantify directed hyphal growth as well as the differences in the experimental conditions used in these studies. In this respect, the development of a standardized plate assay in our laboratory that allows to quantify chemotropism in *F. oxysporum* represents a major methodological breakthrough for this field of research (Turrà, El Ghalid et al. 2015). The use of this assay was a pre-requisite for the purification and identification of the three class III peroxidases TMP1, TMP2 and CEVI-1 as chemoattractants of *F.oxysporum*. Our finding adds a new role to the already extensive catalog of these enzymes known to function in diverse physiological processes such as cell wall modification and pathogen defense (Jeon, Goh et al. 2008).

Purification of the chemoattractant signals from tomato root exudates was performed using solvent partitioning and size exclusion methods, followed by FPLC and separation by SDS-PAGE. Prior to their characterization by LC-ESI-MS/MS, the protein fractions and single protein bands were tested for their chemotropic activity. A similar procedure was followed previously to isolate and identify the signal compounds from *Lotus japonicus* which induce hyphal growthbranching in AM mycorrhizal fungi (Akiyama, Matsuzaki et al. 2005). Importantly, the concentration of recombinant tomato peroxidase that elicited the optimal chemotropic response in *F. oxysporum* was 3 to 4 magnitudes lower than those of α-pheromone (378 μM) and glutamate (2.95 mM), suggesting that secreted tomato peroxidases have a high chemoattractant activity.

The results obtained from heterologous expression of TMP2 and CEVI-1 in *E. coli* indicated that the chemoattractant activity of the two peroxidases is comparable, since both recombinant proteins triggered a similar chemotropic response in *F. oxysporum*. Although we need to take into account that refolding of the two proteins was incomplete, this suggests that different class III peroxidase isoenzymes may have similar chemoattractant activity towards *F. oxysporum*. Thus, chemotropic sensing is probably the sum of the collective activity of multiple secreted peroxidases. In line with

this idea, expression levels of individual peroxidase genes did not correlate with the chemoattractant activity of the corresponding root exudates, suggesting the contribution of additional genes to this activity. Our VIGS experiments corroborate this hypothesis since they suggest that partial silencing of one or several peroxidase genes has no clear effect on the total enzymatic activity of root exudates.

The role of secreted peroxidases in plant metabolism is intimately linked to the range of physiological reducing substrates. Thus, expression of certain peroxidase genes in plants has been linked to ROS-associated defense reponses (Choi and Hwang 2012) and to reinforcement of the cell wall barrier through the formation of lignin and suberin polymers (Whetten, MacKay et al. 1998). We noted that the transcript levels of *TMP1* and *CEVI-1* increased dramatically after infection of tomato plants by *F.oxysporum*. These findings are in agreement with those of Taheri et al, who reported an increase of *CEVI-1* expression after infection by *R. solani*, coinciding with an increase in lignification (Taheri and Tarighi 2011). Collectively, this suggests that TMP1 and CEVI-1 are defense-related peroxidases induced in tomato roots by infection with *F. oxysporum* .However, in our chemotropism assay re-orientation of *F. oxysporum* germ tubes towards tomato roots occurs during the first 13h of the interaction, prior to the transcriptional increase of defense-related peroxidase genes. Therefore, we propose that *F. oxysporum* recognize and growth towards the tomato plant root prior to the establishment of defense mechanisms in the host.

Class III plant peroxidases are targeted to the secretory pathway, often with the cell wall as final destination (Hiraga, Sasaki et al. 2001). In tomato plant, TMP1, TMP2 and CEVI-1 were described to localize to the wall where they function in polymerization of suberin and lignin (Roberts and Kolattukudy 1989; Taheri and Tarighi 2011). In addition, studies in Fabaceae, Graminea and Solanaceae suggest that class III peroxidases can also be released from the plant roots into the rhizosphere where they take part in the oxidative degradation of soil compounds (Gramss, Voigt et al. 1999). Here we isolated TMP1, TMP2 and CEVI-1 from tomato root exudate, demonstrating that these enzymes were released into the extracellular space. Class III peroxidases thus

appear to have a dual role, first in structural modification of the plant cell wall and second as signal compounds in the rhizosphere.

In summary, we identified TMP1, TMP2 and CEVI-1 class III peroxidases as the major chemoattractant compounds secreted from tomato roots that trigger chemotropic sensing in *F. oxysporum*. Recombinant peroxidases produced in *E. coli* demonstrated that both TMP2 and CEVI-1 elicited a similar chemotropic response in the fungus indicating that chemotropic sensing involves the sum of secreted peroxidases enzymatic activities. Additionally, our VIGS experiment confirmed our previous findings by showing that the expression level of our three identified peroxidases does not correlate with the total peroxidase enzymatic activity in tomato root exudates.

Why has F. oxysporum *recruited class III peroxidases for chemotropic sensing of plant roots?*

How has a fungal pathogen such as *F. oxysporum* evolved the capacity to use peroxidases as chemoattractant signals for locating its host? Plant roots are known to exude a large variety of chemical compounds that may attract or somehow influence microorganisms in the rhizosphere. In 1960 Frenzel reported a list of compounds secreted from different parts of the root. His study which mainly focused on amino acids, demonstrated that aspartic acid was secreted from the entire root, while asparagine and threonine were preferentially released from the meristem and the root elongation zone and glutamic acid, leucine, phenylalanine and valine from the root hair zone (Frenzel 1957; Frenzel 1960). The oomycete pathogen *Phytophthora cinnamomi* was shown to display both zoospore chemotaxis and hyphal chemotropism towards the roots of the host plant avocado. The attraction was particularly strong in the region of root elongation, suggesting that the unknown chemoattractant could be mainly exuded from this region (Zentmyer 1961; Morris, Bone et al. 1998). While the root tip zone was previously considered as a major site of exudation (Pearson and Parkinson 1961; Schroth and Snyder 1961), our data indicate that *F. oxysporum* preferentially colonizes tomato roots in the maturation zone, which exhibits with the highest peroxidase enzymatic activity. Since the maturation zone covers a large part of the root, we

speculate that *F. oxysporum* uses class III peroxidases as chemoattractants to ensure an optimal colonization of the host root.

An important feature of class III peroxidases is their ubiquitous presence in all developmental stages, from the first hours of the plant's life until its last moments (Passardi, Theiler et al. 2007). In aggrement with this, we detected peroxidase enzymatic activity in roots of small seedlings, 2 week-old plants and 1 month-old plants (data not shown). These results indicate that peroxidases are continuously secreted by the roots and therefore represent suitable chemoattractant signals to locate and infect the host plant.

Analysis of the protein sequence of the three identified tomato peroxidases, in particular the region of "reactivity with reductants" suggested that TMP1 and TMP2 catalyze the oxidation of the same substrate, whereas CEVI-1 may oxidizes a different type of reductant. In agreement with other reports, and by using different chromogenic substrates such as ABTS, DAB and guaiacol, we demonstrated that class III peroxidases from tomato roots lack a strict substrate specificity. This suggests that several different peroxidases can oxidize a similar substrate and consequently fulfill redundant catalytic function, and loss of a particular peroxidase could be compensated by the other peroxidase isoenzymes. This would explain the observed lack of correlation between transcript levels of *TMP1*, *TMP2* and *CEVI-1* and total peroxidase activity in root exudates of VIGS silenced plants.

In summary, we proposed three main advantageous reasons explaining why *F .oxysporum* selected class III peroxidases to recognize its host: (1) contrarily to other substances and except from the root tip, class III peroxidases are secreted from the whole root. (2) class III peroxidases are secreted from tomato plant roots at developmental stages and (3) class III peroxidases present a large enzymes family. Thus class III peroxidases are redundant proteins that are constitutively expressed and localised in the major part of the tomato roots. We suggested that these temporal and spatial specificities benefit to the fungus to optimally recognise its host.

Are products of peroxidase enzymatic activity and reactive oxygen species the elicitors of chemotropism in F. oxysporum*?*

Our experiments demonstrate that peroxidase enzymatic activity was essential for chemoattraction by tomato root exudate, since the chemotropic response was abolished by specific enzyme inhibitors such as SHAM or by targeted mutation of catalytically essential amino acid residues in heterologously expressed TMP2. The complete loss of chemoattraction upon peroxidase inactivation was somewhat unexpected, since root exudates are composed by a variety of compounds, including nutrients such as sugars or amino acids (Badri and Vivanco 2009). Moreover, previous work by our group demonstrated that *F. oxysporum* also displays chemotropism response towards nutrients, although this response requires much higher concentrations of chemoattractant (Turrà, El Ghalid et al. 2015). It is likely that the absence of a chemotropic response to tomato root exudate in the presence of peroxidase inhibitors is due to the low concentrations of nutrients. Collectively, this suggests that peroxidases are the dominant chemoattractants present in root exudate.

How do plant peroxidases elicit directed hyphal growth in fungi? We found here that different types of ROS also elicit a strong chemotropic response in *F. oxysporum*, including oxidized ABTS derived as a result of HRP activity or H_2O_2, a non-radical oxidant. ROS are by-products of oxygen metabolism that have been known for a long time as damaging cellular compounds (Gough and Cotter 2011). ROS are produced by innate immune cells such as leucocytes to kill microbial pathogens (Lamb and Dixon 1997; Kovtun, Chiu et al. 2000). Moreover, recent work suggests that ROS also regulate crucial aspects of cell biology such as differentiation, host-pathogen interactions, mutualistic symbiosis and chemotaxis (Brun, Malagnac et al. 2009; Enyedi and Niethammer 2013). Due to their rapid diffusion and versatile biological activity, ROSare good candidates for cell-cell signalling.Using an *in vitro* chemotaxis assay, Klyubin et al, demonstrated that mouse peritoneal neutrophils move towards hydrogen peroxide, suggesting that H_2O_2 induces a positive chemotropic response during the host-pathogen interaction (Klyubin, Kirpichnikova et al. 1996). Moreover, injured cell barriers or oncogene-transformed cells emit a gradient of H_2O_2 to rapidly recruit inflammatory cells (Niethammer, Grabher et al. 2009). Interestingly, we found that *F. oxysporum* was repelled by high concentrations of H_2O_2, demonstarting that

chemoattraction can be inverted at supra-optimal concentrations. In animals, high concentrations of ROS induce the oxidative innate immune defense and pathogen killing (Rada and Leto 2008), while low concentrations are non-toxic for leucocytes and can regulate inflammation by activating pro-inflammatory signaling cascades, leading to chemotactic cytokine production (Hayden and Ghosh 2012). The mechanism of action of ROS is still unknown, and it is not clear whether these molecules act as a 'true' chemoattractants. Three hypotheses have been proposed: (1) ROS promote chemotropism by acting as chemoattractants, (2) ROS increase the chemotropic sensitivity of the cells towards chemoattractants; and (3) ROS trigger chemoattractant production and secretion (Hayden and Ghosh 2012).

What is the origin of the ROS chemoattractants? The main known producers of cellular ROS, including H_2O_2 are NADPH oxidases (NOX), a class of enzymes localized at the plasma membrane which form an enzymatic complex catalyzing the reduction of O_2 to the superoxide $O_2^{\cdot -}$ using NADPH or NADH as electrons donors (Bedard and Krause 2007). Subsequently, $O_2^{\cdot -}$ is converted to H_2O_2 spontaneously or by superoxide dismutase (Caliskan and Cuming 1998). H_2O_2 can also be generated by other enzymes such as apoplastic oxalate oxidase (Caliskan and Cuming 1998), diamine oxidase (Federico and Angelini 1986). Less commonly, class III peroxidases can also generate H_2O_2 (Elstner and Heupel 1976; Federico and Angelini 1986), although hydrogen peroxidase generally functions rather as a substrate of peroxidase reactions (Chen and Schopfer 1999). In the saprophytic fungus *Podospora anserina*, hyphal re-orientation is dependent on the NOX PaNox2, its activator PaNoxR and the tetraspanin membrane protein PaPls1. Because NOX appear to be present only in multicellular organisms, it was proposed they evolved in eukaryotic cells to mediate cell-cell communication, informing the adjacent cells about the nutritional status (Lalucque and Silar 2003). Our results suggest that NOX may act as general regulators of chemotropic sensing in *F. oxysporum,* since application of DPI, a specific inhibitor of the NOX complex, drastically reduced the chemotropic response towards glutamate and α-pheromone. Further studies, using targeted NOX deletion mutants are needed to confirm this hypothesis.

The molecular mechanisms used by H_2O_2 and the NOX complex to regulate the directed hyphal growth in fungi are yet to be discovered. For example, it is not clear whether the hydrogen peroxide is generated by NOX activity or by a different source. Interestingly, these two ROS compounds did not induce the same pattern of chemoattraction. While oxidized ABTS presents a bell shaped dose-response curve, H_2O_2 was active over a large range of concentrations reaching from nanomolar to millimolar. The H_2O_2 that triggers chemotropism in *F. oxysporum* could also originate from plant roots. In fact, H_2O_2 produced by root hairs and essential for root hair growth (Foreman, Demidchik et al. 2003). Moreover, H_2O_2 is important in the formation of lignin by peroxidases. Interestingly, H_2O_2 accumulates in the root maturation zone, which corresponds to the region of most intense peroxidase activity (Dunand, Crevecoeur et al. 2007).

In summary, non-radicalized (H_2O_2) and radicalized ROS (produced from the peroxidase enzymatic activity) are the key components that elicit a chemotropic response in *F. oxysporum*. The exact mechanism by which class III peroxidases enzymatic activity and generally ROS trigger directed hyphal growth in the fungus is yet to be deciphered and several questions remain unsolved: What is the origins of the different type of ROS and how do they induce the chemotropic sensing in *F.oxysporum*? And what is the role of the NADPH complex in this phenomenon? Several ongoing projets in our laboratory aim to answer these questions.

Role of the Ste2 receptor and the Mpk1 MAPK in chemotropic sensing

It was previously shown that tomato root exudates elicit chemotropism in *F. oxysporum* through the Ste2 receptor and the MAPK Mpk1 (Turra, El Ghalid et al. 2015). In aggrement with these findings, we suggested here that the products generated by enzymatic activity of class III peroxidases, ABTS and H_2O_2 trigger chemotropism in *F. oxysporum* through the same signaling pathway. Although, it is not clear whether peroxidases activate the Ste2 receptor directly or through an intermediate molecule, we currently favor the second hypothesis, based on our finding that non-specific oxidized products such as oxidized ABTS elicit a robust chemotropic response. However, it is

also possible that the peroxidases and radicalized ABTS can independently oxidize the receptor.

Our results demonstrate that Ste2 receptor mediates the chemotropic response towards H_2O_2, since a complete loss of chemoattraction was observed in the *ste2*Δ mutant. Interestingly, the chemotropic response is still active in the mutant at very high concentrations, suggesting that Ste2 can be bypassed by an excess of H_2O_2. In mammalian cells, several studies proposed that oxidants could mimic growth factors through the reversible oxidation of receptors or regulatory proteins (Bauskin, Alkalay et al. 1991; Hardwick and Sefton 1995; Nathan 2003). H_2O_2 was able to stimulate the tyrosine of the fibroblast growth factor receptor type I (FGFRI) in growth-arrested vascular smooth muscle cells (VSMC) and to activate the downstream signaling pathway (Rao 1997). Moreover, H_2O_2 had the ability to diffuse through the membrane and to activate downstream regulator of the signaling pathway such as ERKs enzymes (Rao 1997).

NOX activity was found to be enhanced upon stimulation of receptors such as the growth-factor receptor (Gough and Cotter 2011). However, in the case of *F. oxysporum,* our results suggest that NOX may act upstream the Ste2 receptor because the chemotropic response towards H_2O_2 was abolished in the *ste2*Δ mutant. To our knowledge, this would be the first evidence suggesting that NOX acts upstream of a cell receptor. However, we cannot discard that the H_2O_2 originates from distinct sources as mentioned above. Although the exact mechanism of chemoattraction by ROS remains to be elucidated, our results strongly indicate that Ste2 is essential for chemotropic sensing of all the types of ROS studied.

Why has *F. oxysporum* recruited a cognate sex pheromone receptor for chemotropic sensing of host signals? To date, Ste2 receptor was thought to function exclusively in α-pheromone sensing (Burkholder and Hartwell 1985; Segall 1993; Arkowitz 2009). Preliminary experiments suggested that *F. oxysporum* germlings exposed simultaneously to competing gradients of α-pheromone and HRP re-orient growth

preferentially towards the peroxidase (data not shown). Thus, in presence of both mating and host signals, *F. oxysporum* appears to preferentially infect the host. However, more thorough studies are needed in order to exclude artefacts such as differences in chemoattractant concentrations. It is interesting, however, that the concentration of HRP required to induce chemotropism in *F. oxysporum* is much lower than that required for α-pheromone.

What is the possible function of the Mpk1 cell wall integrity pathway in chemotropic sensing of host signals? It has been well documented that the Mpk1 cascade is involved in cell defense reponse mechanisms that protect the fungus against deleterious compounds from plants such as components of the plant immune response (Turra, Segorbe et al. 2014). It is attractive to speculate that *F. oxysporum* could use the Mpk1 pathway to simultaneously fulfill two functions, namely to recognize and to grow towards plant roots while activating the defense mechanisms against harmful plant compounds, the latter being the more ancestral function of the Mpk1 signaling cascade. Interestingly, we found that ROS, and particularly H_2O_2 are chemoattractants at low concentrations but repellents at high concentrations. Recruitment of the same signaling pathway for attraction as well as defense responses could ensure a fine and rapid regulation of the response of the fungus during infection, considering that the concentration of ROS increases in the vicinity of the roots.

In summary, class III peroxidases and its enzymatic activity-derived products, the oxidised ABTS signal through the 7TM receptor Ste2 and the cell wall integrity pathway Mpk1 to trigger directed hyphal growth in *F. oxysporum*. In agreement to these findings, the non-radicalized oxidant H_2O_2 was also found to require the Ste2 receptor at low concentrations (signaling concentration). Several hypotheses have been thought to explain why and how ROS activate the Ste2-α-pheromone receptor and its downstream pathway and yet studies have to be conducted on this topic.

HRP oxidized products are modified by **F. oxysporum** *to trigger chemotropic sensing*

We observed that the green color of the oxidized ABTS generated by HRP disappeared gradually in presence of *F. oxysporum,* suggesting that radical compounds may be modified by the fungus to trigger chemotropic sensing. The molecular events leding to these changes are currently under investigation, but several possible scenarios can be drawn. (1) secreted peroxidases are degraded or internalized by the fungus and consequently cannot carry out the continued oxidation of ABTS; (2) oxidized ABTS is internalized by the fungus; and (3) oxidized ABTS is reduced by the fungus.

In *S. cerevisiae*, endocytosis and degradation of α-pheromone are two essential processes for the maintenance of polarized growth during mating (Arkowitz 2009). In the absence of pheromone, receptors, endosomal and vacuole compartments are distributed homogeneously over the cell surface (Jackson and Hartwell 1990; Davis, Horecka et al. 1993; Stefan and Blumer 1994; Ayscough and Drubin 1998). When α-factor binds to Ste2 receptors, these are internalized (Schandel and Jenness 1994) and then reappear on the cell surface in a polarized manner (Jenness and Spatrick 1986; Stefan and Blumer 1994; Ayscough and Drubin 1998). It has been proposed that receptor internalization and recycling plays an important role in signal amplification and desensitization (Arkowitz 2009). Likewise, in the corn smut fungus *U. maydis*, filamentous growth and pathogenicity depend on apical endocytic recycling by early endosomes (Steinberg 2007). Extracellular degradation of pheromones is performed by specific mating-pheromone proteases that are either secreted or attached to the cell wall of the recepient cells (Ciejek and Thorner 1979; Ballensiefen and Schmitt 1997; Moukadiri, Jaafar et al. 1999). A gradient of secreted protease is thought to steepen the pheromone gradient (Arkowitz 2009). Finally, our third hypothesis implies that the oxidized ABTS would have the ability to oxidize a fungal compound(s) such as a receptor thereby returning to its reduced form.

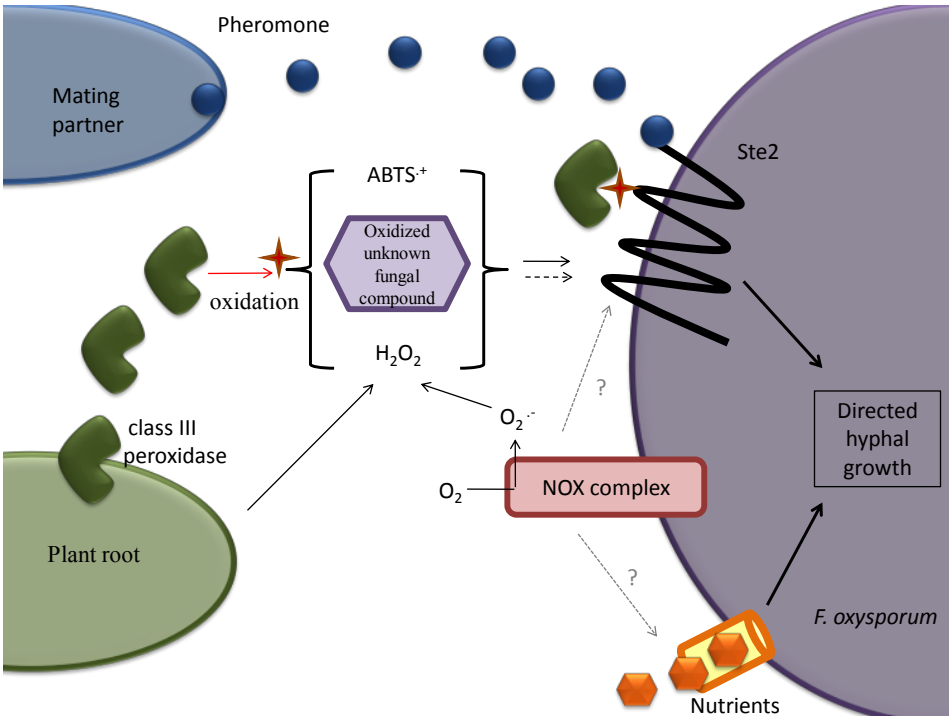

Figure 50. Schematic model of the proposed mechanisms whereby class III peroxidases elicit hyphal chemotropism in *F. oxysporum*. The dark green structure represents the peroxidase, the red star represents the oxidation reaction, the blue circle represents the pheromone and the orange diamond the nutrients. The α-pheromone (blue circle) binds to the 7TM Ste2 receptor to induce directed hyphal growth of *F. oxsyporum* towards its mating partner. The nutrients (orange diamond) elicit a chemotropic response in the fungus via unknown sensor/transporter(s). Two main hypotheses are given to explain how plant secreted peroxidases (dark green structure) trigger the chemotropic sensing in *F. oxsyporum*: (1) class III peroxidases oxidize (oxidation is represented by the red star) the Ste2 receptor. (2) Class III peroxidases enzymatic activity-derived products such as the oxidized ABTS, an unknown fungal oxidant and H_2O_2 activate directly or indirectly, by oxidation or not the Ste2 receptor. H_2O_2 is originated from either the plant root or from the class III peroxidases enzymatic activity or from a product of the NOX complex activity. This latter complex governs the direct hyphal growth of *F. oxysporum* towards the nutrients and the H_2O_2, however its exact role is yet unknown.

Further work is needed to elucidate the exact mechanism of fungal chemoattraction by plant peroxidases. Although direct oxidation of the Ste2 receptor cannot be totally discarded, our data strongly suggest that an unknown intermediate fungal compound is required. In aggrement with this hypothesis, we found that ABTS oxidated by the secreted plant peroxidase HRP triggers chemotropic growth in *F. oxysporum*. We

propose that the intermediate signal compounds could be the hydogren peroxide or extra-cellular or cell-wall associated fungal compounds. For example, H_2O_2 can either originates from plant roots, from the enzymatic activity of secreted peroxidases or from the NOX complex since we demonstrated that this complex governs directed hyphal growth of substrates signaling either through the Fmk1 or the Mpk1 pathway. In turn, ROS could either directly or indirectly activate the Ste2 receptor. It is currently unknown whether NOX direclty activate chemotropic signaling pathways or if ROS produced through their activity are needed for this activation.

What is the chemical nature of the putative intermediate compound signaling between plant secreted peroxidases and the Ste2 receptor? Our results showing that commercial HRP alone can induce chemotropic growth in *F. oxysporum* without the presence of additional plant compounds, suggest that the intermediate signaling molecule must originate from the fungus itself. Possible candidates are membrane- or cell wall-associated or extracellular compounds. A less likely possibility is that peroxidases through an unknown mechanism induce the production and polarized secretion of α-pheromone which would then bind to the Ste2 receptor and induce directed hyphal growth. Among cell surface compounds, membrane lipids may be of particular interest. In *S. cerevisae*, several lipids have been associated with directed hyphal growth. Some of these such as phosphatidylserine, a phospholipid involved in the internalization of the integral membrane protein Arn1(Guo, Au et al. 2010) localize to the inner leaflet of the plasma membrane and accumulate mainly at the bud and the bud neck plasma membrane (Fairn, Hermansson et al. 2011). Others localize to the outer leaflet of the plasma membrane, such as phosphatidylethanolaminewhich localizes particularily to the sites of polarized growth. In *S. pombe*, mutants affected in phosphatidylethanolamine biosynthesis have severe morphological defects, indicating that this lipid could be important for polarized growth (Luo, Matsuo et al. 2009). Furthermore, phospholipid flippase was shown to be important for polarized growth of *S. cerevisiae*: phospholipid flippase mutants over-activate the downstream signaling pathway leading to hyperpolarized growth. Phosphatidylinositol 4,5-bisphosphate (PI(4,5)P2) was found to be essential for endocytosis and exocytosis in both *S. cerevisiae* and *S. pombe* (He, Xi et al. 2007; Sun, Carroll et al. 2007; Zhang, Orlando et

al. 2008; Yakir-Tamang and Gerst 2009; Bendezu and Martin 2011; Sun and Drubin 2012). Finally, sterols and sphingolipids, two important classes of lipids essential for membrane permeability and fluidity, were reported to play a role in *S. cerevisiae* polarized growth, since the relevant mutants showed defects in (Munn, Heese-Peck et al. 1999; Zanolari, Friant et al. 2000; Heese-Peck, Pichler et al. 2002). Collectively these results from the yeasts indicate that membrane lipids could function as substrates of class III peroxidases during chemotropic sensing.

Reactive oxygen species, more than chemoattractants

ROS induce morphological changes in F. oxysporum

In our study we observed the formation of bulge-like structures in *F. oxysporum* germlings exposed to a gradient of oxidized ABTS. Interestingly, these round-shaped structures bear similarity to the appresoria such as those developed by the oomycete pathogen *Phytophtora infestans* (Grenville-Briggs, Anderson et al. 2008), but are much smaller than those formed by the leaf pathogen *Magnaporthe oryzae* (de Jong, McCormack et al. 1997). It was suggested that the formation of appressoria is mainly induced in response to surface signaling and that chemical signals are less important for this mechanism (Gow 1993). Our results indicate that physical contact with the host surface is not required for the formation of appressoria-like structure in *F. oxysporum* since these morphological changes were observed on a plate under chemotropic assay conditions in the absence of physical contact with the roots. Interestingly, the morphological changes in *F. oxysporum* occurred preferentially at high concentration of oxidized ABTS that are supra-optimal for chemotropism. We hypothesize that *F. oxysporum* may initially sense and re-orients its germ tube towards a gradient of host chemoattractant, and then form appressorium-like infection structures once the concentration of chemoattractant reaches a supra-optimal level.

In appressorium-forming species such as *M.oryzae, Colletotrichum lagenarium, C. heterostrophus,* and *Pyrenophora teres*, mutants lacking the Fus3/Kss1 MAPK ortholog fail to differentiate appressoria indicating that this pathway is essential for the

morphogenetic transition (Lev et al., 1999; Takano et al., 2000; Xu and Hamer 1996; Ruiz-Roldan et al., 2001). In this study, we demonstrated that *F. oxysporum* forms appresorium-like structures when exposed to a gradient of oxidized ABTS which activates the Ste2 receptor and the Mpk1 MAPK. However, we can not discard that the Fmk1 pathway is also involved in such process.

ROS stimulate germination and hyphal fusion in F. oxysporum

Strigolactones secreted from *L. japonicus* roots were found to stimulate seed germination in the parasitic weeds Striga and Orobanche and to induce extensive hyphal branching in AM fungi (Akiyama and Hayashi 2006). Both phenomena have been described as the first developmental steps in host recognition. Likewise, Steinberg et al, showed that certain fractions of tomato root exudate were able to stimulate branching and hyphal extension of *F. oxysporum* (Steinberg, Whipps et al. 1999a). In aggrement with these reports, our preliminary results show that *F. oxysporum* undergoes hyphal fusion when exposed to a gradient of recombinant TMP2 peroxidase. Additionally, we observed that products of peroxidase enzymatic activity, and more generally ROS, have a stimulating effect on the germination of *F. oxysporum* microconidia when used at non-toxic concentrations (data not shown). These preliminary observations suggest, that besides eliciting directed hyphal growth host chemoattractants also promote other developmental processes such as spore germination and hyphal fusion in *F. oxysporum*.

In summary, our data suggest that peroxidase-derived tomato root signals induce specific morphological changes in *F. oxysporum* which look similar to appresoria. Therefore, we propose that ROS signals may not only promote chemotropic sensing but also additional pre-infection processes required for sucessful establishment of the tomato-*F. oxysporum* interaction.

Role of chemotropism in host specificity

In 1905, Massee suggested that "immune plants owe their immunity to the absence of chemotropic substances" (Massee 1905). This early hypothesis was revived a century later by several studies. Morris and Ward found that six distinct species of *Phytophtora*

and one species of *Pythium*failed to display sensitivity towards isoflavones from soybean while *Phytophtora sojae*, a soybean pathogen, did. They suggested that the specific attraction to soybean isoflavones might be part of the mechanism that determines host range of oomycete pathogens (Morris and Ward 1992). Likewise, Sbrana and Giovannetti showed that the AM fungus *G. mosseae* was able to reorient hyphal growth across a filter membrane towards the roots of the host plant, but not towards non-hosts (Sbrana and Giovannetti 2005).

In contrast to these studies, we demonstrated that root exudates from wheat, a non-host plant, elicit a strong chemotropic response in *F. oxysporum* through the activity of secreted peroxidases. This finding suggests that chemotropic sensing of the fungus does not differentiate between host and non-host plants during pre-infection stages. Interestingly, it was shown that *F. oxysporum* f. sp. *lycopersici* can colonize the non-host plant maize by penetrating the roots and growing until the stem without causing apparent symptoms (Antonio, personal communication). Steinberg et al, also proposed that recognition mechanisms between the host plant and pathogenic or non-pathogenic strains of *F. oxysporum* may take place on or within the root rather than outside of the root, since mycelial development of three different *F. oxysporum* strains including pathogenic and non-pathogenic ones was similar in the rhizosphere of wheat and and tomato plants (Steinberg, Whipps et al. 1999b). Although the molecular basis of host/non-host discrimination in *F. oxysporum* is still unknown, subsequent studies revealed that the race-cultivar specific resistance response to *F. oxysporum*, which is based on gene-for-gene interactions occurs in the xylem contact cells (Rep, van der Does et al. 2004). In this response, fungal avirulence proteins secreted during colonization of the xylem mediate pathogen recognition and resistance through the product of a cognate *R* gene. However, loss of the avirulence genes can lead to a small reduction in virulence on the susceptible plant cultivar (Rep, van der Does et al. 2004).
Trichoderma species are well known for their ability to control Fusarium wilt disease of tomato by establishing an endophytic interaction with the host plant (Harman, Howell et al. 2004). Interestingly, preliminary experiments in our laboratory suggest that HRP also elicits chemotropic growth in Trichoderma (Turrà, personal communication). This

finding suggests that class III peroxidases could have a conserved function in chemotropism of soil-inhabiting fungi towards plant roots.

Chemical signals mediating plant-microbe communication

Class III peroxidases have previously been implicated in communication between plant roots and bacteria. During the interaction between *Medicago sativa* and the rhizobium *Sinorhizobium meliloti*, an increase in the exudation of several root proteins was observed, including peroxidases (De-la-Pena, Lei et al. 2008). Moreover, expression of *srprx1* encoding a class III peroxidase, in the *Sesbania rostrata* roots was induced by nodulation factors of the bacterial symbiont *Azorhizobium caulinodans* but not by wounding or pathogen attack, suggesting a specific role in the plant-symbiont interaction (Den Herder, Lievens et al. 2007).

Other classes of plant compounds have also been shown to function as signals during the interaction with microbial symbionts or pathogens. Lectins comprise a large group of carbohydrate binding proteins, which have also been associated with the interaction between roots and bacteria (Wen, VanEtten et al. 2007; De-la-Pena, Lei et al. 2008). Similar to class III peroxidases, lectins were found to play a dual role, participating both in the defense against certain pathogens and in the recognition of compatible symbionts (Sharon and Lis 2004; De Hoff, Brill et al. 2009).

It was demonstrated that zoospores of oomyctes exhibit positive chemotaxis towards root compounds (Zentmyer 1961; Carlile 1983; Morris and Ward 1992; Sekizaki, Yokosawa et al. 1993). For example, zoospores of *Phytophthora sojae* are attracted bydaidzein and genistein, two isoflavones secreted by soybean roots (Morris and Ward 1992; Tyler, Wu et al. 1996). In *Rhizobium* and *Bradyrhizobium* bacteria, plant

isoflavones induce the expression of nodulation genes. *Rhizobium meliloti* was shown to exhibit chemotaxis towards the nodulation gene-inducing signals from alfalfa roots (Dharmatilake and Bauer 1992). These findings suggest that flavones and their deratives play a general role in host-microbe communication.

Branching factors (BFs) secreted by roots, such as strigolacones have been the subject of multiple studies (Akiyama, Matsuzaki et al. 2005). BF from common basil eliciting hyphal branching in the AM fungus *Glomus mosseae* was partially identified as a low molecular weight compound (<500 kDa) (Giovannetti, Sbrana et al. 1996). Other studies suggested that BFs were lipophilic compounds present in the host plants of AM fungi but absent in non-hosts (Buee, Rossignol et al. 2000; Nagahashi and Douds 2000).

Phenolic compounds including flavonoids such as quercetin have been considered as candidates for BFs and germination stimulants, since they play an important role in symbiotic and pathogenic plant interactions with microbes (Gianinazzi-Pearson, Branzanti et al. 1989; Peters and Varma 1990; Tsai and Phillips 1991; Becard, Douds et al. 1992). Interestingly, certain class III peroxidases catalyze the oxidation of lignin and suberin, two phenolic compounds involved in cell wall structure. It is attractive to speculate that these compounds could also be secreted into the extracellular space where they could act as chemoattractants. However, other studies have questioned the role of flavonoids as BFs by showing that mutant plants affected in the flavonoid biosynthesis pathway can still induce hyphal branching in AM fungi (Buee, Rossignol et al. 2000). Other works argued against the role of flavonoid in hyphal branching after detecting significant amounts of quercetin, myricetin and kaempferol in non-mycorrhizal plants such as *A. thaliana* (Burbulis, Pelletier et al. 1996). However, we found that non-host plants can also trigger chemotropism in *F. oxysporum* through peroxidase activity, suggesting that this mechansim is broadly conserved and not host-specific. Our results suggest that flavonoids may function as general BF signals for AM fungi, while class III peroxidases may function as general chemoattractants for *F. oxysporum* and, possibly, other fungal pathogens.

Apart from root-microbe interactions, diffusible chemoattractants from lily stigma have been reported to induce a positive chemotropic response in pollen tubes. The chemoattractant was identified as a member of the family of plantacyanin-like proteins (Kim, Mollet et al. 2003). Similar to class III peroxidases, plantacyanin-like proteins localize to the cell wall and can catalyse redox reactions (Battistuzzi, Borsari et al. 1997). While their exact function is unknown, microarray studies in *Arabidopsis* and *Medicago* suggest that plantacyanins are multifunctional proteins expressed in several plant organs (Fedorova, van de Mortel et al. 2002; Whitham, Quan et al. 2003). Thus, two biologically diverse processes such as pollination and root-fungus ineraction require signaling enzymes with similar functions.

It will now be interesting to investigate a possible link between the signaling mechanism of class III peroxidases and more generally redox-associated enzymes described as chemoattractants in the literature. We speculate that class III peroxidases could function as general regulators of chemotropic sensing and activate, by oxidation, the chemotropic potential of a wide range of compounds that were described as chemoattractants in other studies.

Outlook

The unexpected identification of class III peroxidases as plant root chemoattractants opens new avenues for studying the molecular basis of the tomato-*F. oxysporum* interaction. Our finding answers a long-standing question in *F. oxysporum* biology and may be of general importance for chemoattraction between plants and root-colonizing fungi. However, many new questions emerge from our work regarding the signals generated by secreted plant peroxidases as well as the underlying mechanisms that lead to chemotropic growth in the fungus. Perhaps the most fascinating of these is whether ROS could be used by *F. oxysporum* and by other fungi as a general means of communication. Studying early signaling events during hyphal fusion in Neurospora, Fleissner et al. proposed some years ago that genetically identical cells in the same developmental state chemotropically sense each other by rapidly alternating their

physiological state between signal sending and receiving mode (Fleissner, Leeder et al. 2009). While the signaling pathway involved in this process was partially identified, the signal itself remains to be discovered. Given their physical and chemical properties, ROS and particularly H_2O_2 are good candidates for volatile and short-lived signaling molecules. In addition, preliminary data suggest that peroxidases may also govern more complex mechanisms such as the development of sexual structures. Although a sexual cycle has not been described so farin *F. oxysporum*, we observed the formation of multi-hyphal structures in presence of H_2O_2 (data not shown) that were reminiscent of initial fruiting bodies formed by *P. anserina* (Lysek 1976).

This present work identified ROS as major compounds triggering directed hyphal growth in *F. oxysporum* towards both the host and non-host plants indicating that the recognition plant-fungus takes place further during the infection. *F. oxysporum* infects hundreds of crops and we speculate that it might use class III peroxidases as a general means to re-orient hyphal growth towards plant roots. Other studies showed that ROS also trigger chemotropic response in other fungal species such as fungal symbionts belonging to Trichoderma spp. and also mediates interaction between plants and bacteria. Together, our study and these findings suggest ROS may govern the interaction between plant and microbes in a general manner. Finally, the hypothesis that fungi may use ROS to undergo vegetative fusion and mating also place them as putative candidates for cell-cell communication.

Conclusiones/Conclusions

Conclusiones

- Las cascadas MAPK Fmk1 y Mpk1 contribuyen positivamente a la expresión del gen *fpr1* en condiciones de crecimiento invasivo.

- Los genes regulados por la ruta Fmk1 no están conservados entre *S. cerevisiae* y *F. oxysporum*.

- Las peroxidasas de tipo III TMP1 , TMP2 y CEVI - 1 secretadas por las raíces de tomate inducen el quimiotropismo en *F. oxysporum*.

- La actividad enzimática es necesario para la quimioatracción por peroxidasas.

- Las peroxidasas del rábano picante y las secretadas por las raices de trigo también inducen el quimiotropismo a través de su actividad enzimática.

- Las especies reactivas de oxígeno (ERO) radicalizadas y non-radicalizadas como el ABTS oxidado y el H_2O_2 provocan una fuerte respuesta quimiotrópica en *F. oxysporum.*

- El receptor Ste2 y la MAPK Mpk1 de *F. oxysporum* son esenciales para la respuesta quimiotrópica a peroxidasa y a ERO.

- La actividad peroxidasa induce cambios morfológicos en *F. oxyporum.*

- Las peroxidasas de tipo III podrían representar un mecanismo general para la detección quimiotrópica de los raíces por los hongos del suelo.

Conclusions

- The Fmk1 and Mpk1 MAPK pathways contribute positively to the expression of *fpr1* under invasive growth-inducing conditions.
- The regulation of genes functioning downstream of the Fmk1 MAPK pathway are not conserved between *S. cerevisiae* and *F. oxysporum*.
- The class III peroxidases TMP1, TMP2 and CEVI-1 are chemoattractants secreted by tomato roots that elicit hyphal chemotropism in *F. oxysporum*
- Peroxidase enzymatic activity is required for chemoattraction.
- Commercial horseradish peroxidase and root exudates from wheat also elicit chemotropism in *F. oxysporum* through their peroxidase enzymatic activity.
- Non-radicalized and radicalized reactive oxygen species (ROS) such as the oxidized ABTS and H_2O_2 trigger directed hyphal growth in *F. oxysporum*.
- The seven transmembrane-receptor Ste2 and the MAPK Mpk1 are required for chemotropic sensing of peroxidase and ROS.
- Peroxidase activity induces morphological changes in *F. oxyporum*.
- Class III peroxidases could represent a general mechanism for chemotropic sensing of plant roots by soil-inhabiting fungi.

References

Agrios, G. N. (1997). Plant Pathology, 4th Edn. Academic Press, San Diego, California.

Agrios, G. N. (2005b). Plant Pathology, 5th Edn. Academic Press, New York, USA.

Akiyama, K. and H. Hayashi (2006). "Strigolactones: chemical signals for fungal symbionts and parasitic weeds in plant roots." Ann Bot **97**(6): 925-931.

Akiyama, K., K. Matsuzaki and H. Hayashi (2005). "Plant sesquiterpenes induce hyphal branching in arbuscular mycorrhizal fungi." Nature **435**(7043): 824-827.

Andrews, D. L., J. D. Egan, M. E. Mayorga and S. E. Gold (2000). "The *Ustilago maydis* ubc4 and ubc5 genes encode members of a MAP kinase cascade required for filamentous growth." Mol Plant Microbe Interact **13**(7): 781-786.

Arie, T., I. Kaneko, T. Yoshida, M. Noguchi, Y. Nomura and I. Yamaguchi (2000). "Mating-type genes from asexual phytopathogenic ascomycetes *Fusarium oxysporum* and *Alternaria alternata*." Mol Plant Microbe Interact **13**(12): 1330-1339.

Arkowitz, R. A. (2009). "Chemical gradients and chemotropism in yeast." Cold Spring Harb Perspect Biol **1**(2): a001958.

Armstrong, G. M. and J. K. Armstrong (1981). "Formae speciales and races of *Fusarium oxysporum* causing wilt diseases." In: Nelson, P.E., Toussoun, T.A., Cook, R.J.(eds). Fusarium: Diseases, Biology and Taxonomy. Pennsylvania State University Press, University Park, London.

Ayscough, K. R. and D. G. Drubin (1998). "A role for the yeast actin cytoskeleton in pheromone receptor clustering and signalling." Curr Biol **8**(16): 927-930.

Azpiroz-Leehan, R. and K. A. Feldmann (1997). "T-DNA insertion mutagenesis in Arabidopsis: going back and forth." Trends Genet **13**(4): 152-156.

Backhouse, D., L. W. Burgess and B. A. Summerell (2001). "Biogeography of Fusarium." Pages 122-136 in: 2001 *Fusarium* Paul E. Nelson Memorial Symposium. B. A. Summerell, J. F. Leslie, D. Backhouse, P. Bryden, and L. W. Burgess, eds. The American Phytopathological Society Press. St. Paul, MN.

Badri, D. V. and J. M. Vivanco (2009). "Regulation and function of root exudates." Plant Cell Environ **32**(6): 666-681.

Ballensiefen, W. and H. D. Schmitt (1997). "Periplasmic Bar1 protease of *Saccharomyces cerevisiae* is active before reaching its extracellular destination." Eur J Biochem **247**(1): 142-147.

Banuett, F. and I. Herskowitz (1994). "Identification of fuz7, a *Ustilago maydis* MEK/MAPKK homolog required for a-locus-dependent and -independent steps in the fungal life cycle." Genes Dev **8**(12): 1367-1378.

Bar, E. E., A. T. Ellicott and D. E. Stone (2003). "Gbetagamma recruits Rho1 to the site of polarized growth during mating in budding yeast." J Biol Chem **278**(24): 21798-21804.

Barrett, D. M., E. L. Garcia, G. F. Russel, E. Ramirez and A. Shirazi (2000). "Blanch Time and Cultivar Effects on Quality of Frozen and Stored Corn and Broccoli." Journal of food science **65**: 534-540.

Bartel, D. P. (2004). "MicroRNAs: genomics, biogenesis, mechanism, and function." Cell **116**(2): 281-297.

Battistuzzi, G., M. Borsari, M. Sola and F. Francia (1997). "Redox thermodynamics of the native and alkaline forms of eukaryotic and bacterial class I cytochromes c." Biochemistry **36**(51): 16247-16258.

Baulcombe, D. C. (1999). "Fast forward genetics based on virus-induced gene silencing." Curr Opin Plant Biol **2**(2): 109-113.

Bauskin, A. R., I. Alkalay and Y. Ben-Neriah (1991). "Redox regulation of a protein tyrosine kinase in the endoplasmic reticulum." Cell **66**(4): 685-696.

Becard, G., D. D. Douds and P. E. Pfeffer (1992). "Extensive In Vitro Hyphal Growth of Vesicular-Arbuscular Mycorrhizal Fungi in the Presence of CO(2) and Flavonols." Appl Environ Microbiol **58**(3): 821-825.

Beckman, C. H. (1987b). The nature of wilt disease of plants. St.Paul, Minn., American Phytopathological Society.

Bedard, K. and K. H. Krause (2007). "The NOX family of ROS-generating NADPH oxidases: physiology and pathophysiology." Physiol Rev **87**(1): 245-313.

Bendezu, F. O. and S. G. Martin (2011). "Actin cables and the exocyst form two independent morphogenesis pathways in the fission yeast." Mol Biol Cell **22**(1): 44-53.

Bendezu, F. O. and S. G. Martin (2013). "Cdc42 explores the cell periphery for mate selection in fission yeast." Curr Biol **23**(1): 42-47.

Berglund, G. I., G. H. Carlsson, A. T. Smith, H. Szoke, A. Henriksen and J. Hajdu (2002). "The catalytic pathway of horseradish peroxidase at high resolution." Nature **417**(6887): 463-468.

Bernards, M. A., W. D. Fleming, D. B. Llewellyn, R. Priefer, X. Yang, A. Sabatino and G. L. Plourde (1999). "Biochemical characterization of the suberization-associated anionic peroxidase of potato." Plant Physiol **121**(1): 135-146.

Bestwick, C. S., I. R. Brown and J. W. Mansfield (1998). "Localized changes in peroxidase activity accompany hydrogen peroxide generation during the development of a nonhost hypersensitive reaction in lettuce." Plant Physiol **118**(3): 1067-1078.

Booth, C. (1971). "The Genus Fusarium." The Eastern Press limited London and Reading, England.

Borchert, R. (1978). "Time course and spatial distribution of phenylalanine ammonia-lyase and peroxidase activity in wounded potato tuber tissue." Plant Physiol **62**(5): 789-793.

Bordallo, J. J., L. V. Lopez-Llorca, H.-B. Jansson, J. Salinas, L. Persmark and L. Asensio (2002). "Colonization of plant roots by egg-parasitic and nematode-trapping fungi." New Phytol **154**: 491-499.

Brand, A. (2012). "Hyphal growth in human fungal pathogens and its role in virulence." Int J Microbiol **2012**: 517529.

Brand, A. and N. A. Gow (2009). "Mechanisms of hypha orientation of fungi." Curr Opin Microbiol **12**(4): 350-357.

Brefeld, O. (1883). "Botanische Untersuchugen uber Hefenpilze." Untersuchungen aus dem Gesamt, ebiet der Mykologie V. Die Brandpilze. I. Leipzig

Brun, S., F. Malagnac, F. Bidard, H. Lalucque and P. Silar (2009). "Functions and regulation of the Nox family in the filamentous fungus Podospora anserina: a new role in cellulose degradation." Mol Microbiol **74**(2): 480-496.

Buee, M., M. Rossignol, A. Jauneau, R. Ranjeva and G. Becard (2000). "The pre-symbiotic growth of arbuscular mycorrhizal fungi is induced by a branching factor partially purified from plant root exudates." Mol Plant Microbe Interact **13**(6): 693-698.

Buehrer, B. M. and B. Errede (1997). "Coordination of the mating and cell integrity mitogen-activated protein kinase pathways in *Saccharomyces cerevisiae*." Mol Cell Biol **17**(11): 6517-6525.

Burbulis, I. E., M. K. Pelletier, C. C. Cain and B. W. Shirley (1996). "Are flavonoids synthesized by a multi-enzyme complex?" SAAS Bull Biochem Biotechnol **9**: 29-36.

Burgess, L. W. (1981). General ecology of the Fusaria. Pennsylvania PA, Pennsylvania State University Press.

Burkholder, A. C. and L. H. Hartwell (1985). "The yeast alpha-factor receptor: structural properties deduced from the sequence of the STE2 gene." Nucleic Acids Res **13**(23): 8463-8475.

Caliskan, M. and A. C. Cuming (1998). "Spatial specificity of H2O2-generating oxalate oxidase gene expression during wheat embryo germination." Plant J **15**(2): 165-171.

Callow, J. A. (1987). Models for host-pathogen interactions.

Cameron, J. N. and M. J. Carlile (1981). "Binding of isovaleraldehyde, an attractant, to zoospores of the fungus Phytophthora palmivora in relation to zoospore chemotaxis." J Cell Sci **49**: 273-281.

Carlile, M. J. (1983). "Motility, taxis, and tropism in Phytophthora". In DC Erwin, S Bartnicki-Garcia, PH Tsao, eds, *Phytophthora*: Its Biology, Taxonomy, Ecology, and Pathology. American Phytopathological Society Press, St. Paul, MN.

Chang, L. and M. Karin (2001). "Mammalian MAP kinase signalling cascades." Nature **410**(6824): 37-40.

Chen, S. X. and P. Schopfer (1999). "Hydroxyl-radical production in physiological reactions. A novel function of peroxidase." Eur J Biochem **260**(3): 726-735.

Chittoor, J. M., J. E. Leach and F. F. White (1997). "Differential induction of a peroxidase gene family during infection of rice by *Xanthomonas oryzae* pv. *oryzae*." Mol Plant Microbe Interact **10**(7): 861-871.

Choi, H. W. and B. K. Hwang (2012). "The pepper extracellular peroxidase CaPO2 is required for salt, drought and oxidative stress tolerance as well as resistance to fungal pathogens." Planta **235**(6): 1369-1382.

Ciejek, E. and J. Thorner (1979). "Recovery of S. cerevisiae a cells from G1 arrest by alpha factor pheromone requires endopeptidase action." Cell **18**(3): 623-635.

Coleman, M., B. Henricot, J. Arnau and R. P. Oliver (1997). "Starvation-induced genes of the tomato pathogen Cladosporium fulvum are also induced during growth in planta." Mol Plant Microbe Interact **10**(9): 1106-1109.

Cosio, C. and C. Dunand (2009). "Specific functions of individual class III peroxidase genes." J Exp Bot **60**(2): 391-408.

Cottle, W. and P. E. Kolattukudy (1982). "Abscisic Acid stimulation of suberization : induction of enzymes and deposition of polymeric components and associated waxes in tissue cultures of potato tuber." Plant Physiol **70**(3): 775-780.

Couteaudier, Y. and C. Alabouvette (1990). "Survival and inoculum potential of conidia and chlamydospores of *Fusarium oxysporum* f.sp. *lini* in soil." Can J Microbiol **36**(8): 551-556.

Cullen, P. J., W. Sabbagh, Jr., E. Graham, M. M. Irick, E. K. van Olden, C. Neal, J. Delrow, L. Bardwell and G. F. Sprague, Jr. (2004). "A signaling mucin at the head of the Cdc42- and MAPK-dependent filamentous growth pathway in yeast." Genes Dev **18**(14): 1695-1708.

Curtis, M. D., A. L. Rae, A. G. Rusu, S. J. Harrison and J. M. Manners (1997). "A peroxidase gene promoter induced by phytopathogens and methyl jasmonate in transgenic plants." Mol Plant Microbe Interact **10**(3): 326-338.

Cyert, M. S. (2003). "Calcineurin signaling in *Saccharomyces cerevisiae*: how yeast go crazy in response to stress." Biochem Biophys Res Commun **311**(4): 1143-1150.

Dalmay, T., A. Hamilton, S. Rudd, S. Angell and D. C. Baulcombe (2000). "An RNA-dependent RNA polymerase gene in Arabidopsis is required for

posttranscriptional gene silencing mediated by a transgene but not by a virus." Cell **101**(5): 543-553.

Dangl, J. L. and J. M. McDowell (2006). "Two modes of pathogen recognition by plants." Proc Natl Acad Sci U S A **103**(23): 8575-8576.

Davis, N. G., J. L. Horecka and G. F. Sprague, Jr. (1993). "Cis- and trans-acting functions required for endocytosis of the yeast pheromone receptors." J Cell Biol **122**(1): 53-65.

Dayan, F. E., A. M. Rimando, S. O. Duke and N. J. Jacobs (1999). "Thiol-dependent degradation of protoporphyrin IX by plant peroxidases." FEBS Lett **444**(2-3): 227-230.

de Bary, A. (1884). Vergleichende Morphologie und Biologie der Pilze, Mycetozoen, und Bacterien. Wilhelm Engelmann.

De Hoff, P. L., L. M. Brill and A. M. Hirsch (2009). "Plant lectins: the ties that bind in root symbiosis and plant defense." Mol Genet Genomics **282**(1): 1-15.

de Jong, J. C., B. J. McCormack, N. Smirnoff and N. J. Talbot (1997). "Glycerol generates turgor in rice blast." Nature **389**: 244–245.

de Marco, A., P. Guzzardi and E. Jamet (1999). "Isolation of tobacco isoperoxidases accumulated in cell-suspension culture medium and characterization of activities related to cell wall metabolism." Plant Physiol **120**(2): 371-382.

De-la-Pena, C., Z. Lei, B. S. Watson, L. W. Sumner and J. M. Vivanco (2008). "Root-microbe communication through protein secretion." J Biol Chem **283**(37): 25247-25255.

Deflorio, R., M. E. Brett, N. Waszczak, E. Apollinari, M. V. Metodiev, O. Dubrovskyi, D. Eddington, R. A. Arkowitz and D. E. Stone (2013). "Phosphorylation of Gbeta is crucial for efficient chemotropism in yeast." J Cell Sci **126**(Pt 14): 2997-3009.

Delgado-Jarana, J., A. L. Martinez-Rocha, R. Roldan-Rodriguez, M. I. Roncero and A. Di Pietro (2005). "*Fusarium oxysporum* G-protein beta subunit Fgb1 regulates hyphal growth, development, and virulence through multiple signalling pathways." Fungal Genet Biol **42**(1): 61-72.

Den Herder, J., S. Lievens, S. Rombauts, M. Holsters and S. Goormachtig (2007). "A symbiotic plant peroxidase involved in bacterial invasion of the tropical legume Sesbania rostrata." Plant Physiol **144**(2): 717-727.

Dharmatilake, A. J. and W. D. Bauer (1992). "Chemotaxis of *Rhizobium* meliloti towards Nodulation Gene-Inducing Compounds from Alfalfa Roots." Appl Environ Microbiol **58**(4): 1153-1158.

Di Pietro, A., F. I. Garcia-MacEira, E. Meglecz and M. I. Roncero (2001). "A MAP kinase of the vascular wilt fungus *Fusarium oxysporum* is essential for root penetration and pathogenesis." Mol Microbiol **39**(5): 1140-1152.

Dignani, M. C. and E. Anaissie (2004). "Human fusariosis." Clin Microbiol Infect **10 Suppl 1**: 67-75.

Dinesh-Kumar, S. P., R. Anandalakshmi, R. Marathe, M. Schiff and Y. Liu (2003). "Virus-induced gene silencing." Methods Mol Biol **236**: 287-294.

Divon, H. H., B. Rothan-Denoyes, O. Davydov, D. I. P. A and R. Fluhr (2005). "Nitrogen-responsive genes are differentially regulated in planta during *Fusarium oxyspsorum* f. sp. *lycopersici* infection." Mol Plant Pathol **6**(4): 459-470.

Donofrio, N. M., Y. Oh, R. Lundy, H. Pan, D. E. Brown, J. S. Jeong, S. Coughlan, T. K. Mitchell and R. A. Dean (2006). "Global gene expression during nitrogen starvation in the rice blast fungus, *Magnaporthe grisea*." Fungal Genet Biol **43**(9): 605-617.

Duarte-Vazquez, M. A., B. E. Garcia-Almendarez, C. Regalado and J. R. Whitaker (2001). "Purification and properties of a neutral peroxidase isozyme from turnip (*Brassica napus* L. var. *purple* Top White Globe) roots." J Agric Food Chem **49**(9): 4450-4456.

Dunand, C., M. Crevecoeur and C. Penel (2007). "Distribution of superoxide and hydrogen peroxide in Arabidopsis root and their influence on root development: possible interaction with peroxidases." New Phytol **174**(2): 332-341.

Ekengren, S. K., Y. Liu, M. Schiff, S. P. Dinesh-Kumar and G. B. Martin (2003). "Two MAPK cascades, NPR1, and TGA transcription factors play a role in Pto-mediated disease resistance in tomato." Plant J **36**(6): 905-917.

Elion, E. A. (2000). "Pheromone response, mating and cell biology." Curr Opin Microbiol **3**(6): 573-581.

Elion, E. A., B. Satterberg and J. E. Kranz (1993). "FUS3 phosphorylates multiple components of the mating signal transduction cascade: evidence for STE12 and FAR1." Mol Biol Cell **4**(5): 495-510.

Elstner, E. F. and A. Heupel (1976). "Formation of hydrogen peroxide by isolated cell walls from horseradish (*Armoracia lapathifolia* Gilib.)." Planta **130**(2): 175-180.

Enyedi, B. and P. Niethammer (2013). "H2O2: a chemoattractant?" Methods Enzymol **528**: 237-255.

Fairn, G. D., M. Hermansson, P. Somerharju and S. Grinstein (2011). "Phosphatidylserine is polarized and required for proper Cdc42 localization and for development of cell polarity." Nat Cell Biol **13**(12): 1424-1430.

Farman, M. L., Y. Eto, T. Nakao, Y. Tosa, H. Nakayashiki, S. Mayama and S. A. Leong (2002). "Analysis of the structure of the AVR1-CO39 avirulence locus in virulent rice-infecting isolates of *Magnaporthe grisea*." Mol Plant Microbe Interact **15**(1): 6-16.

Fawal, N., Q. Li, B. Savelli, M. Brette, G. Passaia, M. Fabre, C. Mathe and C. Dunand (2013). "PeroxiBase: a database for large-scale evolutionary analysis of peroxidases." Nucleic Acids Res **41**(Database issue): D441-444.

Federico, R. and R. Angelini (1986). "Occurrence of diamine oxidase in the apoplast of pea epicotyls." Planta **167**(2): 300-302.

Fedorova, M., J. van de Mortel, P. A. Matsumoto, J. Cho, C. D. Town, K. A. VandenBosch, J. S. Gantt and C. P. Vance (2002). "Genome-wide identification of nodule-specific transcripts in the model legume *Medicago truncatula*." Plant Physiol **130**(2): 519-537.

Fire, A., S. Xu, M. K. Montgomery, S. A. Kostas, S. E. Driver and C. C. Mello (1998). "Potent and specific genetic interference by double-stranded RNA in Caenorhabditis elegans." Nature **391**(6669): 806-811.

Fleissner, A., A. C. Leeder, M. G. Roca, N. D. Read and N. L. Glass (2009). "Oscillatory recruitment of signaling proteins to cell tips promotes coordinated behavior during cell fusion." Proc Natl Acad Sci U S A **106**(46): 19387-19392.

Flor, H. H. (1947). "Inheritance of pathogenicity in *Melampsora lini*." Phytopathology **32**: 653-669.

Flor, H. H. (1971). "Current status of the gene for gene concept." Annu Rev Phytopathol. **9**: 275-296.

Foreman, J., V. Demidchik, J. H. Bothwell, P. Mylona, H. Miedema, M. A. Torres, P. Linstead, S. Costa, C. Brownlee, J. D. Jones, J. M. Davies and L. Dolan (2003). "Reactive oxygen species produced by NADPH oxidase regulate plant cell growth." Nature **422**(6930): 442-446.

Fravel , D., C. Olivain and C. Alabouvette (2003). "*Fusarium oxysporum* and its biocontrol." New Phytologist **157**: 493-502.

Frenzel, B. (1957). "Zur abgabe von aminosauren und amiden an dasnahrmedium durch die wurzeln von *Helianthus annus*." Planta **49**: 210–234.

Frenzel, B. (1960). "Zur atiologie der anreicherung von aminosaurenund amiden in wurzelraum von *Helianthes annus*. Ein Beitragzur Klarung der Probleme der Rhizosphare. ." Planta **55**: 169–207.

Fulton, H. R. (1906). "Chemotropism of fungi." Bot. Gaz **41**: 81-108.

Gadea, J., M. E. Mayda, V. Conejero and P. Vera (1996). "Characterization of defense-related genes ectopically expressed in viroid-infected tomato plants." Mol Plant Microbe Interact **9**(5): 409-415.

Gajhede, M., D. J. Schuller, A. Henriksen, A. T. Smith and T. L. Poulos (1997). "Crystal structure of horseradish peroxidase C at 2.15 A resolution." Nat Struct Biol **4**(12): 1032-1038.

Gelin-Licht, R., S. Paliwal, P. Conlon, A. Levchenko and J. E. Gerst (2012). "Scp160-dependent mRNA trafficking mediates pheromone gradient sensing and chemotropism in yeast." Cell Rep **1**(5): 483-494.

Gianinazzi-Pearson, V., B. Branzanti and S. Gianinazzi (1989). "In vitro enhancement of spore germination and early hyphal growth of a vesicular-arbuscular mycorrhizal fungus by host root exudates and plant flavonoids." Symbiosis **7**: 243–255.

Giovannetti, M., C. Sbrana, A. Silvia and L. Avio (1996). "Analysis of factors involved in fungal recognition response to host-derived signals by arbuscular mycorrhizal fungi." New Phytologist **133**: 65–71.

Gough, D. R. and T. G. Cotter (2011). "Hydrogen peroxide: a Jekyll and Hyde signalling molecule." Cell Death Dis **2**: e213.

Gow, N. A. (1993). "Nonchemical signals used for host location and invasion by fungal pathogens." Trends Microbiol **1**(2): 45-50.

Gramss, G., K. Voigt and B. Kirsche (1999). " Oxidoreductase enzymes liberated by plant roots and their effects on soil humic material." Chemosphere **38**: 1481-1494

Grenville-Briggs, L. J., V. L. Anderson, J. Fugelstad, A. O. Avrova, J. Bouzenzana, A. Williams, S. Wawra, S. C. Whisson, P. R. Birch, V. Bulone and P. van West (2008). "Cellulose synthesis in *Phytophthora infestans* is required for normal appressorium formation and successful infection of potato." Plant Cell **20**(3): 720-738.

Guo, Y., W. C. Au, M. Shakoury-Elizeh, O. Protchenko, M. Basrai, W. A. Prinz and C. C. Philpott (2010). "Phosphatidylserine is involved in the ferrichrome-induced plasma membrane trafficking of Arn1 in Saccharomyces cerevisiae." J Biol Chem **285**(50): 39564-39573.

Gustin, M. C., J. Albertyn, M. Alexander and K. Davenport (1998). "MAP kinase pathways in the yeast *Saccharomyces cerevisiae*." Microbiol Mol Biol Rev **62**(4): 1264-1300.

Hadwiger, J. A., C. Wittenberg, H. E. Richardson, M. de Barros Lopes and S. I. Reed (1989). "A family of cyclin homologs that control the G1 phase in yeast." Proc Natl Acad Sci U S A **86**(16): 6255-6259.

Hanahan, D. (1985). "Techniques for transformation of *Escherichia coli*". In: Glover D M, editor. DNA cloning: a practical approach. Vol. 1. Oxford, United Kingdom: IRL Press.

Hardwick, J. S. and B. M. Sefton (1995). "Activation of the Lck tyrosine protein kinase by hydrogen peroxide requires the phosphorylation of Tyr-394." Proc Natl Acad Sci U S A **92**(10): 4527-4531.

Harman, G. E., C. R. Howell, A. Viterbo, I. Chet and M. Lorito (2004). "Trichoderma species--opportunistic, avirulent plant symbionts." Nat Rev Microbiol **2**(1): 43-56.

Harrison, S. J., M. D. Curtis, C. L. McIntyre, D. J. Maclean and J. M. Manners (1995). "Differential expression of peroxidase isogenes during the early stages of infection of the tropical forage legume Stylosanthes humilis by *Colletotrichum gloeosporioides*." Mol Plant Microbe Interact **8**(3): 398-406.

Hartmann, C. and P. R. Ortiz de Montellano (1992). "Baculovirus expression and characterization of catalytically active horseradish peroxidase." Arch Biochem Biophys **297**(1): 61-72.

Hayden, M. S. and S. Ghosh (2012). "NF-kappaB, the first quarter-century: remarkable progress and outstanding questions." Genes Dev **26**(3): 203-234.

He, B., F. Xi, X. Zhang, J. Zhang and W. Guo (2007). "Exo70 interacts with phospholipids and mediates the targeting of the exocyst to the plasma membrane." EMBO J **26**(18): 4053-4065.

Heese-Peck, A., H. Pichler, B. Zanolari, R. Watanabe, G. Daum and H. Riezman (2002). "Multiple functions of sterols in yeast endocytosis." Mol Biol Cell **13**(8): 2664-2680.

Henriksen, A., A. T. Smith and M. Gajhede (1999). "The structures of the horseradish peroxidase C-ferulic acid complex and the ternary complex with cyanide suggest how peroxidases oxidize small phenolic substrates." J Biol Chem **274**(49): 35005-35011.

Hinman, R. L. and J. Lang (1965). "Peroxidase-Catalyzed Oxidation of Indole-3-Acetic Acid." Biochemistry **4**: 144-158.

Hiraga, S., H. Ito, H. Yamakawa, N. Ohtsubo, S. Seo, I. Mitsuhara, H. Matsui, M. Honma and Y. Ohashi (2000). "An HR-induced tobacco peroxidase gene is responsive to spermine, but not to salicylate, methyl jasmonate, and ethephon." Mol Plant Microbe Interact **13**(2): 210-216.

Hiraga, S., K. Sasaki, H. Ito, Y. Ohashi and H. Matsui (2001). "A large family of class III plant peroxidases." Plant Cell Physiol **42**(5): 462-468.

Hiraga, S., K. Yamamoto, H. Ito, K. Sasaki, H. Matsui, M. Honma, Y. Nagamura, T. Sasaki and Y. Ohashi (2000). "Diverse expression profiles of 21 rice peroxidase genes." FEBS Lett **471**(2-3): 245-250.

Ho, S. N., H. D. Hunt, R. M. Horton, J. K. Pullen and L. R. Pease (1989). "Site-directed mutagenesis by overlap extension using the polymerase chain reaction." Gene **77**(1): 51-59.

Hohmann, S., M. Krantz and B. Nordlander (2007). "Yeast osmoregulation." Methods Enzymol **428**: 29-45.

Horan, D. P. and G. A. Chilvers (1990). "Chemotropism - the key to ectomycorrhizal formation?" New Phytol **116**: 297-301.

Hou, Z., C. Xue, Y. Peng, T. Katan, H. C. Kistler and J. R. Xu (2002). "A mitogen-activated protein kinase gene (MGV1) in Fusarium graminearum is required for female fertility, heterokaryon formation, and plant infection." Mol Plant Microbe Interact **15**(11): 1119-1127.

Howes, B. D., N. C. Veitch, A. T. Smith, C. G. White and G. Smulevich (2001). "Haem-linked interactions in horseradish peroxidase revealed by spectroscopic analysis of the Phe-221-->Met mutant." Biochem J **353**(Pt 2): 181-191.

Huertas-Gonzalez, M. D., M. C. Ruiz-Roldan, F. I. Garcia Maceira, M. I. Roncero and A. Di Pietro (1999). "Cloning and characterization of pl1 encoding an in planta-secreted pectate lyase of *Fusarium oxysporum*." Curr Genet **35**(1): 36-40.

Isaacson, R. E. (2002). "Genomics and the prospects for the discovery of new targets for antibacterial and antifungal agents." Curr Pharm Des **8**(13): 1091-1098.

Ito, H., S. Hiraga, H. Tsugawa, H. Matsui, M. Honma, Y. Otsuki, T. Murakami and Y. Ohashi (2000). "Xylem-specific expression of wound-inducible rice peroxidase genes in transgenic plants." Plant Sci **155**(1): 85-100.

Izumitsu, K., A. , D. Yoshimi, A. M. Kubo, Y. Saitoh and C. Tanaka (2009). "The MAPKK kinase ChSte11 regulates sexual/asexual development, melanization, pathogenicity, and adaptation to oxidative stress in *Cochliobolus heterostrophus*." Curr Genet **55(4)**: 439-448.

Izumitsu, K., A. Yoshimi, D. Kubo, A. Morita, Y. Saitoh and C. Tanaka (2009). "The MAPKK kinase ChSte11 regulates sexual/asexual development, melanization, pathogenicity, and adaptation to oxidative stress in *Cochliobolus heterostrophus*." Curr Genet **55**(4): 439-448.

Jackson, C. L. and L. H. Hartwell (1990). "Courtship in *S. cerevisiae*: both cell types choose mating partners by responding to the strongest pheromone signal." Cell **63**(5): 1039-1051.

Jaffe, L. F. (1966). "On Autotropism in *Botrytis*: Measurement Technique and Control by CO2." Plant Physiol **41**: 303-306.

Jansson, H.-B., T. Johansson, B. Nordbring-Herts, A. Tunlid and G. Odham (1988). "Chemotropic growth of germ tubes of *Cochliobolus sativus* to barley roots or root exudates." Trans. Br. Mycol. Soc **90**: 647-650.

Jenczmionka, N. J., F. J. Maier, A. P. Losch and W. Schafer (2003). "Mating, conidiation and pathogenicity of Fusarium graminearum, the main causal agent of the head-blight disease of wheat, are regulated by the MAP kinase gpmk1." Curr Genet **43**(2): 87-95.

Jenczmionka, N. J. and W. Schafer (2005). "The Gpmk1 MAP kinase of *Fusarium graminearum* regulates the induction of specific secreted enzymes." Curr Genet **47**(1): 29-36.

Jenness, D. D. and P. Spatrick (1986). "Down regulation of the alpha-factor pheromone receptor in *S. cerevisiae*." Cell **46**(3): 345-353.

Jeon, J., J. Goh, S. Yoo, M. H. Chi, J. Choi, H. S. Rho, J. Park, S. S. Han, B. R. Kim, S. Y. Park, S. Kim and Y. H. Lee (2008). "A putative MAP kinase kinase kinase, MCK1, is required for cell wall integrity and pathogenicity of the rice blast fungus, *Magnaporthe oryzae*." Mol Plant Microbe Interact **21**(5): 525-534.

Joobeur, T., J. J. King, S. J. Nolin, C. E. Thomas and R. A. Dean (2004). "The Fusarium wilt resistance locus Fom-2 of melon contains a single resistance gene with complex features." Plant J **39**(3): 283-297.

Jung, U. S. and D. E. Levin (1999). "Genome-wide analysis of gene expression regulated by the yeast cell wall integrity signalling pathway." Mol Microbiol **34**(5): 1049-1057.

Jung, U. S., A. K. Sobering, M. J. Romeo and D. E. Levin (2002). "Regulation of the yeast Rlm1 transcription factor by the Mpk1 cell wall integrity MAP kinase." Mol Microbiol **46**(3): 781-789.

Kammen, A. v. (1997). "Virus-induced gene silencing in infected and transgenic plants." Trends in Plant Science **2**: 409–411.

Kawaoka, A., T. Kawamoto, M. Sekine, K. Yoshida, M. Takano and A. Shinmyo (1994). "A cis-acting element and a trans-acting factor involved in the wound-induced expression of a horseradish peroxidase gene." Plant J **6**(1): 87-97.

Kelley, J. B., G. Dixit, J. B. Sheetz, S. P. Venkatapurapu, T. C. Elston and H. G. Dohlman (2015). "RGS proteins and septins cooperate to promote chemotropism by regulating polar cap mobility." Curr Biol **25**(3): 275-285.

Khan, M. R., S. Fischer, D. Egan and F. M. Doohan (2006). "Biological control of fusarium seedling blight disease of wheat and barley." Phytopathology **96**(4): 386-394.

Kim, S., J. C. Mollet, J. Dong, K. Zhang, S. Y. Park and E. M. Lord (2003). "Chemocyanin, a small basic protein from the lily stigma, induces pollen tube chemotropism." Proc Natl Acad Sci U S A **100**(26): 16125-16130.

Kjaersgard, I. V., H. M. Jespersen, S. K. Rasmussen and K. G. Welinder (1997). "Sequence and RT-PCR expression analysis of two peroxidases from *Arabidopsis thaliana* belonging to a novel evolutionary branch of plant peroxidases." Plant Mol Biol **33**(4): 699-708.

Klahre, U., P. Crete, S. A. Leuenberger, V. A. Iglesias and F. Meins, Jr. (2002). "High molecular weight RNAs and small interfering RNAs induce systemic posttranscriptional gene silencing in plants." Proc Natl Acad Sci U S A **99**(18): 11981-11986.

Klyubin, I. V., K. M. Kirpichnikova and I. A. Gamaley (1996). "Hydrogen peroxide-induced chemotaxis of mouse peritoneal neutrophils." Eur J Cell Biol **70**(4): 347-351.

Kojima, K., T. Kikuchi, Y. Takano, E. Oshiro and T. Okuno (2002). "The mitogen-activated protein kinase gene MAF1 is essential for the early differentiation phase of appressorium formation in Colletotrichum lagenarium." Mol Plant Microbe Interact **15**(12): 1268-1276.

Kolattukudy, P. E. (1980). "Biopolyester membranes of plants: cutin and suberin." Science **208**(4447): 990-1000.

Kono, Y., H. Yamamoto, M. Takeuchi and H. Komada (1995). "Alterations in superoxide dismutase and catalase in *Fusarium oxysporum* during starvationinduced differentiation." Biochim Biophys Acta **1268**: 35–40.

Koske, R. E. (1982). "Evidence for a volatile attractant from plant roots affecting germ tubes of a VA mycorrhizal fungus." Transact Br Mycol Soc **79**(2): 305-310.

Koua, D., L. Cerutti, L. Falquet, C. J. Sigrist, G. Theiler, N. Hulo and C. Dunand (2009). "PeroxiBase: a database with new tools for peroxidase family classification." Nucleic Acids Res **37**(Database issue): D261-266.

Kovtun, Y., W. L. Chiu, G. Tena and J. Sheen (2000). "Functional analysis of oxidative stress-activated mitogen-activated protein kinase cascade in plants." Proc Natl Acad Sci U S A **97**(6): 2940-2945.

Kraus, P. R. and J. Heitman (2003). "Coping with stress: calmodulin and calcineurin in model and pathogenic fungi." Biochem Biophys Res Commun **311**(4): 1151-1157.

Kricka, L. J. (1995). Nonisotopic Probing, Blotting, and Sequencing, 2nd Ed. Academic Press, San Diego, CA, USA.

Kuldau, G. A. and I. E. Yates. (2000). "Evidence for Fusarium endophytes in cultivated and wild plants." In: Bacon, C.W.; White Jr., J.F. (eds). Biology and evolution of microbial endophytes. Dekker, New York, USA: 85-117.

Kurjan, J. (1993). "The pheromone response pathway in *Saccharomyces cerevisiae*." Annu Rev Genet **27**: 147-179.

Laemmli, U. K. (1970). "Cleavage of structural proteins during the assembly of the head of bacteriophage T4." Nature **227**(5259): 680-685.

Lagrimini, L. M. and S. Rothstein (1987). "Tissue specificity of tobacco peroxidase isozymes and their induction by wounding and tobacco mosaic virus infection." Plant Physiol **84**(2): 438-442.

Lalucque, H. and P. Silar (2003). "NADPH oxidase: an enzyme for multicellularity?" Trends Microbiol **11**(1): 9-12.

Lamb, C. and R. A. Dixon (1997). "The Oxidative Burst in Plant Disease Resistance." Annu Rev Plant Physiol Plant Mol Biol **48**: 251-275.

Lanver, D., A. Mendoza-Mendoza, A. Brachmann and R. Kahmann (2010). "Sho1 and Msb2-related proteins regulate appressorium development in the smut fungus *Ustilago maydis*." Plant Cell **22**(6): 2085-2101.

Larena, I., P. Melgarejo and A. De Cal (2002). "Production, Survival, and Evaluation of Solid-Substrate Inocula of *Penicillium oxalicum*, a Biocontrol Agent Against Fusarium Wilt of Tomato." Phytopathology **92**(8): 863-869.

Larkin, R. P. and D. R. Fravel (2002). "Effects of Varying Environmental Conditions on Biological Control of Fusarium Wilt of Tomato by Nonpathogenic *Fusarium* spp." Phytopathology **92**(11): 1160-1166.

Leeder, A. C., J. Palma-Guerrero and N. L. Glass (2011). "The social network: deciphering fungal language." Nat Rev Microbiol **9**(6): 440-451.

Lev, S. and B. A. Horwitz (2003). "A mitogen-activated protein kinase pathway modulates the expression of two cellulase genes in *Cochliobolus heterostrophus* during plant infection." Plant Cell **15**(4): 835-844.

Lev, S., A. Sharon, R. Hadar, H. Ma and B. A. Horwitz (1999). "A mitogen-activated protein kinase of the corn leaf pathogen *Cochliobolus heterostrophus* is involved in conidiation, appressorium formation, and pathogenicity: diverse roles for mitogen-activated protein kinase homologs in foliar pathogens." Proc Natl Acad Sci U S A **96**(23): 13542-13547.

Levin, D. E. (2005). "Cell wall integrity signaling in *Saccharomyces cerevisiae*." Microbiol Mol Biol Rev **69**(2): 262-291.

Link (1809). "Fusarium." Mag. Ges. Naturf. Freunde, Berlin **3**: 10

Liu, W., X. Zhou, G. Li, L. Li, L. Kong, C. Wang, H. Zhang and J. R. Xu (2011). "Multiple plant surface signals are sensed by different mechanisms in the rice blast fungus for appressorium formation." PLoS Pathog **7**(1): e1001261.

Liu, Y., M. Schiff and S. P. Dinesh-Kumar (2002). "Virus-induced gene silencing in tomato." Plant J **31**(6): 777-786.

Liu, Y., M. Schiff, R. Marathe and S. P. Dinesh-Kumar (2002). "Tobacco Rar1, EDS1 and NPR1/NIM1 like genes are required for N-mediated resistance to tobacco mosaic virus." Plant J **30**(4): 415-429.

Livak, K. J. and T. D. Schmittgen (2001). "Analysis of relative gene expression data using real-time quantitative PCR and the 2(-Delta Delta C(T)) Method." Methods **25**(4): 402-408.

Lo, W. S. and A. M. Dranginis (1996). "FLO11, a yeast gene related to the STA genes, encodes a novel cell surface flocculin." J Bacteriol **178**(24): 7144-7151.

Lo, W. S. and A. M. Dranginis (1998). "The cell surface flocculin Flo11 is required for pseudohyphae formation and invasion by *Saccharomyces cerevisiae*." Mol Biol Cell **9**(1): 161-171.

Lopez-Berges, M. S., N. Rispail, R. C. Prados-Rosales and A. Di Pietro (2010). "A nitrogen response pathway regulates virulence functions in *Fusarium oxysporum* via the protein kinase TOR and the bZIP protein MeaB." Plant Cell **22**(7): 2459-2475.

Luo, J., Y. Matsuo, G. Gulis, H. Hinz, J. Patton-Vogt and S. Marcus (2009). "Phosphatidylethanolamine is required for normal cell morphology and cytokinesis in the fission yeast *Schizosaccharomyces pombe*." Eukaryot Cell **8**(5): 790-799.

Lysek, G. (1976). "Formation of perithecia in colonies of Podospora anserina." Planta **133**(1): 81-83.

Ma, L. J., H. C. van der Does, K. A. Borkovich, J. J. Coleman, M. J. Daboussi, A. Di Pietro, M. Dufresne, M. Freitag, M. Grabherr, B. Henrissat, P. M. Houterman, S. Kang, W. B. Shim, C. Woloshuk, X. Xie, J. R. Xu, J. Antoniw, S. E. Baker, B. H. Bluhm, A. Breakspear, D. W. Brown, R. A. Butchko, S. Chapman, R. Coulson, P. M. Coutinho, E. G. Danchin, A. Diener, L. R. Gale, D. M. Gardiner, S. Goff, K. E. Hammond-Kosack, K. Hilburn, A. Hua-Van, W. Jonkers, K. Kazan, C. D. Kodira, M. Koehrsen, L. Kumar, Y. H. Lee, L. Li, J. M. Manners, D. Miranda-Saavedra, M. Mukherjee, G. Park, J. Park, S. Y. Park, R. H. Proctor, A. Regev, M. C. Ruiz-Roldan, D. Sain, S. Sakthikumar, S. Sykes, D. C. Schwartz, B. G. Turgeon, I. Wapinski, O. Yoder, S. Young, Q. Zeng, S. Zhou, J. Galagan, C. A. Cuomo, H. C. Kistler and M. Rep (2010). "Comparative genomics reveals mobile pathogenicity chromosomes in Fusarium." Nature **464**(7287): 367-373.

Mader, M., J. Ungemach and P. Schloss (1980). "The role of peroxidase isoenzyme groups of Nicotiana tabacum in hydrogen peroxide formation." Planta **147**(5): 467-470.

Madhani, H. D., T. Galitski, E. S. Lander and G. R. Fink (1999). "Effectors of a developmental mitogen-activated protein kinase cascade revealed by expression signatures of signaling mutants." Proc Natl Acad Sci U S A **96**(22): 12530-12535.

Madhani, H. D., C. A. Styles and G. R. Fink (1997). "MAP kinases with distinct inhibitory functions impart signaling specificity during yeast differentiation." Cell **91**(5): 673-684.

Madrid, M. P., A. Di Pietro and M. I. Roncero (2003). "Class V chitin synthase determines pathogenesis in the vascular wilt fungus *Fusarium oxysporum* and mediates resistance to plant defence compounds." Mol Microbiol **47**(1): 257-266.

Martienssen, R. A. (1998). "Functional genomics: probing plant gene function and expression with transposons." Proc Natl Acad Sci U S A **95**(5): 2021-2026.

Marzluf, G. A. (1997). "Genetic regulation of nitrogen metabolism in the fungi." Microbiol Mol Biol Rev **61**(1): 17-32.

Massee, G. (1905). "On the origin of parasitism in fungi." Phil. Trans. Royal Soc **197**: 7-24.

Mayda, E., C. Marques, V. Conejero and P. Vera (2000). "Expression of a pathogen-induced gene can be mimicked by auxin insensitivity." Mol Plant Microbe Interact **13**(1): 23-31.

Mehrabi, R., S. Ding and J. R. Xu (2008). "MADS-box transcription factor mig1 is required for infectious growth in *Magnaporthe grisea*." Eukaryot Cell **7**(5): 791-799.

Meno, K., S. Jennings, A. T. Smith, A. Henriksen and M. Gajhede (2002). "Structural analysis of the two horseradish peroxidase catalytic residue variants H42E and R38S/H42E: implications for the catalytic cycle." Acta Crystallogr D Biol Crystallogr **58**(Pt 10 Pt 2): 1803-1812.

Merlini, L., O. Dudin and S. G. Martin (2013). "Mate and fuse: how yeast cells do it." Open Biol **3**(3): 130008.

Metodiev, M. V., D. Matheos, M. D. Rose and D. E. Stone (2002). "Regulation of MAPK function by direct interaction with the mating-specific Galpha in yeast." Science **296**(5572): 1483-1486.

Mey, G., K. Held, J. Scheffer, K. B. Tenberge and P. Tudzynski (2002). "CPMK2, an SLT2-homologous mitogen-activated protein (MAP) kinase, is essential for pathogenesis of *Claviceps purpurea* on rye: evidence for a second conserved pathogenesis-related MAP kinase cascade in phytopathogenic fungi." Mol Microbiol **46**(2): 305-318.

Mey, G., B. Oeser, M. H. Lebrun and P. Tudzynski (2002). "The biotrophic, non-appressorium-forming grass pathogen *Claviceps purpurea* needs a Fus3/Pmk1 homologous mitogen-activated protein kinase for colonization of rye ovarian tissue." Mol Plant Microbe Interact **15**(4): 303-312.

Michielse, C. B. and M. Rep (2009). "Pathogen profile update: *Fusarium oxysporum*." Mol Plant Pathol **10**(3): 311-324.

Michielse, C. B., R. van Wijk, L. Reijnen, B. J. Cornelissen and M. Rep (2009). "Insight into the molecular requirements for pathogenicity of *Fusarium oxysporum* f. sp. *lycopersici* through large-scale insertional mutagenesis." Genome Biol **10**(1): R4.

Miyoshi, M. (1894). "Über Chemotropismus der Pilze." Bot. Zeit. **52**: 1-28.

Mohan, R., P. Vijayan and P. E. Kolattukudy (1993). "Developmental and tissue-specific expression of a tomato anionic peroxidase (tap1) gene by a minimal promoter, with wound and pathogen induction by an additional 5'-flanking region." Plant Mol Biol **22**(3): 475-490.

Moore, T. I., C. S. Chou, Q. Nie, N. L. Jeon and T. M. Yi (2008). "Robust spatial sensing of mating pheromone gradients by yeast cells." PLoS One **3**(12): e3865.

Morawski, B., Z. Lin, P. Cirino, H. Joo, G. Bandara and F. H. Arnold (2000). "Functional expression of horseradish peroxidase in *Saccharomyces cerevisiae* and *Pichia pastoris*." Protein Eng **13**(5): 377-384.

Morris, P. F., E. Bone and B. M. Tyler (1998). "Chemotropic and contact responses of phytophthora sojae hyphae to soybean isoflavonoids and artificial substrates." Plant Physiol **117**(4): 1171-1178.

Morris, P. F. and E. W. B. Ward (1992). "Chemoattraction of zoospores of the soybean pathogen *Phytophthora sojae* by isoflavones." Physiol Mol Plant Pathol **40**: 17–22.

Moukadiri, I., L. Jaafar and J. Zueco (1999). "Identification of two mannoproteins released from cell walls of a *Saccharomyces cerevisiae* mnn1 mnn9 double mutant by reducing agents." J Bacteriol **181**(16): 4741-4745.

Muehlstein, L. K., J. P. Amon and D. L. Leffler (1988). "Chemotaxis in the Marine Fungus *Rhizophydium littoreum*." Appl Environ Microbiol **54**(7): 1668-1672.

Muller, P., G. Weinzierl, A. Brachmann, M. Feldbrugge and R. Kahmann (2003). "Mating and pathogenic development of the Smut fungus *Ustilago maydis* are regulated by one mitogen-activated protein kinase cascade." Eukaryot Cell **2**(6): 1187-1199.

Munn, A. L., A. Heese-Peck, B. J. Stevenson, H. Pichler and H. Riezman (1999). "Specific sterols required for the internalization step of endocytosis in yeast." Mol Biol Cell **10**(11): 3943-3957.

Murray, M. G. and W. F. Thompson (1980). "Rapid isolation of high molecular weight plant DNA." Nucleic Acids Res **8**(19): 4321-4325.

Nagahashi, G. and D. D. Douds (2000). "Partial separation of root exudate compounds and their effects upon the growth of germinated spores of AM fungi." Mycological Research **104**: 1453–1464.

Nasmyth, K. and L. Dirick (1991). "The role of SWI4 and SWI6 in the activity of G1 cyclins in yeast." Cell **66**(5): 995-1013.

Nathan, C. (2003). "Specificity of a third kind: reactive oxygen and nitrogen intermediates in cell signaling." J Clin Invest **111**(6): 769-778.

Neiman, A. M., B. J. Stevenson, H. P. Xu, G. F. Sprague, Jr., I. Herskowitz, M. Wigler and S. Marcus (1993). "Functional homology of protein kinases required for sexual differentiation in *Schizosaccharomyces pombe* and *Saccharomyces cerevisiae* suggests a conserved signal transduction module in eukaryotic organisms." Mol Biol Cell **4**(1): 107-120.

Nelson, P. E. (1981). Life cycle and epidemiology of *Fusarium oxysporum*: Academic Press, Inc., New York.

Nern, A. and R. A. Arkowitz (1998). "A GTP-exchange factor required for cell orientation." Nature **391**(6663): 195-198.

Nern, A. and R. A. Arkowitz (1999). "A Cdc24p-Far1p-Gbetagamma protein complex required for yeast orientation during mating." J Cell Biol **144**(6): 1187-1202.

Niethammer, P., C. Grabher, A. T. Look and T. J. Mitchison (2009). "A tissue-scale gradient of hydrogen peroxide mediates rapid wound detection in zebrafish." Nature **459**(7249): 996-999.

O'Donnell, K., H. C. Kistler, E. Cigelnik and R. C. Ploetz (1998). "Multiple evolutionary origins of the fungus causing Panama disease of banana: concordant evidence from nuclear and mitochondrial gene genealogies." Proc Natl Acad Sci U S A **95**(5): 2044-2049.

Ori, N., Y. Eshed, I. Paran, G. Presting, D. Aviv, S. Tanksley, D. Zamir and R. Fluhr (1997). "The I2C family from the wilt disease resistance locus I2 belongs to the nucleotide binding, leucine-rich repeat superfamily of plant resistance genes." Plant Cell **9**(4): 521-532.

Paliwal, S., P. A. Iglesias, K. Campbell, Z. Hilioti, A. Groisman and A. Levchenko (2007). "MAPK-mediated bimodal gene expression and adaptive gradient sensing in yeast." Nature **446**(7131): 46-51.

Panwar, V., B. McCallum and G. Bakkeren (2013). "Endogenous silencing of *Puccinia triticina* pathogenicity genes through in planta-expressed sequences leads to the suppression of rust diseases on wheat." Plant J **73**(3): 521-532.

Parinov, S., M. Sevugan, D. Ye, W. C. Yang, M. Kumaran and V. Sundaresan (1999). "Analysis of flanking sequences from dissociation insertion lines: a database for reverse genetics in Arabidopsis." Plant Cell **11**(12): 2263-2270.

Park, G., C. Xue, L. Zheng, S. Lam and J. R. Xu (2002). "MST12 regulates infectious growth but not appressorium formation in the rice blast fungus *Magnaporthe grisea*." Mol Plant Microbe Interact **15**(3): 183-192.

Passardi, F., G. Theiler, M. Zamocky, C. Cosio, N. Rouhier, F. Teixera, M. Margis-Pinheiro, V. Ioannidis, C. Penel, L. Falquet and C. Dunand (2007). "PeroxiBase: the peroxidase database." Phytochemistry **68**(12): 1605-1611.

Pearson, R. and D. Parkinson (1961). "The sites of excretion of older bean plants to *R. solani*. ninhydrin-positive substances by broad bean seedlings." Plant Soil **13**: 391-396.

Perez-Nadales, E., M. F. Almeida Nogueira, C. Baldin, S. Castanheira, M. El Ghalid, E. Grund, K. Lengeler, E. Marchegiani, P. V. Mehrotra, M. Moretti, V. Naik, M. Oses-Ruiz, T. Oskarsson, K. Schafer, L. Wasserstrom, A. A. Brakhage, N. A. Gow, R. Kahmann, M. H. Lebrun, J. Perez-Martin, A. Di Pietro, N. J. Talbot, V. Toquin, A. Walther and J. Wendland (2014). "Fungal model systems and the elucidation of pathogenicity determinants." Fungal Genet Biol **70C**: 42-67.

Perez-Nadales, E. and A. Di Pietro (2011). "The membrane mucin Msb2 regulates invasive growth and plant infection in *Fusarium oxysporum*." Plant Cell **23**(3): 1171-1185.

Perez-Nadales, E. and A. Di Pietro (2015). "The transmembrane protein Sho1 cooperates with the mucin Msb2 to regulate invasive growth and plant infection in *Fusarium oxysporum*." Mol Plant Pathol **16**(6): 593-603.

Peters, N. K. and D. P. S. Varma (1990). "Phenolic compounds as regulators of gene expression in plant-microbe interactions." Molecular Plant-Microbe Interactions **3**: 4-8.

Petrova, N. S., M. A. Zenkova and E. L. Chernolovskaya (2013). "Structure - Functions Relations in Small Interfering RNAs", Practical Applications in Biomedical Engineering, Dr. Adriano Andrade (Ed.), ISBN: 978-953-51-0924-2, InTech, DOI: 10.5772/53945.

Pfaffl, M. W. (2001). "A new mathematical model for relative quantification in real-time RT-PCR." Nucleic Acids Res **29**(9): e45.

Pfeffer, W. (1883). "Locomotorische Richtungsbewegungen durch chemische Reize." Ber. Deutsch. Bot. Gesells **I**: 532.

Pietro, A. D., M. P. Madrid, Z. Caracuel, J. Delgado-Jarana and M. I. Roncero (2003). "*Fusarium oxysporum*: exploring the molecular arsenal of a vascular wilt fungus." Mol Plant Pathol **4**(5): 315-325.

Ponferrada-Marin, M. I., T. Roldan-Arjona and R. R. Ariza (2009). "ROS1 5-methylcytosine DNA glycosylase is a slow-turnover catalyst that initiates DNA demethylation in a distributive fashion." Nucleic Acids Res **37**(13): 4264-4274.

Poulos, T. L. and J. Kraut (1980). "The stereochemistry of peroxidase catalysis." J Biol Chem **255**(17): 8199-8205.

Prados Rosales, R. C. and A. Di Pietro (2008). "Vegetative hyphal fusion is not essential for plant infection by *Fusarium oxysporum*." Eukaryot Cell **7**(1): 162-171.

Prados-Rosales, R. C., R. Roldan-Rodriguez, C. Serena, M. S. Lopez-Berges, J. Guarro, A. Martinez-del-Pozo and A. Di Pietro (2012). "A PR-1-like protein of *Fusarium oxysporum* functions in virulence on mammalian hosts." J Biol Chem **287**(26): 21970-21979.

Prinz, S., I. Avila-Campillo, C. Aldridge, A. Srinivasan, K. Dimitrov, A. F. Siegel and T. Galitski (2004). "Control of yeast filamentous-form growth by modules in an integrated molecular network." Genome Res **14**(3): 380-390.

Puhalla, J. E. (1968). "Compatibility reactions on solid medium and interstrain inhibition in *Ustilago maydis*." Genetics **60**: 461-474.

Qi, M. and E. A. Elion (2005). "MAP kinase pathways." J Cell Sci **118**(Pt 16): 3569-3572.

Qi, Z., Q. Wang, X. Dou, W. Wang, Q. Zhao, R. Lv, H. Zhang, X. Zheng, P. Wang and Z. Zhang (2012). "MoSwi6, an APSES family transcription factor, interacts with MoMps1 and is required for hyphal and conidial morphogenesis, appressorial function and pathogenicity of *Magnaporthe oryzae*." Mol Plant Pathol **13**(7): 677-689.

Rada, B. and T. L. Leto (2008). "Oxidative innate immune defenses by Nox/Duox family NADPH oxidases." Contrib Microbiol **15**: 164-187.

Rao, G. N. (1997). "Protein tyrosine kinase activity is required for oxidant-induced extracellular signal-regulated protein kinase activation and c-fos and c-jun expression." Cell Signal **9**(2): 181-187.

Ratcliff, F., A. M. Martin-Hernandez and D. C. Baulcombe (2001). "Technical Advance. Tobacco rattle virus as a vector for analysis of gene function by silencing." Plant J **25**(2): 237-245.

Read, N. D., A. B. Goryachev and L. A. (2011). "The mechanistic basis of self-fusion between conidial anastomosis tubes during fungal colony initiation." Fungal Biol Rev **26**: 1-11.

Rep, M., H. C. van der Does, M. Meijer, R. van Wijk, P. M. Houterman, H. L. Dekker, C. G. de Koster and B. J. Cornelissen (2004). "A small, cysteine-rich protein secreted by *Fusarium oxysporum* during colonization of xylem vessels is required for I-3-mediated resistance in tomato." Mol Microbiol **53**(5): 1373-1383.

Rispail, N. and A. Di Pietro (2009). "Fusarium oxysporum Ste12 controls invasive growth and virulence downstream of the Fmk1 MAPK cascade." Mol Plant Microbe Interact **22**(7): 830-839.

Rispail, N. and A. Di Pietro (2010). "The two-component histidine kinase Fhk1 controls stress adaptation and virulence of *Fusarium oxysporum*." Mol Plant Pathol **11**(3): 395-407.

Rispail, N., D. M. Soanes, C. Ant, R. Czajkowski, A. Grunler, R. Huguet, E. Perez-Nadales, A. Poli, E. Sartorel, V. Valiante, M. Yang, R. Beffa, A. A. Brakhage, N. A. Gow, R. Kahmann, M. H. Lebrun, H. Lenasi, J. Perez-Martin, N. J. Talbot, J. Wendland and A. Di Pietro (2009). "Comparative genomics of MAP kinase and calcium-calcineurin signalling components in plant and human pathogenic fungi." Fungal Genet Biol **46**(4): 287-298.

Roberts, E. and P. E. Kolattukudy (1989). "Molecular cloning, nucleotide sequence, and abscisic acid induction of a suberization-associated highly anionic peroxidase." Mol Gen Genet **217**(2-3): 223-232.

Roberts, E., T. Kutchan and P. E. Kolattukudy (1988). "Cloning and sequencing of cDNA for a highly anionic peroxidase from potato and the induction of its mRNA in suberizing potato tubers and tomato fruits." Plant Mol Biol **11**(1): 15-26.

Robinson, P. M., D. Park and T. A. Graham (1968). "Autotropism in fungal spores." J. Exp. Bot. **19**: 125-134.

Rodriguez-Lopez, J. N., A. T. Smith and R. N. Thorneley (1996). "Role of arginine 38 in horseradish peroxidase. A critical residue for substrate binding and catalysis." J Biol Chem **271**(8): 4023-4030.

Romano, N. and G. Macino (1992). "Quelling: transient inactivation of gene expression in Neurospora crassa by transformation with homologous sequences." Mol Microbiol **6**(22): 3343-3353.

Rosskopf, E. N., D. O. Chellemi, N. Kokalis-Burelle and G. T. Church (2005) "Alternatives to Methyl Bromide: A Florida Perspective." APSnet Features. Online. APSnet Features. doi: 10.1094/APSnetFeature/2005-0605.

Rui, O. and M. Hahn (2007). "The Slt2-type MAP kinase Bmp3 of *Botrytis cinerea* is required for normal saprotrophic growth, conidiation, plant surface sensing and host tissue colonization." Mol Plant Pathol **8**(2): 173-184.

Ruiz-Roldan, M. C., F. J. Maier and W. Schafer (2001). "PTK1, a mitogen-activated-protein kinase gene, is required for conidiation, appressorium formation, and pathogenicity of *Pyrenophora teres* on barley." Mol Plant Microbe Interact **14**(2): 116-125.

Saito, H. (2010). "Regulation of cross-talk in yeast MAPK signaling pathways." Curr Opin Microbiol **13**(6): 677-683.

Sambrook, J., Fritsch, E.F., and Maniatis, T. (1989). Molecular cloning: A laboratory manual. 2nd Edn. Cold Spring Harbour Laboratory Press, Cold Spring Harbour, New York.

Sasaki, K., T. Iwai, S. Hiraga, K. Kuroda, S. Seo, I. Mitsuhara, A. Miyasaka, M. Iwano, H. Ito, H. Matsui and Y. Ohashi (2004). "Ten rice peroxidases redundantly respond to multiple stresses including infection with rice blast fungus." Plant Cell Physiol **45**(10): 1442-1452.

Sasaki, T., T. Matsumoto, K. Yamamoto, K. Sakata, T. Baba, Y. Katayose, J. Wu, Y. Niimura, Z. Cheng, Y. Nagamura, B. A. Antonio, H. Kanamori, S. Hosokawa, M. Masukawa, K. Arikawa, Y. Chiden, M. Hayashi, M. Okamoto, T. Ando, H. Aoki, K. Arita, M. Hamada, C. Harada, S. Hijishita, M. Honda, Y. Ichikawa, A. Idonuma, M. Iijima, M. Ikeda, M. Ikeno, S. Ito, T. Ito, Y. Ito, A. Iwabuchi, K. Kamiya, W. Karasawa, S. Katagiri, A. Kikuta, N. Kobayashi, I. Kono, K. Machita, T. Maehara, H. Mizuno, T. Mizubayashi, Y. Mukai, H. Nagasaki, M. Nakashima, Y. Nakama, Y. Nakamichi, M. Nakamura, N. Namiki, M. Negishi, I. Ohta, N. Ono, S. Saji, K. Sakai, M. Shibata, T. Shimokawa, A. Shomura, J. Song, Y. Takazaki, K. Terasawa, K. Tsuji, K. Waki, H. Yamagata, H. Yamane, S. Yoshiki, R. Yoshihara, K. Yukawa, H. Zhong, H. Iwama, T. Endo, H. Ito, J. H. Hahn, H. I. Kim, M. Y. Eun, M. Yano, J. Jiang and T. Gojobori (2002). "The genome sequence and structure of rice chromosome 1." Nature **420**(6913): 312-316.

Savenkova, M. I., S. L. Newmyer and P. R. Montellano (1996). "Rescue of His-42 --> Ala horseradish peroxidase by a Phe-41 --> His mutation. Engineering of a surrogate catalytic histidine." J Biol Chem **271**(40): 24598-24603.

Sbrana, C. and M. Giovannetti (2005). "Chemotropism in the arbuscular mycorrhizal fungus *Glomus mosseae*." Mycorrhiza **15**(7): 539-545.

Schamber, A., M. Leroch, J. Diwo, K. Mendgen and M. Hahn (2010). "The role of mitogen-activated protein (MAP) kinase signalling components and the Ste12 transcription factor in germination and pathogenicity of *Botrytis cinerea*." Mol Plant Pathol **11**(1): 105-119.

Schandel, K. A. and D. D. Jenness (1994). "Direct evidence for ligand-induced internalization of the yeast alpha-factor pheromone receptor." Mol Cell Biol **14**(11): 7245-7255.

Schreurs, W. J., R. L. Harold and F. M. Harold (1989). "Chemotropism and branching as alternative responses of Achlya bisexualis to amino acids." J Gen Microbiol **135**(9): 2519-2528.

Schroth, M. N. and W. C. Snyder (1961). "Effect of host exudates on chlamydospores germination of the bean root rot of fungus, *Fusarium solani* f. *phaseoli*." Phytopathology **51**: 389-393

Schuller, D. J., N. Ban, R. B. Huystee, A. McPherson and T. L. Poulos (1996). "The crystal structure of peanut peroxidase." Structure **4**(3): 311-321.

Segall, J. E. (1993). "Polarization of yeast cells in spatial gradients of alpha mating factor." Proc Natl Acad Sci U S A **90**(18): 8332-8336.

Sekizaki, H., R. Yokosawa, C. Chinen, H. Adachi and Y. Yamane (1993). "Studies on zoospore attracting activity. II. Synthesis of isoflavones and their attracting activity to Aphanomyces euteiches zoospore." Biol Pharm Bull **16**(7): 698-701.

Senthil-Kumar, M. and K. S. Mysore (2014). "Tobacco rattle virus-based virus-induced gene silencing in Nicotiana benthamiana." Nat Protoc **9**(7): 1549-1562.

Sharon, N. and H. Lis (2004). "History of lectins: from hemagglutinins to biological recognition molecules." Glycobiology **14**(11): 53R-62R.

Shim, W. B. and L. D. Dunkle (2003). "CZK3, a MAP kinase kinase kinase homolog in Cercospora zeae-maydis, regulates cercosporin biosynthesis, fungal development, and pathogenesis." Mol Plant Microbe Interact **16**(9): 760-768.

Smith, A. T., N. Santama, S. Dacey, M. Edwards, R. C. Bray, R. N. Thorneley and J. F. Burke (1990). "Expression of a synthetic gene for horseradish peroxidase C in *Escherichia coli* and folding and activation of the recombinant enzyme with Ca2+ and heme." J Biol Chem **265**(22): 13335-13343.

Snoeijers, S. S., A. Perez-Garcia, M. H. A. J. Joosten and P. J. G. M. De Wit (2000). "The effect of nitrogen on disease development and gene expression in bacterial and fungal pathogens." European Journal of Plant Pathology **106**: 493–506.

Snyder, W. C. and H. N. Hansen (1940). "The species concept in Fusarium." Am. J. Bot. **27**: 64-67.

Speulman, E., P. L. Metz, G. van Arkel, B. te Lintel Hekkert, W. J. Stiekema and A. Pereira (1999). "A two-component enhancer-inhibitor transposon mutagenesis system for functional analysis of the Arabidopsis genome." Plant Cell **11**(10): 1853-1866.

Stadler, D. R. (1952). "Chemotropism in Rhizopus nigricans; The staling reaction. ." J. Cell. Physiol. **39**: 449-474.

Stefan, C. J. and K. J. Blumer (1994). "The third cytoplasmic loop of a yeast G-protein-coupled receptor controls pathway activation, ligand discrimination, and receptor internalization." Mol Cell Biol **14**(5): 3339-3349.

Steinberg, C., J. M. Whipps, D. A. Wood, J. Fenlon and C. Alabouvette (1999a). "Mycelial development of *Fusarium oxysporum* in the vicinity of tomato roots." Mycological Research **103**: 769-778.

Steinberg, G. (2007). "On the move: endosomes in fungal growth and pathogenicity." Nature Reviews Microbiology **5**: 309-316.

Stephenson, S. A., J. R. Green, J. M. Manners and D. J. Maclean (1997). "Cloning and characterisation of glutamine synthetase from Colletotrichum gloeosporioides and demonstration of elevated expression during pathogenesis on Stylosanthes guianensis." Curr Genet **31**(5): 447-454.

Stevenson, I. L. and S. A. Becker (1972). "The fine structure and development of chlamydospores of *Fusarium oxysporum*." Can J Microbiol **18**(7): 997-1002.

Strange, B. (1890). Ueber chemotactische Reizbewegungen, Bot. Zeit. .

Sun, Y., S. Carroll, M. Kaksonen, J. Y. Toshima and D. G. Drubin (2007). "PtdIns(4,5)P2 turnover is required for multiple stages during clathrin- and actin-dependent endocytic internalization." J Cell Biol **177**(2): 355-367.

Sun, Y. and D. G. Drubin (2012). "The functions of anionic phospholipids during clathrin-mediated endocytosis site initiation and vesicle formation." J Cell Sci **125**(Pt 24): 6157-6165.

Swingle, W. T. (1896). Bordeaux mixture, its chemistry, physical properties, and toxic effect on fungi and algae, Div. Veg. Phys. and Path. U. S. Dept. Agric. Bull.

Taheri, P. and S. Tarighi (2012). "The Role of Pathogenesis-Related Proteins in the Tomato-Rhizoctonia solani Interaction." Journal of Botany. Doi.org/doi:10.1155/2012/137037.

Taheri, P. and S. Tarighi (2011). "A survey on basal resistance and riboflavin-induced defense responses of sugar beet against *Rhizoctonia solani*." J Plant Physiol **168**(10): 1114-1122.

Takken, F. and M. Rep (2010). "The arms race between tomato and *Fusarium oxysporum*." Mol Plant Pathol **11**(2): 309-314.

Talbot, N. J., D. J. Ebbole and J. E. Hamer (1993). "Identification and characterization of MPG1, a gene involved in pathogenicity from the rice blast fungus *Magnaporthe grisea*." Plant Cell **5**(11): 1575-1590.

Tavernier, V., S. Cadiou, K. Pageau, R. Lauge, M. Reisdorf-Cren, T. Langin and C. Masclaux-Daubresse (2007). "The plant nitrogen mobilization promoted by *Colletotrichum lindemuthianum* in Phaseolus leaves depends on fungus pathogenicity." J Exp Bot **58**(12): 3351-3360.

Teichert, I., E. K. Steffens, N. Schnass, B. Franzel, C. Krisp, D. A. Wolters and U. Kuck (2014). "PRO40 is a scaffold protein of the cell wall integrity pathway, linking the MAP kinase module to the upstream activator protein kinase C." PLoS Genet **10**(9): e1004582.

Terpe, K. (2006). "Overview of bacterial expression systems for heterologous protein production: from molecular and biochemical fundamentals to commercial systems." Appl Microbiol Biotechnol **72**(2): 211-222.

Theorell, H. (1950). "Research on peroxidases and catalases." Rend Ist Sup Sanit **13**(11-12): 876-893.

Tissier, A. F., S. Marillonnet, V. Klimyuk, K. Patel, M. A. Torres, G. Murphy and J. D. Jones (1999). "Multiple independent defective suppressor-mutator transposon insertions in Arabidopsis: a tool for functional genomics." Plant Cell **11**(10): 1841-1852.

Tognolli, M., C. Penel, H. Greppin and P. Simon (2002). "Analysis and expression of the class III peroxidase large gene family in *Arabidopsis thaliana*." Gene **288**(1-2): 129-138.

Truckses, D. M., L. S. Garrenton and J. Thorner (2004). "Jekyll and Hyde in the microbial world." Science **306**(5701): 1509-1511.

Tsai, S. M. and D. A. Phillips (1991). "Flavonoids released naturally from alfalfa promote development of symbiotic glomus spores in vitro." Appl Environ Microbiol **57**(5): 1485-1488.

Turra, D. and A. Di Pietro (2015). "Chemotropic sensing in fungus-plant interactions." Curr Opin Plant Biol **26**: 135-140.

Turra, D., M. El Ghalid, F. Rossi and A. Di Pietro (2015). "Fungal pathogen uses sex pheromone receptor for chemotropic sensing of host plant signals." Nature **accepted**.

Turra, D., D. Segorbe and A. Di Pietro (2014). "Protein kinases in plant-pathogenic fungi: conserved regulators of infection." Annu Rev Phytopathol **52**: 267-288.

Tyler, B. M., M. Wu, J. Wang, W. Cheung and P. F. Morris (1996). "Chemotactic Preferences and Strain Variation in the Response of Phytophthora sojae Zoospores to Host Isoflavones." Appl Environ Microbiol **62**(8): 2811-2817.

Unver, T. and H. Budak (2009). "Virus-induced gene silencing, a post transcriptional gene silencing method." Int J Plant Genomics **2009**: 198680.

Vadaie, N., H. Dionne, D. Akajagbor, D. Krysan and P. Cullen (2008). "Cleavage of the signaling mucin Msb2 by the aspartyl protease Yps1 is required for MAPK activation in yeast." J Cell Biol **181**(7): 1073-1081.

Valtz, N., M. Peter and I. Herskowitz (1995). "FAR1 is required for oriented polarization of yeast cells in response to mating pheromones." J Cell Biol **131**(4): 863-873.

van den Ackerveken, G. F. J. M., J. A. L. van Kan, M. H. A. J. Joosten, H. Muisers and P. J. G. M. De Wit (1994). "Nitrogen limitation induces expression of the avirulence gene avr9 in the tomato pathogen *Cladosporium fulvum*." Molecular Plant–Microbe Interactions **3**: 277-285.

Veitch, N. C. (2004). "Horseradish peroxidase: a modern view of a classic enzyme." Phytochemistry **65**(3): 249-259.

Vera, P., P. Tornero and V. Conejero (1993). "Cloning and expression analysis of a viroid-induced peroxidase from tomato plants." Mol Plant Microbe Interact **6**(6): 790-794.

Verna, J., A. Lodder, K. Lee, A. Vagts and R. Ballester (1997). "A family of genes required for maintenance of cell wall integrity and for the stress response in *Saccharomyces cerevisiae*." Proc Natl Acad Sci U S A **94**(25): 13804-13809.

Vitali, A., B. Botta, G. Delle Monache, S. Zappitelli, P. Ricciardi, S. Melino, R. Petruzzelli and B. Giardina (1998). "Purification and partial characterization of a peroxidase from plant cell cultures of *Cassia didymobotrya* and biotransformation studies." Biochem J **331**(Pt 2): 513-519.

Voinnet, O. (2001). "RNA silencing as a plant immune system against viruses." Trends Genet **17**(8): 449-459.

Wang, K. (2006). Agrobacterium Protocols. Totowa, NJ, USA, Human Press.

Wang, Y. and H. G. Dohlman (2004). "Pheromone signaling mechanisms in yeast: a prototypical sex machine." Science **306**(5701): 1508-1509.

Wen, F., H. D. VanEtten, G. Tsaprailis and M. C. Hawes (2007). "Extracellular proteins in pea root tip and border cell exudates." Plant Physiol **143**(2): 773-783.

Whetten, R. W., J. J. MacKay and R. R. Sederoff (1998). "Recent Advances in Understanding Lignin Biosynthesis." Annu Rev Plant Physiol Plant Mol Biol **49**: 585-609.

Whitham, S. A., S. Quan, H. S. Chang, B. Cooper, B. Estes, T. Zhu, X. Wang and Y. M. Hou (2003). "Diverse RNA viruses elicit the expression of common sets of genes in susceptible Arabidopsis thaliana plants." Plant J **33**(2): 271-283.

Wollenweber, H. W. (1931). "Fusarium-Monographie. Fungi parasitici et saprophytici." Zeitschrift für Parasitenkunde **3**: 269-516.

Wollenweber, H. W. and O. A. Reinking (1935). "Die Fusarien: ihre Beschreibung." Schadwirkung und Bekämpfung: 1-355.

Woronin, M. (1888). Ueber die Sklerotienkrankheit der Vaccinieen-Beeren, Mem. Acad. Imp. Sci. St. Petersbourg VII.

Xu, J. R. and J. E. Hamer (1996). "MAP kinase and cAMP signaling regulate infection structure formation and pathogenic growth in the rice blast fungus *Magnaporthe grisea*." Genes Dev **10**(21): 2696-2706.

Xu, J. R., C. J. Staiger and J. E. Hamer (1998). "Inactivation of the mitogen-activated protein kinase Mps1 from the rice blast fungus prevents penetration of host cells but allows activation of plant defense responses." Proc Natl Acad Sci U S A **95**(21): 12713-12718.

Yakir-Tamang, L. and J. E. Gerst (2009). "A phosphatidylinositol-transfer protein and phosphatidylinositol-4-phosphate 5-kinase control Cdc42 to regulate the actin cytoskeleton and secretory pathway in yeast." Mol Biol Cell **20**(15): 3583-3597.

Yang, L., L. Ukil, A. Osmani, F. Nahm, J. Davies, C. P. De Souza, X. Dou, A. Perez-Balaguer and S. A. Osmani (2004). "Rapid production of gene replacement constructs and generation of a green fluorescent protein-tagged centromeric marker in *Aspergillus nidulans*." Eukaryot Cell **3**(5): 1359-1362.

Young, S. A., A. Guo, J. A. Guikema, F. F. White and J. E. Leach (1995). "Rice cationic peroxidase accumulates in xylem vessels during incompatible interactions with *Xanthomonas oryzae* pv *oryzae*." Plant Physiol **107**(4): 1333-1341.

Zanolari, B., S. Friant, K. Funato, C. Sutterlin, B. J. Stevenson and H. Riezman (2000). "Sphingoid base synthesis requirement for endocytosis in *Saccharomyces cerevisiae*." EMBO J **19**(12): 2824-2833.

Zentmyer, G. A. (1961). "Chemotaxis of Zoospores for Root Exudates." Science **133**(3464): 1595-1596.

Zhang, H., C. Xue, L. Kong, G. Li and J. R. Xu (2011). "A Pmk1-interacting gene is involved in appressorium differentiation and plant infection in *Magnaporthe oryzae*." Eukaryot Cell **10**(8): 1062-1070.

Zhang, X., K. Orlando, B. He, F. Xi, J. Zhang, A. Zajac and W. Guo (2008). "Membrane association and functional regulation of Sec3 by phospholipids and Cdc42." J Cell Biol **180**(1): 145-158.

Zheng, L., M. Campbell, J. Murphy, S. Lam and J. R. Xu (2000). "The BMP1 gene is essential for pathogenicity in the gray mold fungus *Botrytis cinerea*." Mol Plant Microbe Interact **13**(7): 724-73.